SPATIAL AND TEMPORAL CONTROLS ON BIOGEOCHEMICAL INDICATORS AT THE SMALL-SCALE INTERFACE BETWEEN A CONTAMINATED AQUIFER AND WETLAND SURFACE WATER

A Dissertation

by

SUSAN ENID BAEZ-CAZULL

Submitted to the Office of Graduate Studies of
Texas A&M University
in partial fulfillment of the requirements for the degree of

DOCTOR OF PHILOSOPHY

December 2007

Major Subject: Geology

SPATIAL AND TEMPORAL CONTROLS ON BIOGEOCHEMICAL INDICATORS AT THE SMALL-SCALE INTERFACE BETWEEN A CONTAMINATED AQUIFER AND WETLAND SURFACE WATER

A Dissertation

by

SUSAN ENID BAEZ-CAZULL

Submitted to the Office of Graduate Studies of
Texas A&M University
in partial fulfillment of the requirements for the degree of

DOCTOR OF PHILOSOPHY

Approved by:

Chair of Committee,	Jennifer T. McGuire
Committee Members,	Hongbin Zhang
	Anne Raymond
	Ethan Grossman
	Dan Thornton
Head of Department,	John Spang

December 2007

Major Subject: Geology

ABSTRACT

Spatial and Temporal Controls on Biogeochemical Indicators at the Small-Scale Interface Between a Contaminated Aquifer and Wetland Surface Water.

(December 2007)

Susan Enid Baez-Cazull, B.S., University of Puerto Rico at Río Piedras

Chair of Advisory Committee: Dr. Jennifer T. McGuire

This high-resolution biogeochemical study investigated spatial and temporal variability in the mixing interface zones within a wetland-aquifer system near a municipal landfill in the city of Norman, Oklahoma. Steep biogeochemical gradients indicating zones of enhanced microbial activity (e.g. iron/sulfate reduction and fermentation) were found at centimeter-scale hydrological and lithological interfaces. The small resolution study was achieved by combining passive diffusion samplers with capillary electrophoresis for chemical analysis. The spatial and temporal variability of biogeochemical processes found at the interfaces was evaluated in a depth profile over a period of three years. Correlations between geochemical parameters were determined using Principal Component Analysis (PCA) and the principal factors obtained were interpreted as a dominant biogeochemical process. Factors scores were mapped by date and depth to determine the spatial-temporal associations of the dominant processes. Fermentation was the process controlling the greatest variability in the dataset followed by iron/sulfate reduction, and methanogenesis.

The effect of seasonal and hydrologic changes on biogeochemistry was evaluated from samples collected in a wet/dry period from three locations exhibiting upward, downward, and negligent hydrologic flow between aquifer and wetland. PCA was used to identify the principal biogeochemical processes and to obtain factor scores for evaluating significant seasonal and hydrological differences via analysis of variance. Iron and sulfate reduction were dominated by changes in water table levels and water flow paths, whereas methanogenesis and bacterial barite utilization were dominated by season and associated with a site with negligible flow. A preliminary study on microbial response to changes in geochemical nutrients (e.g. electron acceptors and electron donors) was conducted using in situ microcosms with the purpose of quantifying iron and sulfate reduction rates. Problems encountered in the experiment such as leaks in the microcosms did not allow the determination of respiration rates, therefore the experiments will be repeated in the future. The results suggest that iron and sulfate reduction were stimulated with the addition of sulfate and ferrihydrite (electron acceptors) and acetate and lactate (electron donors). This research demonstrates the importance of assessing biogeochemical processes at interface zones at appropriate scales and reveals the seasonal and hydrological controls on system processes.

Para mi Mamá, mi Papá y mis hermanos quienes me han dado todo su amor y apoyo.

For Levi who has believed in me and has given me all the support and strength.

Y para tí Abuela por siempre estar conmigo.

Because their love is all I need.

ACKNOWLEDGMENTS

I would like to express my sincere thanks to my advisor, Dr. Jennifer T. McGuire, for her guidance, encouragement and friendship. I would like to thank my research group, in particular Tara Kneeshaw who has been there for me helping in many sampling trips and has been an unconditional friend. My sincere thanks to Erik Smith for all his assistance in sampling trips, assistance with the CE instrument, and creation of sampling equipment; without him the task would have been much difficult. In addition, I owe thanks to the U.S. Geological Survey, to Isabelle Cozzarelli, Jeanne Jaeschke, Mary A. Voytek, Scott Christenson, Jason Masoner, and James Greer. I would also like to thank Dr. Anne Raymond for all the professional and personal advice she has given me.

I am indebted to the National Science Foundation, Biocomplexity in the Environment, the Center of Environmental and Rural Health at TAMU, the Conoco Phillips Fellowship, the Robert Berg Fellowship, and the Geology & Geophysics Department at TAMU for funding my research.

TABLE OF CONTENTS

CHAPTER Page

LIST OF FIGURES

FIGURE Page

FIGURE Page

FIGURE Page

LIST OF TABLES

CHAPTER I

INTRODUCTION

To assess the quality of freshwater resources it is necessary to characterize the biogeochemical conditions and hydrological processes that exert a control on the composition of surface water and groundwater. This dissertation characterizes biogeochemical processes in a freshwater system and determines the seasonal and hydrological controls on these processes by presenting a high-resolution biogeochemical study targeting the mixing interface zones within a wetland-aquifer system near the Norman Landfill in Norman, Oklahoma.

In a wetland system, the most biogeochemically active zone is near the surface, where the system experiences changes in temperature, precipitation, infiltration, vegetation, and nutrient loading (Hunt et al., 1997). In this zone enhanced biogeochemical activity is observed due to the availability of electron acceptors and electron donors. However, in this study other interfaces found with depth have shown evidence for enhanced biogeochemical activity such as the interface between wetland pore water and anaerobic groundwater (Baez-Cazull et al., 2007a), where electron acceptors and electron donors come into contact.

This dissertation follows the style and format of Applied Geochemistry.

The interaction of a wetland and aquifer system can present unique conditions for biogeochemical cycling at these interfaces as they are subject to seasonal conditions and heterogeneous distribution of chemicals in the systems. The research presented in this dissertation is divided in four chapters that address the spatial and temporal variability of biogeochemical processes associated with the interactions of the wetland and aquifer systems. The goals for each chapter are 1) identify biogeochemical processes taking place with depth in the wetland aquifer system associated with available electron acceptors and donors found in lithological boundaries, the sediment-water interface, and the wetland pore water-aquifer water interface, 2) determine the spatial and temporal variability of dominant biogeochemical processes at these interfaces, 3) evaluate the seasonal and hydrological controls on the biogeochemical processes, and 4) determine sulfate and iron reduction rates of native microbial organisms after the introduction of electron donors and electron acceptors simulating a recharge event. These goals are discussed in detail in Chapters II to V.

The purpose of Chapter II is to identify the most active zones of biogeochemical cycling within the wetland-aquifer system characterized by steep geochemical gradients. The research presents field-laboratory methods to describe resulting gradients at fine spatial resolution. In past field investigations, it has been difficult to obtain geochemical and microbiological measurements at sufficiently fine spatial resolution to describe biogeochemical processes and observe the resulting geochemical gradients. Discrete pore water samples were collected at a high resolution (centimeter intervals) using passive diffusion samplers “peepers”. In combination with analysis by capillary

electrophoresis, a suite of geochemical parameters such as anions, cations, and organic acids were analyzed on small sample volumes. Steep geochemical gradients were observed on a centimeter-scale at transition zones between lithological and surface water/groundwater boundaries associated with areas of increased microbial activity, and biogeochemical processes occurring with depth at the wetland-aquifer system were identified.

Chapter III describes the spatial and temporal variability of dominant biogeochemical processes occurring in the wetland-aquifer system from geochemical pore water data collected at centimeter interval depths over a period of three years. In a wetland-aquifer system the changes in biogeochemical processes respond to solute transport processes, biological activities, and solid phase composition which can vary on small spatial and temporal scales (Brune et al., 2000; Hunt et al., 1997; Kappler et al., 2005). In biogeochemical studies, these processes are often interpreted from the analysis of geochemical parameters such as redox couples (e.g. H_2S and SO_4^{2-}). One caveat with this approach is that many geochemical parameters are affected by multiple hydro-bio-geo-chemical processes and expected relationships cannot be easily discerned from geochemical datasets due to the effects of multiple processes on a single geochemical indicator. To interpret processes, it was important to determine the correlations between parameters to identify the contributing process(es) for each parameter. Therefore, geochemical parameters were analyzed using multivariate statistics to determine dominant biogeochemical processes such as iron reduction, sulfate reduction, and methanogenesis. The use of multivariate statistics was practical for reducing the large

dataset and for exposing significant relationships among geochemical parameters. Multivariate statistical analyses provided details on the correlations between parameters revealing obscured relationships between hydro-bio-geochemical parameters to give new insights into the processes controlling the variability in the dataset. The use of PCA for exploring parameter correlations and the mapping of factor scores improved the understanding and interpretation of processes controlling the surface water and groundwater composition affected by seasonal changes and hydrologic fluctuations. This study demonstrates the value of using multivariate statistics to reveal biogeochemical relationships and enhance understanding of complex system dynamics.

The purpose of Chapter IV is to determine the controls of seasonal hydrologic conditions on dominant biogeochemical processes resulting from the linkages of the wetland-aquifer system. Most studies approach these systems separately targeting biogeochemical processes occurring in either the wetland or aquifer. However, shallow unconfined aquifer systems are often connected hydrologically to surface wetland systems resulting in linked biogeochemical processes. Environmental conditions affecting the distribution of biogeochemical processes in the wetland include: temperature and precipitation, changes in hydrological flowpaths, and changes in water table levels. These factors determine the supply of electron acceptors and nutrients to the system over spatial and temporal scales. For example, variable flowpaths bring waters with limiting solutes (ex., nutrients, electron donors, or electron acceptors) into contact enhancing microbial activities and organic matter mineralization. Thus, the observed temporal and spatial heterogeneity in biogeochemistry is the result of the

complex hydrology and seasonal changes that the wetland and aquifer share (Baez-Cazull et al., 2007a; Baez-Cazull et al., 2007b). To evaluate the seasonal hydrologic controls on biogeochemistry in this system, field geochemical data were collected during the wet spring season in May and during the dry fall season in September 2005 from vertical profiles spanning the wetland-aquifer interface. The effect of changing hydrologic conditions was studied from the analysis of three locations that exhibited different flow direction and aquifer seepage rates: 1) high discharge to the wetland system, 2) high recharge to the aquifer system, and 3) low/negligible discharge rate. Multivariate statistics were used to explore significant relationships among geochemical parameters and evaluate changing processes. Principal Component Analysis (PCA) was used to determine dominant biogeochemical processes by exploring parameter correlations. Factor scores obtained from PCA were entered in Analysis of Variance (ANOVA) for the determination of significant differences in the means among sites representing different seasonal hydrologic regimes. The combination of these statistical techniques allowed for interpretation of the role of seasonal hydrologic fluctuations in controlling surface water and groundwater composition.

Chapter V discusses a preliminary experiment with the aims of understanding microbial respiration rates responding to changes in geochemical conditions. Recharge events were simulated by adding geochemical solutions containing electron acceptors and/or electron donors to a community of anaerobes contained in the microcosms with the purpose of quantifying metabolic rates and changes in community structure. In dynamic systems such as wetland and aquifers, changes in electron acceptors and

electron donors are driven by seasonal cycles and hydrological changes which result in adaptation and competition between microbial communities adjusting to the new environmental conditions. A series of in situ experiments were carried at a region above the wetland-aquifer interface, consisting of small chambers that allow colonization of native microorganisms and provide the loci for introducing the experimental solutions. This zone has been previously characterized with variable concentrations of organic acids suggesting that it is a zone of active microbial metabolism. The experiments were designed to quantify ideal iron and sulfate reduction rates from an in situ incubated bacterial community responding to a simulated recharge event by 1) addition of electron acceptors (sulfate and ferrihydrite) and 2) addition of electron acceptors and electron donors, with the assumption that the observed changes in TEAPs are a result of the adaptation of microorganisms to the changing geochemical conditions. During experimentation, there were some problems encountered with the design of the equipment which caused some of the solutions to leak. Therefore accurate analysis of sulfate and iron reduction could not be attributed to the organisms in the microcosms. The discussion in this chapter is intended to give information on the design and methodology for the improvement of future experiments.

CHAPTER II

CHARACTERIZATION OF BIOGEOCHEMICAL GRADIENTS AT A WETLAND-AQUIFER INTERFACE USING CAPILLARY ELECTROPHORESIS*

SYNOPSIS

Steep biogeochemical gradients were measured at mixing interfaces in a wetland-aquifer system impacted by landfill leachate in Norman, Oklahoma. Using cm-scale passive diffusion samplers, water samples were collected in a depth profile spanning the surface water and various sedimentary layers. Biogeochemical process indicators, including organic acids, were analyzed by capillary electrophoresis and field techniques to maximize small sample volumes available from pore waters at the centimeter scale. Steep concentration gradients were observed at the sediment-water interface as well as at mixing interfaces between waters in various sedimentary units. At the sediment-water interface, iron reduction and sulfate reduction coexist, likely due to heterogeneity in the iron phases present in the system. Within the wetland sediments, heterogeneities in organic carbon and available electron acceptors allow for build-up of organic acids and indicators of microbial activity.

*Reproduced with permission from Baez-Cazull, S.; McGuire, J.T.; Cozzarelli, I.M.; Raymond, A.; Welsh, L. Applied Geochemistry 2007 in press. Copyright © 2007, Elsevier, DOI: 10.1016/j.apgeochem.2007.06.003

These findings support the hypothesis that increased biogeochemical cycling occurs at interfaces between environments of differing redox potential where limiting electron acceptors or donors can come in contact.

INTRODUCTION

To understand and predict the fate and transport of numerous chemical species, including nutrients and contaminants, it is important to identify the most active zones of biogeochemical cycling within a system. It has been proposed that in natural systems, zones with steep biogeochemical gradients may be areas of increased microbial activity (Kappler et al., 2005). Microbial activity is enhanced when concentration gradients of limiting electron acceptors and/or electron donors come in contact, such as in the transition zones between environments of differing redox potential (Koretsky et al., 2003; Llobet-Brossa et al., 2002; McMahon and Chapelle, 1991; Sass et al., 2002; Ulrich et al., 1998). Although the potential importance of transition zones is widely accepted, characterization is challenging because chemical and microbiological measurements must be collected at sufficiently fine spatial resolution to describe resulting gradients. The microbial processes that control natural attenuation of contaminants typically occur at the micrometer to millimeter scale, yet measurements of electron acceptor and donor concentrations are most often made at the meter scale (Kappler et al., 2005). Here we present findings of steep biogeochemical gradients observed at centimeter-scale transition zones in an aquifer-wetland system impacted by landfill leachate.

The reduction-oxidation (redox) potential of a system, influenced by linked hydrological, microbiological, and geochemical processes, largely controls the elemental cycling of nutrients and contaminants (Lyngkilde and Christensen, 1992a; Nicholson et al., 1983; Peterson and Sun, 2000). In subsurface systems, much work has focused on documenting redox zonation and associated biodegradation at the plume scale. Many studies have suggested a sequential pattern of redox zones, each of which is dominated by a single terminal electron accepting process (TEAP) coupled to the oxidation of organic compounds (Baun et al., 2003; Chapelle and McMahon, 1991; Christensen et al., 2000; McGuire et al., 2000). Based on thermodynamic energy yield, microorganisms first use O_2 as an electron acceptor followed by the reduction of alternate electron acceptors including NO_3^-, Fe(III), SO_4^{2-}, and CO_2 (methanogenesis). This results in the characteristic redox zonation observed in sediments (Achtnich et al., 1995; Albrechtsen and Christensen, 1994; Champ et al., 1979; Chapelle et al., 1996; Christensen et al., 2000; Cozzarelli et al., 2000; Lovley and Phillips, 1987; Ludvigsen et al., 1998). However, studies have found TEAPs appear to occur simultaneously at the plume scale, thereby adding complexity to this sequential redox zone model (Blodau et al., 1998; Koretsky et al., 2003; Ludvigsen et al., 1998; McGuire et al., 2002; Motelica-Heino et al., 2003). Complexities in the distribution of TEAPs have also been identified at the "fringe" zones surrounding contaminant plumes where anoxic water contacts more oxic recharge water, creating gradients of electron acceptors and donors (Christensen et al., 2000; Mayer et al., 2001; Tuxen et al., 2006; van Breukelen and Griffioen, 2004; van Breukelen et al., 2003). Similarly, heterogeneities in the spatial distribution of

sediments (e.g., particle size, mineralogy), organic carbon content, and availability of electron acceptors can allow for the coexistence of several carbon oxidation pathways using multiple electron acceptors (Koretsky et al., 2003). Complexities in the redox zonation model illustrate the importance of collecting biogeochemical measurements at sufficiently small spatial intervals to characterize the active zones of biogeochemical cycling. For example, studies by Cozzarelli et al. (2001) and Bekins et al. (2001) observed that iron reduction gradients occurred at centimeter scales in a hydrocarbon contaminated plume due to the heterogeneous distribution of reducible iron minerals.

Quantifying the redox reactions occurring at these relatively small transition zones may be critical to assessing the overall biogeochemical cycling in a system if these zones are indeed areas of enhanced microbial activity. Previous studies have documented enhanced microbial activity at interface zones created by lithologic boundaries (Ulrich et al., 1998) and surface water-groundwater interfaces (Dahm et al., 1998) due to the mixing of electron donors and acceptors. Steep geochemical gradients of metabolic byproducts (i.e. organic acids) have also been observed at the interface between aquifer and aquitard sediments (McMahon and Chapelle, 1991). In a recent study, Tuxen et al. (2006) documented a steep gradient of phenoxy acids and oxygen at the fringe of a contaminant plume where microbial degradation was enhanced, demonstrating the importance of measuring these gradients at small (decimeter) scales. However, few studies have undertaken extensive characterization of the complex biogeochemical processes at relevant sampling scales to describe transition zones.

Past field investigations have been limited by the difficulty in obtaining geochemical measurements at representative spatial scales to characterize the small and transient nature of interface zones (Hunt et al., 1997). The small volumes of fluid available for analytical measurements also limit the characterization of the organic and inorganic species involved in complex redox reactions (Christensen et al., 2000). Commonly used sampling methods including well pumping and pore water extraction from sediment cores raise concerns such as the potential mixing of waters from various zones and sediment disturbances. Water samples reflecting in situ equilibrium conditions at discrete intervals can be collected using passive diffusion samplers or "peepers" (Hesslein, 1976) to limit mixing with adjacent zones. One consequence of using peepers at 0.5 to 1 cm intervals is the small sample volumes obtained. Generally, sample volumes greater than 0.5 mL are required for common analytical techniques for inorganic and organic ions, such as ion chromatography, atomic absorption, and gas chromatography. Using these techniques, the total volumes necessary for complete redox characterization cannot be obtained from cm-scale peepers. Capillary electrophoresis (CE), an emerging technology in environmental sciences, overcomes these volume limitations by requiring very small sample volumes, ~ 1 nL per injection for a chemical suite, and no pre-processing (Linhardt and Toida, 2002). For example, all anionic parameters can be analyzed in triplicate with 10 μL of pipetted sample.

This paper presents a high-resolution biogeochemical study targeting the mixing interface zones within a wetland-aquifer system near the Norman Landfill in Norman, Oklahoma. The site is an ideal location for studying geochemical gradients because the

wetland-aquifer system contains several shallow interfaces where waters of differing redox potential mix. The purpose of this paper is to document the biogeochemical gradients that result at these mixing interfaces and present appropriate field-laboratory methods to describe resulting gradients at sufficiently fine spatial resolution. Emerging CE technology to analyze environmental samples provides the ability to measure biogeochemical indicators on smaller volumes of fluid and thus allow investigations at smaller spatial scales. New knowledge of the importance of interface zones on biogeochemical cycling will allow for improved prediction of chemical fate and transport and assessment of natural attenuation of contaminated sites.

BACKGROUND

Site Description

The Norman Landfill, situated in the Canadian River alluvial plain in central Oklahoma (Figure 2.1), was a municipal, non-restricted solid waste landfill that operated from 1922 to 1985 in the city of Norman, OK. The geologic setting is characterized by moderately permeable alluvial and terrace deposits with a shallow water table that overlies a Permian shale and mudstone confining unit known as the Hennessy Group (Scholl and Christenson, 1998). The reworked alluvium is about 12 meters thick in the landfill area (Stacy, 1961) and the hydraulic conductivity is estimated to range from 7.3×10^{-2} to 2.4×10^{1} meters per day (Scholl and Christenson, 1998). Leachate from the unlined landfill resulted in a groundwater plume that extends downgradient

approximately 250 m from the landfill toward the Canadian River and flows directly beneath the wetland (slough) (Scholl and Christenson, 1998). The wetland is likely a previous location of the main river channel, fed by groundwater discharge and precipitation. The wetland's water levels vary seasonally ranging from approximately 1 m deep in the spring to dry in the summer. Upper sediments have been variably saturated during the summer months.

The Norman Landfill has been designated as a U.S. Geological Survey research site under the USGS Toxic Substances Hydrology Program since 1995. It is the site of active, ongoing investigations into the biogeochemistry of the plume. Recent studies at the site by Lorah et al. (2007) targeting biogeochemical cycling within the wetland system demonstrate the spatial and temporal link between redox conditions in the wetland sediments and fluctuations in groundwater/surface-water levels. Generally, during periods of high recharge, the upgradient bank of the slough had higher concentrations of leachate constituents including ammonium, dissolved organic carbon, iron, and bicarbonate were found in the top 60 cm of the wetland-sediment pore water compared to low recharge periods, indicating that leachate plume water from the aquifer discharged into the wetland. Scholl et al. (2005) also observed that exchange between the wetland and shallow groundwater was episodic and that shallow groundwater downgradient from the slough contained, on average, 29 percent wetland water during periods of high recharge. A generalized conceptual model showing the connection between the wetland (slough) and surrounding aquifer is shown in Figure 2.2.

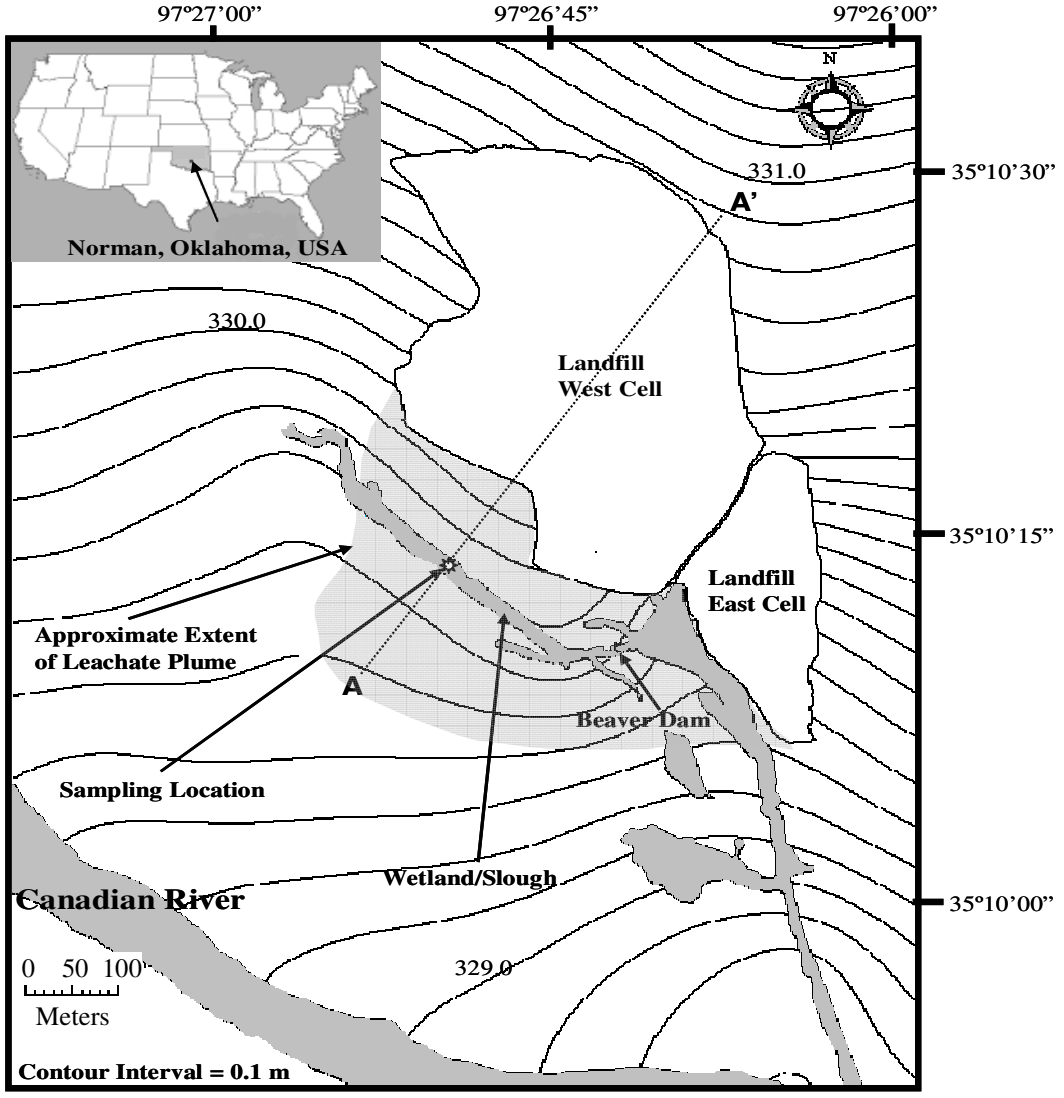

Figure 2.1. Map of the Norman Landfill site in Oklahoma, U.S., showing the sample location. Modified from Scholl and Christenson (1998). Potentiometric lines are shown.

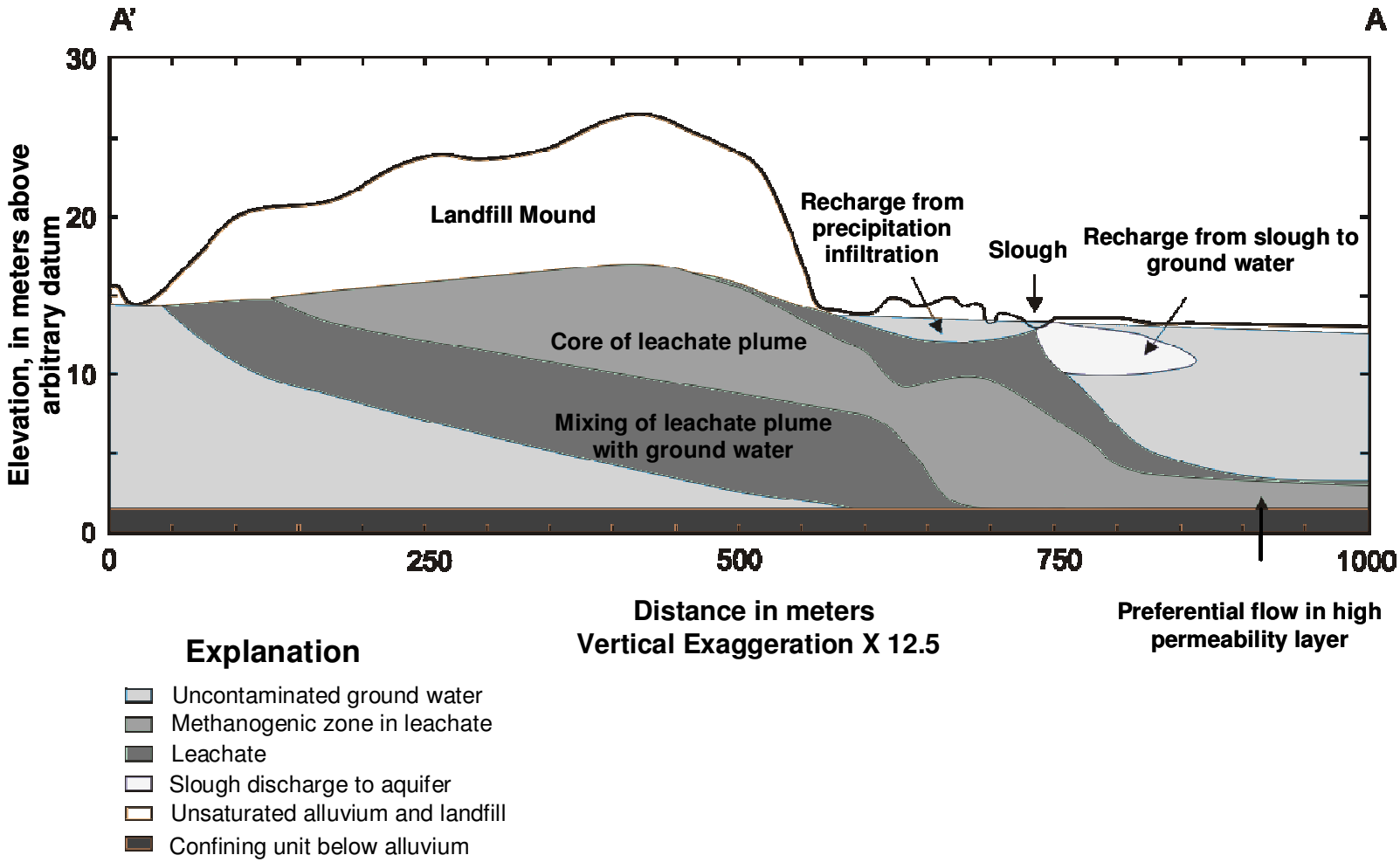

Figure 2.2. Cross-sectional view of the Norman Landfill along section A-A' (as shown in Figure 2.1). The leachate plume and recharge zones are drawn on the basis of chemistry measurements made in the aquifer between 1997 and 2002 (adapted from Scholl et al. (2005)).

Core Description

The surficial sediments of the wetland adjacent to the Norman Landfill consist of alternating units of fluvial silt and sand. The following description is based on the sequence of layers in a shallow core collected near the location of the peepers (Figure 2.3).

Upper Silt Unit (0-40 cm). The upper 40 cm of the core consists of organic-rich silt, referred to as the upper silt unit. The uppermost 10 cm of this unit contain abundant particulate organic matter, including plant fibers, seeds, and insect parts. The organic content of the upper silt unit decreases with depth (Figure 2.4). Snail shells are most abundant in the top 25 cm of the upper silt unit, but occur sporadically throughout the core. When exposed to light, seeds in the upper 18 cm of this unit sprouted. Seeds below 18 cm in the core did not sprout. The upper silt unit is laterally extensive and appears in all cores collected from the wetland (unpublished field data).

Transition Zone (40-46 cm). The next two units in the core together form a highly variable transition zone between the upper silt unit and the underlying coarse sand unit. The upper unit of the transition zone is a 3-4 cm layer of tan, medium to coarse-grained sand, referred to as the upper sand unit. The contact between the upper silt unit and the upper sand unit preserves relict burrows. The lower unit of the transition zone is a thin, organic-rich muddy silt unit, 2-3 cm thick, referred to as the middle silt unit. The contact between the upper sand and middle silt units is erosional.

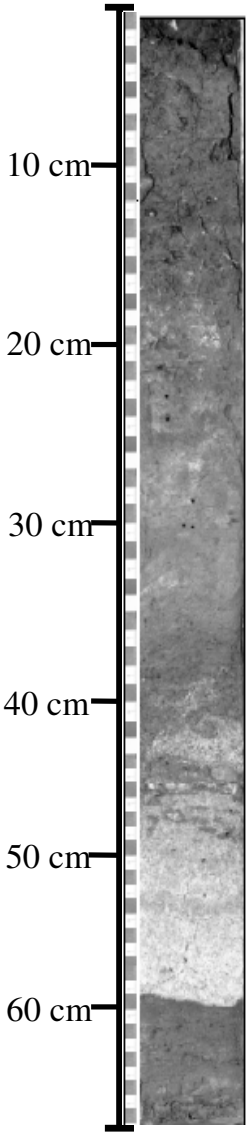

Upper silt unit – 0 to 40 cm (40 cm)

- 0-22 cm: Sediment is mostly silt and fine sand with organic material (green grasses, leaves and fibrous roots in the top 10 cm)
- 23-35 cm: Less organic material, some bioturbation.
- 36-39 cm: Fine sand and yellowish brown fine grains, burrowed contact with coarse sand below.

Transition Zone:

Upper sand unit – 40 to 43-44 cm (3-4 cm)

- Uniform coarse sand. Erosional contact with middle fine grained unit.
-

Middle fine-grained unit – 43 to 44 cm to 46 cm (2-3 cm)

- Burrowed contact with middle sand unit.

Coarse sand unit – 46-59 cm (13 cm)

- Uniform coarse sand. Erosional contact with lower fine-grained unit below.

Lower silt unit – 59-66 cm (7 cm)

- Very dark grayish brown silty mud. Erosional contact with sand below.

Figure 2.3. Photograph of sediment core collected in 2004 near the peeper location. Description of sediment layers corresponding to depth.

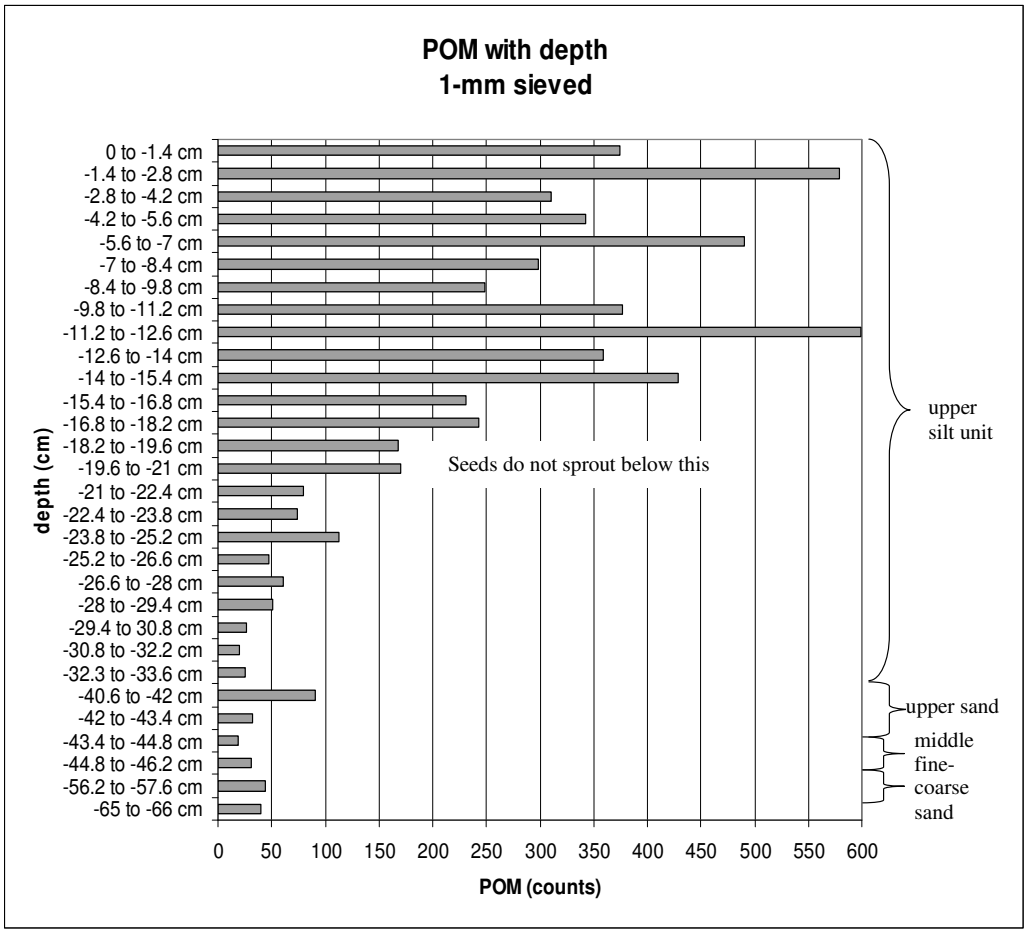

Figure 2.4. Particulate Organic Matter (POM) counts from the >1 mm sieved fraction of the core shown in Figure 2.3. Sand units yielded little or no POM, and therefore, not all sand units from the core were sieved and thus do not appear on this diagram creating a non-linear scale. Analyzed by Lisa Welsh at Geology & Geophysics, TAMU.

Coarse Sand Unit (46-59 cm). The middle fine-grained unit overlies a clean, grey, coarse-grained sand unit, 13 cm thick, referred to as the coarse sand unit. This unit is laterally extensive and the combination of coarse grain size and light grey color make it easy to identify in all cores collected from the wetland (unpublished field data). The contact between the middle silt unit (at the bottom of the transition zone) and the coarse sand unit contains relict burrows. No peeper data were collected below 52 cm in the coarse sand unit.

Lower Silt Unit (59-66 cm). The coarse sand unit overlies an organic-rich silt layer, 7 cm thick, referred to as the lower silt unit. Like the coarse sand unit, the lower silt unit is laterally extensive and was observed in a core collected 5 m from the peeper (unpublished field data). The contact between the coarse sand layer and the lower silt unit is erosional.

Lower Sand Unit (66-76 cm). At the bottom of this core, the lower silt unit appears to have overlain a sandy layer, which was not retained during extraction. In a core collected 5 m from the peeper (unpublished field data), the lower silt unit overlies a fine-grained sand layer, which is at least 14 cm thick, referred to as the Lower Sand Unit.

The silt/sand couplets in these cores record three depositional sequences. We interpret the coarse sand layers as flood deposits and the overlying organic-rich silts as wetland sediments. One implication of this depositional interpretation is that sand units reflect rapid deposition during floods, whereas silt layers may have accumulated slowly over a series of years. The contacts between the sand units and the underlying organic-

rich silt units are erosional; the contacts between the sand units and the overlying organic-rich silt units contain relict burrows indicating the influence of aquatic invertebrates (probably crayfish).

MATERIALS AND METHODS

In Situ Measurements

Water samples were collected during the "wet" spring season in May 2003 from the wetland adjacent to the Norman Landfill using peepers (Hesslein, 1976). Two peepers with 0.45-µm Millipore® membrane[1] were used to obtain vertical profiles of surface water, pore water, and groundwater with a 0.5 to 1 cm-resolution. The peepers have a total of 37 horizontal ports in which, the first 22 ports have apertures and spacing of 0.5 cm followed by 15 ports with apertures and spacing of 1 cm. The peepers span a vertical profile 52 cm deep. This peeper design allows us to obtain discrete water samples at small spatial resolution by limiting the vertical mixing of adjacent water masses during sampling.

Peeper ports were filled with nanopure water (18 mΩ) and deoxygenated with nitrogen for three days to remove oxygen from the water and plastic samplers. Peepers were then transported in an anaerobic PVC-constructed chamber to the site and maintained under deoxygenated conditions until insertion into the wetland sediments. The peepers were positioned in the wetland for 2 weeks (April-May 2003) to allow equilibration and diffusion of solutes between the nanopure water and surrounding pore

water (Azcue et al., 1996; Jacobs, 2002; Webster et al., 1998). The peepers were positioned 40 cm apart in the center of the wetland parallel to groundwater flow at two different depths. In peeper 1 the first 21 cm sampled the water column and the next 29 cm sampled the sediment pore water. Peeper 2 was buried completely in the sediments capturing the sediment pore water down to a depth of 52 cm below the sediment-water interface (0 cm). After two weeks of equilibration, the peepers were retrieved and processed immediately in an anaerobic glove bag filled with an N_2 atmosphere.

From the peeper ports, 12 mL of sample were obtained, 2 mL were used for the analysis of alkalinity, 2.5 mL for dissolved iron, and 3 mL for hydrogen sulfide, and were measured in the field using methods of electrometric Gran titration and colorimetric spectroscopy modified for low sample volumes (APHA et al., 2005). Cations, anions, organic acids, and ammonium were analyzed in the laboratory from 1 mL of water collected for each. Cations were preserved in 1% trace metal grade hydrochloric acid, anions were preserved in 0.5% formaldehyde, organic acids and ammonium were flash-frozen with dry ice and stored. Dissolved oxygen, pH, conductivity, temperature and redox potential were measured at the wetland using a 600 XLM YSI Hydrodata multiparameter meter (Yellow Springs, OH USA).

Capillary Electrophoresis Analyses

An Agilent Technologies capillary electrophoresis (CE) instrument with a photo diode array detector was used for analyzing anions (SO_4^{-2}, Cl^-, NO_3^-, NO_2^-), cations (Ca^{+2}, Mg^{+2}, K^+, NH_4^+, Na^+), and organic acids (acetate, butyrate, oxalate, lactate,

propionate). A 56 cm fused silica capillary was used (50 µm I.D, 150 µM at the detection window). Tapered polypropylene vials were filled with ~30 µL of sample. The samples were injected by hydrostatic pressure followed by a 2 second injection of electrolyte (each injection consumed ~1 nL/sample). The temperature was held constant at 25ºC. Table 2.1 shows the conditions for each analysis.

Saturation Indices

Mineral equilibria were evaluated using saturation indices (SI) calculated with the program PHREEQC-2 (Parkhurst, 1995) and the PHREEQC database. All measured inorganic species were included in the speciation model as were pH and an approximate temperature of 15.9ºC deduced from the measured temperature of the bottom waters. Due to the high concentrations of organic acids found in the system, the alkalinity values obtained from Gran titration (i.e., the total acid neutralizing capacity (ANC)) were corrected for the contribution of organic acids. It has been demonstrated that small chain organic acids contribute to the total titrated alkalinity (Baedecker and Cozzarelli, 1992; Devlin, 1991; Hemond, 1990), and thus uncorrected field data may overestimate HCO_3^- concentrations. Although previous studies have shown a complex relationship between observed alkalinity and organic acid concentration, Baedecker and Cozzarelli (1992) demonstrated that acetate contributed linearly to alkalinity in well-buffered solutions with bicarbonate concentrations of 100 microequivalents. Thus, in the high bicarbonate system of the Norman Landfill wetland, a reasonable correction would be to assume that

Table 2.1. Capillary electrophoresis setup conditions for the analysis of major ions.

Analytes / CE Conditions	**Cl^-, Br^-, NO_3^-, NO_2^-, and SO_4^{2-}**	**Ca^{2+}, Mg^{2+}, Na^+, K^+, Fe^{2+}, and (NH_4^+)[a]**	**Formic, Acetic, Propionic, and Butyric acids**
Buffer Solution	Chromate Electrolyte Solution from Waters	IonPhor Cation DDP Electrolyte Buffer Concentrate from Dionex	Chromate Electrolyte Solution from Waters
Sample detection Wavelength, bandwidth (nm)	325, 10	450, 80	315, 20
Reference detection Wavelength, bandwidth (nm)	375, 40	230, 20	375, 40
Voltage (kV)	10	20	10
Current (μA)	14	300	14
Hydrostatic Injection	35 mbar: 2 second with electrolyte 15 second with sample 2 second electrolyte	50 mbar: 0.1 second with sample 2 second with electrolyte	35mbar: 15 second with sample 2 second with electrolyte
Duration of run (min)	15	10	12
Conditioning between sample runs	5 min. water 5 min. 0.1 N NaOH[b] 5 min. electrolyte solution	5 min. water 5 min. electrolyte solution	3 min. water 3 min. 0.1 N NaOH[b] 5 min. electrolyte solution
Dilution	No dilution	1:10	1:10

[a] Samples were not diluted and the sample injection time was 1 second.

[b] One disadvantage with this method is the use of a NaOH flush between runs. This was added to eliminate memory effects but resulted in rapid degradation of the interior of the fused silica capillaries and thus should be avoided if possible. Other possible rinses to avoid memory effects include using sodium borate or sodium phosphate adjusted to a pH of 9.

the low molecular weight organic acids detected in these waters (acetate, propionate, and butyrate) were titrated in the field. Field alkalinity values were corrected by subtracting the sum of the milliequivalents of acetate, propionate, and butyrate and the remaining alkalinity was assumed to be HCO_3^-. These corrected values were included in the PHREEQC input files used to generate the saturation indices to determine mineral equilibria. It should be noted that a comparison of the SI for calcite, siderite, and mackinawite calculated with corrected and uncorrected alkalinities show that the values were only minimally affected (ex., ~0.1 lower for calcite), even for the samples with the highest observed organic acid concentrations.

RESULTS

Wetland Surface Water Description

The shallow surface water, ~1 meter, was found to be stratified with respect to water parameters such as temperature, redox potential (ORP), oxygen levels, and pH (Table 2.2). A dense layer of aquatic grasses was observed covering the surface water at the end of April 2003 when the peepers were placed in the sediments. At this time, the water column was found to be stratified with high levels of dissolved oxygen at the top of the surface water (covered by grasses) and high pH presumably due to high levels of photosynthesis. Below the plant cover, the oxygen concentrations and pH decreased. In May 2003, when the peepers were retrieved, the vegetation was decaying and the bottom water was anoxic and free of nitrate.

Table 2.2. Parameters of the water column at the time of peepers' insertion.

Water Column	Temperature (°C)	pH	Dissolved Oxygen (mg/L)	Specific Conductivity (µS/cm)
Surface	19.50	8.13	~15.50[a]	1578
Bottom	15.86	7.21	3.09	1742

[a] Reading did not stabilize. Measurements taken near photosynthesizing plants, system was out of equilibrium.

Sulfur

Dissolved sulfate concentrations were high in the water column with a maximum of 646 µM (Figure 2.5). A significant decrease in concentration was observed at the sediment-water interface (0 cm depth, Figure 2.5) from 584 µM to 15.0 µM across a 4 cm interval. This decrease in sulfate at the sediment-water interface is spatially concurrent with an increase in hydrogen sulfide (Figure 2.5). Hydrogen sulfide concentrations were highest at the sediment-water interface (1004 µM) and were, on average, 5.7 times higher in the water column than in the sediments. Within the sediment profile (-1 to -28 cm), sulfate concentrations were low and remain relatively constant (fluctuating from 12 µM to 15 µM), and the average hydrogen sulfide

concentrations were 3 times higher than sulfate concentrations (Figure 2.5). Below -29 cm, sulfate decreased sharply to levels below detection limits (<5 µM) while sulfide gradually increased to a maximum of 257 µM just below the transition to the coarse sand unit (~ -46 cm).

Iron

Fe^{2+} concentrations in the water column were low, with an average of 5 µM (Figure 2.5) except one locally reduced zone at 14 cm above the sediment-water interface, where Fe^{2+} values were 100 µM. At the sediment-water interface, Fe^{2+} concentration increased steeply coincident with the sharp decrease in sulfate (Figure 2.6). With increasing depth in the sediments, ferrous iron generally decreased ranging from 869 µM to 39.0 µM (at -5 to -52 cm). In the upper sediments (-1 to -28 cm), Fe^{2+} concentrations were 46 and 15 times higher than the concentrations of sulfate and sulfide respectively. Below -30 cm, dissolved iron concentrations decreased to the lowest values, concomitant with increased sulfide concentrations.

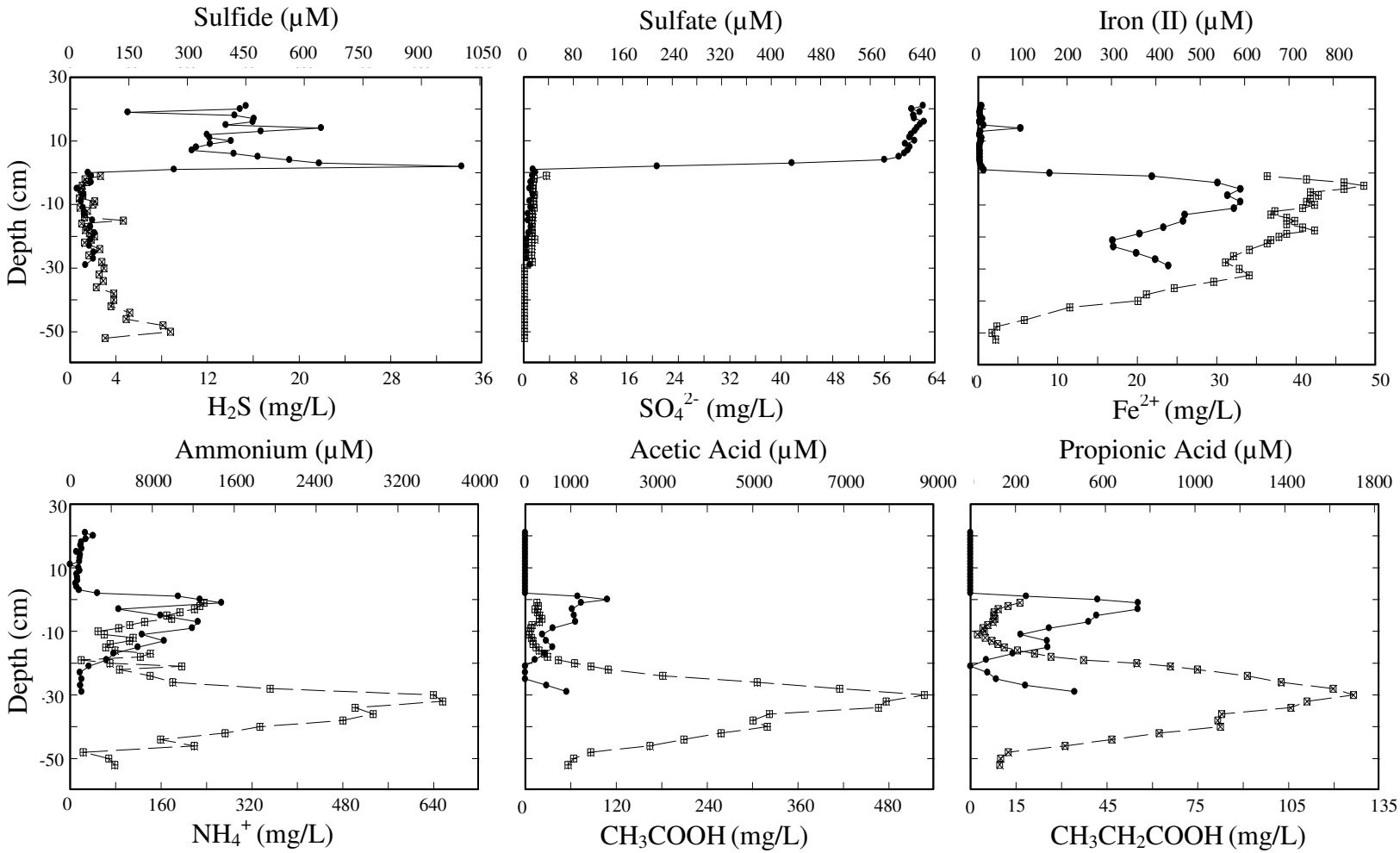

Figure 2.5. Depth profiles for chemical concentrations. A depth of zero represents the sediment-water interface. Peeper 1 filled circles, peeper 2 crossed squares.

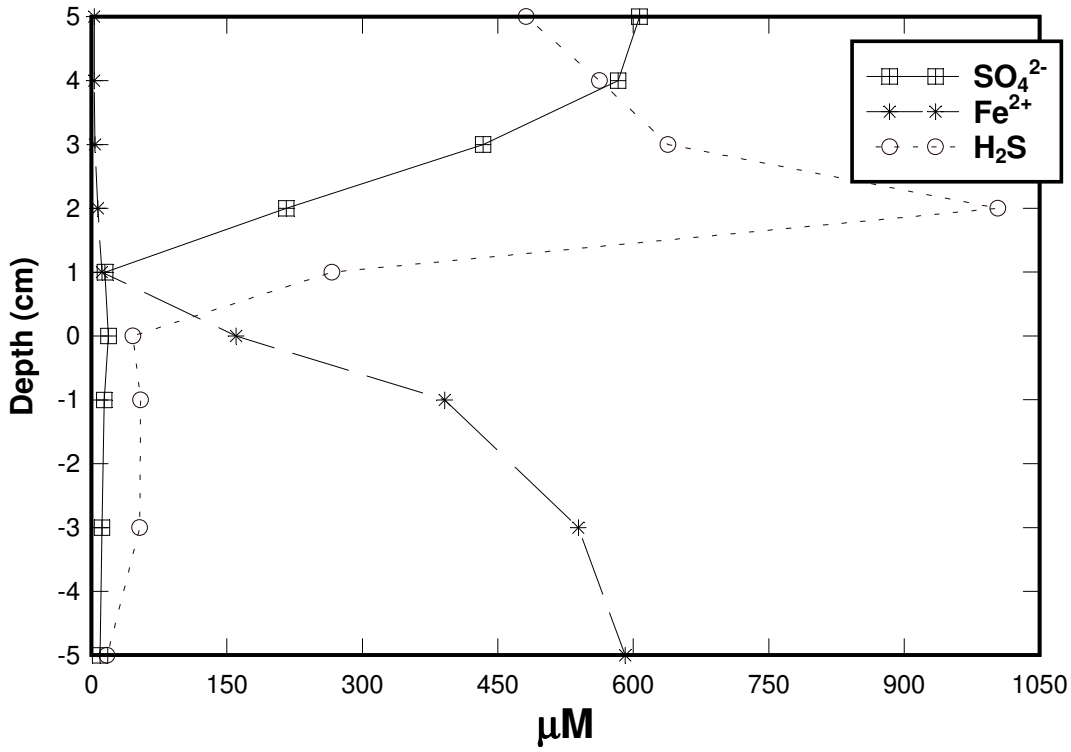

Figure 2.6. Enlarged profile from depth 5 cm to -5 cm showing the concentrations of sulfate, iron (II) and hydrogen sulfide from peeper 1 at the sediment-water interface (zero depth).

Nitrogen

Concentrations of nitrate and nitrite were both below detection limits (9.7 and 13.0 µM respectively) in all samples for both peepers. Elevated ammonium concentrations were found throughout the depth profile and showed significant gradients related to mixing interfaces (Figure 2.5). At the sediment-water interface (0 cm depth), the ammonium gradient reached a concentration of 14.8 mM over 3 cm. Similarly, a second maximum of 36.3 mM is observed at -32 cm over a spatial interval of ~5 cm.

This peak occurs in the lower portion of the upper silt layer just above the transition zone to the coarse sand.

Organic Acids

Waters were analyzed for acetate, butyrate, propionate, oxalate, and lactate. Oxalate and lactate were not detected in the profile. The trends for acetate, butyrate and propionate were similar, although concentrations were greatest for acetate (Figure 2.5). Sharp concentration gradients of organic acids were similar to those observed for NH_4^+. At the sediment-water interface, a peak is observed; acetate reached a high concentration of 1.80 mM, propionate 0.75 mM and butyrate 0.08 mM. A second peak of high organic acid concentrations coincides with the location of the NH_4^+ peak (Figure 2.5) just above the transition zone. Here acetate reached a high concentration of 8.8 mM, and propionate and butyrate reached 1.7 mM. In the coarse sand layer, acetate decreased to a minimum of 0.94 mM, propionate to 0.13 mM, and butyrate to 0.074 mM.

Cl, Cations, pH and Alkalinity

Chloride concentrations gradually increased with depth (Figure 2.7) in both peepers but the overall concentrations were higher in peeper 2 than peeper 1. In peeper 1, the lowest concentration of chloride, ~1.8 mM, was observed in the surface water. Chloride concentrations, increased in the sediments to a maximum of 3.5 mM at 29 cm depth. Concentrations in peeper 2 were 5.1 mM in the upper silt layer and gradually increased to a maximum of 7.4 mM in the coarse sand layer (Figure 2.7).

The pH was highest in the water column (~8.5) and decreased sharply to ~7.5 at the sediment-water interface coincident with the decrease of sulfate. In the upper silt layer the pH values were noisy and have a minimum (~6.9) at approximately the same location as the high concentrations of organic acids (~30 cm) (Figures 2.5 and 2.8). The alkalinity profile shows an oscillating pattern with an average concentration of 15 mM in the water column (Figure 2.8). Within the first 5 cm of the upper silt layer, alkalinity concentrations increased to a maximum of 35 mM. Below this point, oscillating concentrations decreased to 22 mM at ~ 30 cm and fluctuated between 16 mM to 25 mM below this depth (Figure 2.8).

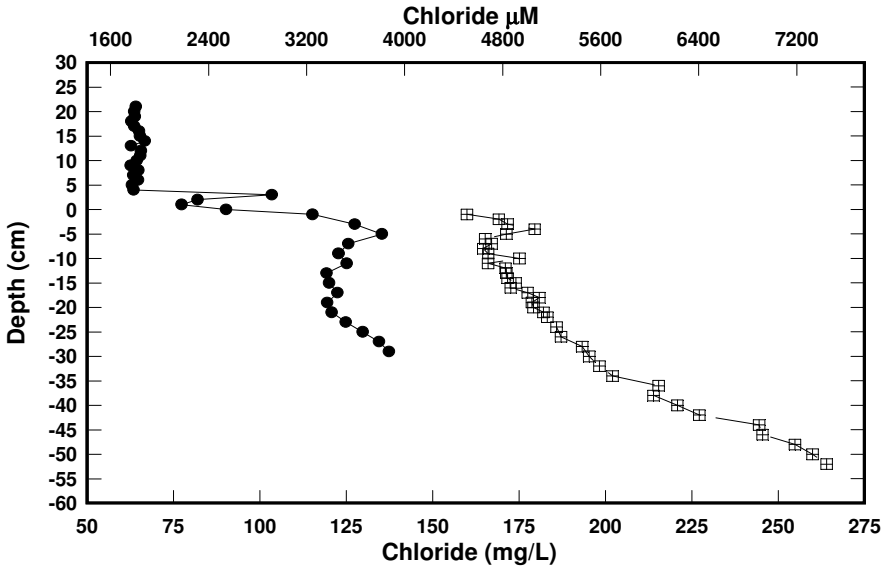

Figure 2.7. Depth profile for chloride. A depth of zero represents the sediment-water interface. Peeper 1 filled circles, peeper 2 crossed squares.

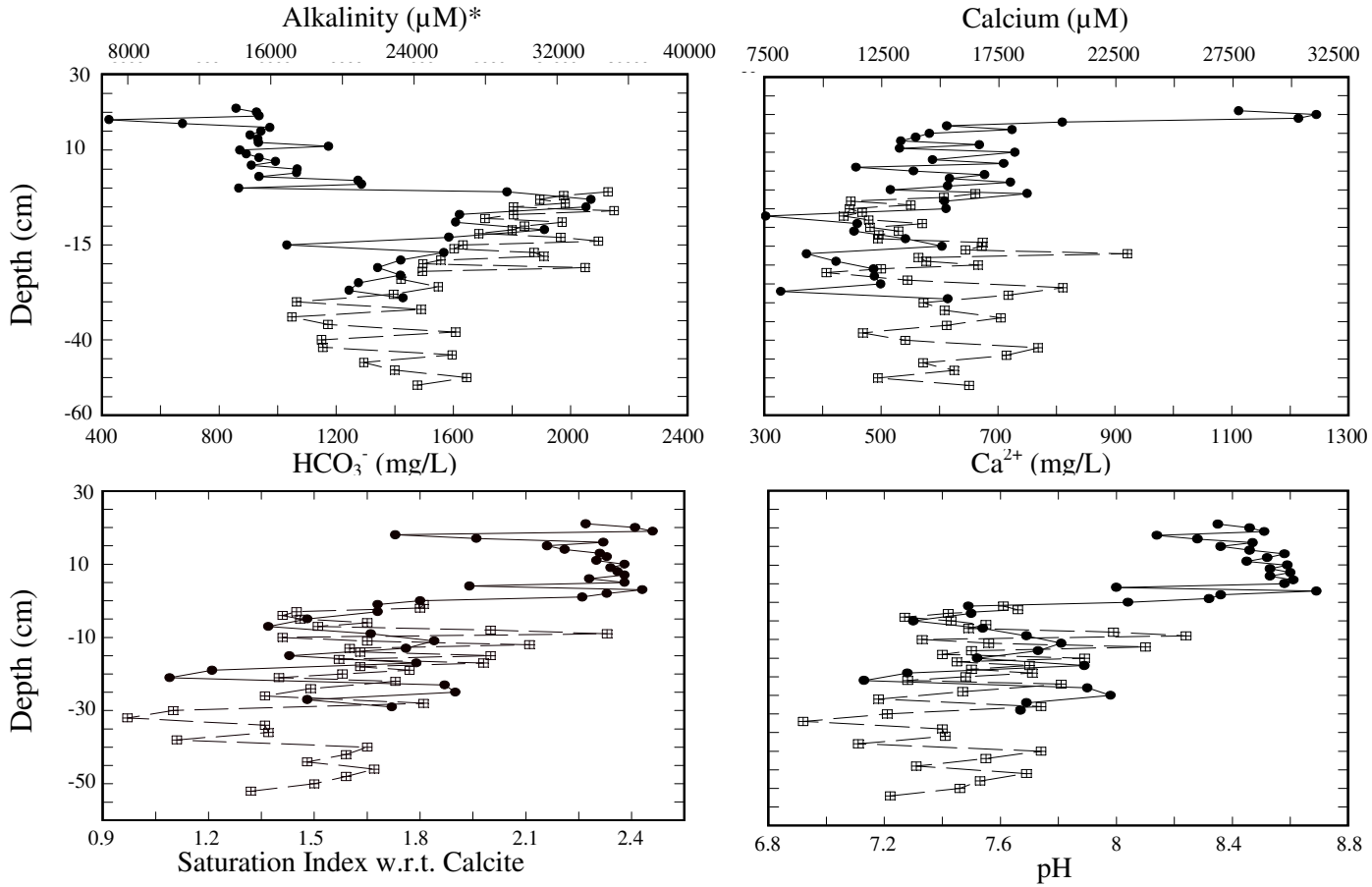

Figure 2.8. Depth profiles for alkalinity, pH, calcium and saturation index with respect to calcite. A depth of zero represents the sediment-water interface. Peeper 1 filled circles, peeper 2 crossed squares. Alkalinity concentrations corrected for the effect of organic acids.

Cation concentrations showed similar cm-scale oscillations and were higher in the water column than in the pore water, with a maximum of 31 mM calcium (Figure 2.8), 12 mM magnesium, 2.2 mM potassium, and 19 mM sodium (data not shown). The highest levels of calcium were observed in the upper portions of the water column near the dense aquatic grasses. Saturation indices (SI) suggest that the entire profile was supersaturated with respect to calcite with average SI values in the water column of 2.3, 1.8 in the upper silt layer, 1.7 in the transition zone, and 1.5 in the coarse sand layer (Figure 2.8). Saturation indices indicate that the water column was undersaturated with respect to siderite, except at 14 cm above the sediment-water interface with an SI of 0.8. The sediments are supersaturated with respect to siderite with values oscillating between 1.6 and 3.0 above 45 cm depth. Below 45 cm depth, SIs decreased to 0.3 (profile not shown).

DISCUSSION

Wetland-Aquifer System

Chloride is a non-reactive anion and has been found to be a good tracer for the presence of water impacted by landfill leachate (Grossman et al., 2002; Röling et al., 2001; van Breukelen and Griffioen, 2004). An observed gradual increase of chloride with depth suggests transport from the underlying landfill leachate into the wetland (Figure 2.7). Both peepers show a similar trend but higher concentrations were observed in peeper 2, which was ~ 40 cm closer to the upgradient bank of the wetland. Overall

concentrations of Fe^{2+} were also higher in peeper 2 perhaps due to the presence of higher concentrations of iron leached from the landfill to be recycled. Because of the reactive nature of iron the trends in Fe^{2+} do not match the trends in Cl^- but suggest that over time the effects of the landfill leachate can be seen in the wetland pore water.

Sulfate, Hydrogen Sulfide, and Iron

The wetland was anoxic and nitrate was absent, making iron and sulfate reduction the most favorable TEAPs at the sediment-water interface. The decrease in sulfate observed at the sediment-water interface (depth 0 cm, Figure 2.5) is attributed to bacterial sulfate reduction as sulfate is considered chemically to be metastable at standard Earth surface temperatures (Nealson, 1997). Sulfate is utilized by sulfate-reducing bacteria as an electron acceptor, which is reduced to hydrogen sulfide to drive metabolism. Because sulfate reduction was occurring in the loose flocculated bottom sediments at the sediment-water interface, it is likely that the sulfide produced was diffusing upward into the water column as observed in the sulfide profile (Figure 2.5). Hydrogen sulfide speciation was evaluated and shows that hydrogen sulfide existed as an ion and not as a dissolved gas. Sulfide concentrations remained high due to the hypoxic nature of the water column (Table 2.2). This is common in meromictic lakes where an oxic/hypoxic stratification in the water column is permanent and hydrogen sulfide diffuses from the bottom sediments into the water column causing a depletion of oxygen (Ciglenecki et al., 2005).

In the sediments, sulfide was present in lower concentrations than in the water primarily due to its high reactivity with Fe^{2+} to form iron sulfides. Saturation indices suggests that the system is supersaturated with respect to mackinawite throughout the profile with higher SIs below the sediment-water interface (2.7-4.1) suggesting that the system precipitated iron sulfides. Iron sulfide minerals including pyrite have been observed at the Norman Landfill site (Breit et al., 2005) and similar environments (Adler et al., 2000; Koretsky et al., 2003). A Spearman's Rank Order Correlation Analysis reveals that sulfide exhibits a significant negative correlation with Fe^{2+} ($r_s = -0.809$, $n = 73$, $p < 0.01$) throughout the profile.

Dissolved iron (Fe^{2+}) in the sediments is a product of the reduction of iron (III) in various forms by abiotic and/or biotic processes. In freshwater aquatic sediments and groundwater at near neutral pH, biotic processes are more important in the reduction of iron (III) than abiotic processes (Lovley et al., 1991). Thus, high concentrations of Fe^{2+} are likely a consequence of the activity of iron reducers (see Figure 2.5 for organic acid and Fe^{2+} concentrations). In addition, the system was supersaturated with respect to siderite. Previous studies have reported waters supersaturated with respect to siderite and authigenic siderite formation in aquifers with active iron reduction (Baedecker et al., 1993; van Breukelen et al., 2004). Examining the profiles in Figure 2.6, an increase in Fe^{2+} is observed just below the decrease in sulfate, near the sediment-water interface. This suggests that either sulfate reduction was occurring above iron reduction in the sediments or sulfate and iron reduction were occurring in the same location but Fe^{2+} is not observed due to precipitation with sulfide. This could be explained by the high

concentrations of organic matter at the sediment-water interface and heterogeneities in the phases of iron oxides being utilized. A study by Cozzarelli et al. (1999a) demonstrated simultaneous occurrence of iron reduction and sulfate reduction for an aquifer contaminated with gasoline. Other studies have documented concurrent dynamics between iron and sulfate reducers. For example, in an acidic lake the availability of sulfate exceeded the availability of reactive iron causing the sulfate reducers to outcompete the iron reducers (Blodau et al., 1998). Blodau et al. found that sulfate reduction and iron reduction occurred simultaneously but higher energy yields were obtained from sulfate reduction than from iron reduction. The result was attributed to low concentrations of bioavailable oxidized iron even though the sediments contained high concentrations of other oxidized iron species. Another study found iron reducers and sulfate reducers existing actively in the same zone (Motelica-Heino et al., 2003). The most unstable iron oxides will be consumed preferentially and the remaining iron oxides become refractory allowing for sulfate reduction. In systems where iron oxides of different stability are present, the boundaries between the zones of iron and sulfate reduction are more diffuse (Postma and Jakobsen, 1996). In our system, the wetland contains high concentrations of sulfate, likely due to dissolution of gypsum naturally present in the Permian rocks (Ulrich et al., 2003), and heterogeneous quantities of iron (Cozzarelli et al., 1999b) with low concentrations of bioavailable iron (Breit et al., 2005). Most of the detectable ferric iron in the aquifer sediments was associated with clays and was very slow to react during reductive dissolution. The reduction of the ferric oxides present in the clay particles was interpreted to be diffusion limited (Breit et

al., 2005). These conditions could allow simultaneous redox reactions at the sediment-water interface. Evidence of the coexistence of iron and sulfate reduction was also observed at 14 cm above the sediment-water interface 100 µM Fe^{2+} and 638 µM sulfide (Figure 2.5). These peaks likely represent a localized anaerobic microzone driven by dense suspended organic material including decaying aquatic grasses. In addition to providing organic matter, the grasses in the water column may serve as a structure on which solid phase iron oxide particles may be present.

In the wetland sediments, the iron and sulfur cycles are linked and trends correlate well to transitions between sedimentary layers (Figure 2.9). Sulfate concentrations were relatively constant with depth (poised at ~15 µM) until 30 cm when a sharp decline to levels below detection limit is observed. Interestingly, changes in sulfate do not correlate with changes in sulfide concentrations (e.g., peaks in sulfide correspond to zones with low/no free sulfate ion). In zones with low/no free sulfate ion, observed sulfide is interpreted to be from either transport processes (i.e., upward movement from the sand layer) or in situ sulfate reduction by bacteria using barite as a sulfate source as has been previously demonstrated at this site (Ulrich et al., 2003).

An increase in hydrogen sulfide (and decrease in Fe^{2+}) occurred below 18cm, the same boundary where seeds were no longer viable and the particulate organic matter concentrations decreased (Figure 2.4). Hydrogen sulfide is generally considered to be toxic to wetland plants (Koch et al., 1990) and may affect seed viability. The increase in H_2S observed in the coarse sand layer (Figure 2.9), may represent an increase in sulfate reduction rates or simply loss of Fe^{2+} from the system through precipitation.

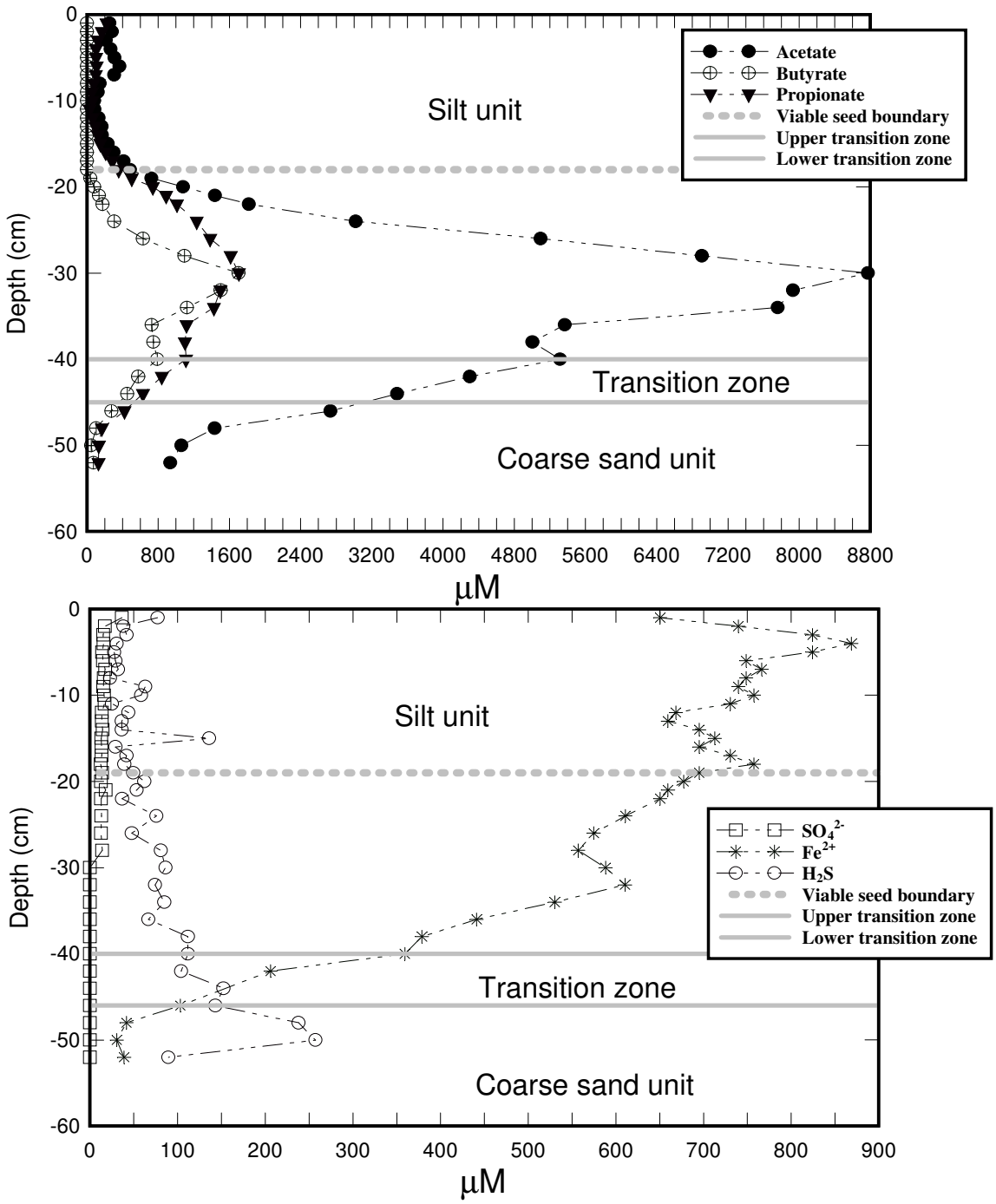

Figure 2.9. Comparison of profiles at peeper 2 for organic acids (top), sulfate, dissolved iron and sulfide (bottom) showing the linkages to the sedimentary units. A depth of zero represents the sediment-water interface.

Organic Acids

Concentrations of organic acids throughout the sediment profile result from the activities of fermentative bacteria (Capone and Kiene, 1988; McMahon and Chapelle, 1991). Fermentative bacteria transform organic substrates to low molecular weight organic acids and hydrogen, which act as electron donors for various terminal electron accepting processes (Ho et al., 2002). Many fermentation products have been studied as indicators of organic carbon decomposition (Ho et al., 2002) and microbial activities (Boschker et al., 1998; Kleikemper et al., 2002). Other studies emphasize the importance of fermentation products on remediation of contaminated subsurface systems (Aulenta et al., 2005). A build-up of organic acids implies that their production exceeds consumption at that location. For example, McMahon and Chapelle (1991) observed that fermentative products were present in greater abundance in aquitard than aquifer sediments related to the availability of electron acceptors.

In this study, high concentrations of fermentation products were found at the sediment-water interface and in the lower portion of the upper silt layer just above the transition zone to the coarse sand. The build up in organic acids (acetate, propionate, and butyrate) at the sediment-water interface is attributed to decomposition of organic material from the wetland (Figure 2.9), such as plant biomass (Kostka et al., 2002). The decay of aquatic grasses provides a source of organic carbon and is likely the trigger for the anaerobic conditions in the surface water. Elevated concentrations of labile organic matter at the sediment-water interface provide the electron donors for iron and sulfate reduction.

The source of the high concentration of organic acids observed above the transition zone (20-42 cm) is uncertain. One possible source is the decomposition of a localized concentration of organic matter. Although, the overall trend of the particulate organic matter found in the core (Figure 2.4) shows a decrease with depth, this does not exclude the possibility that a local organic concentration exists near the peepers given the heterogeneity of the macrobiology in the system. Another possibility is that the organic acids originate from degradation of DOC from the leachate plume. Discharge from the aquifer into the wetland during recharge periods can be a source of DOC to the wetland sediments (Lorah et al., 2007). The gradual increase in chloride concentrations with depth supports that leachate components have migrated upward into the wetland. However, the highest concentrations of DOC (13.3 mM) found in the leachate-contaminated aquifer upgradient from the wetland (Eganhouse et al., 2001) are much lower than the sum of organic acids observed in this study. A likely scenario is that both natural DOC from buried organic matter in the wetland and DOC from leachate contribute to the high acetate concentrations observed.

Below ~18 cm, concentrations of organic acids increase reaching a maximum at ~30 cm due to the low availability of electron acceptors. This is supported by other studies that have shown steep gradients in organic acids associated with abrupt changes in biological activity due to changes in the supply of electron acceptors, temperature, supply of labile organic carbon, or shifts in methanogen population (Cozzarelli et al., 1994; Ho et al., 2002; Shannon and White, 1996). Acetate concentration reaches 8,800 μM, which is 4 times higher than the peak at the sediment-water interface and higher

than levels reported in the literature (Figure 2.9). Studies in diverse sedimentary environments report acetate concentrations such as, 1000 µM in peat bogs (Duddleston et al., 2002; Shannon and White, 1996), 1200 µM (Kostka et al., 2002) and 1600 µM (Hines et al., 1994) in salt-marsh sediments, 60µM (McMahon and Chapelle, 1991) and 500 µM (McMahon, 2001) in aquifer-aquitard sediments, 25 µM in estuarine sediments (Wellsbury and Parkes, 1995), and 10 µM in marine environments (Ho et al., 2002). However, in petroleum deposits low molecular weight organic acids can reach higher concentrations up to 166,500 µM (10,000 mg/L for acetate) (Kharaka et al., 1993).

In addition to finding a steep gradient of organic acids in the upper silt layer, the shape and location of this gradient is also interesting (Figure 2.9). The steep increase in organic acids at 18 cm coincides with the maximum depth of seed viability in the core and with decreased levels of coarse particulate organic matter (Figure 2.4). Loss of seed viability may be a response to increased levels of organic acid in the pore water, as well as increased levels of H_2S. Crop residues have been shown to inhibit seed germination in fields due to high levels of phenolic acid in the soil (Sène et al., 2000). However, almost no data exist on the link between seed viability and the abundance of simple organic acids in wetland soil. The steep increase in organic acids may also signal a change in the quality of particulate organic matter below 18 cm. This is the focus of ongoing studies.

Ammonium and Nitrate

Thermodynamics suggest that nitrate will be one of the first alternate electron acceptors to be utilized by anaerobic bacteria in anoxic aquifers. Nitrate was below detection limits throughout the profiles suggesting that any available nitrate has been consumed and less thermodynamically favorable processes (e.g., sulfate reduction) dominate. The primary nitrogen species in the system is ammonium which originates from both active microbial cycling of wetland organic matter and transport from the landfill leachate plume. Elevated ammonium concentrations were found throughout the sediment profile (Figure 2.5) but generally follow the same trend as acetate, propionate, and butyrate with maximum concentrations at the sediment-water interface and -30 cm depth suggesting a similar source (see "Organic Acids" discussion above). The correlation of NH_4^+ and organic acids is consistent with mineralization of organic matter as noted in other studies (Bally et al., 2004). The high levels of ammonium together with lower pH and higher alkalinities suggest significant organic matter degradation.

Cations and Alkalinity

The alkalinity profile is controlled by TEAPs and mineral precipitation/dissolution reactions. Iron and sulfate reduction increase alkalinity whereas methanogenesis decreases alkalinity (Schlesinger, 1997). In the surface water, alkalinities are lower with the exception of a peak at 14 cm above the sediment water-interface where other TEAP indicators suggest iron and sulfate reduction. At the sediment-water interface, a sharp increase in alkalinity is consistent with the sharp

increase in Fe^{2+} and decrease in sulfate. These trends support the interpretation of active sulfate and iron reduction at 14 cm and at the sediment-water interface. With depth in the sediments, carbonate alkalinity decreases as a result of CO_2 reduction likely by methanogenesis and possible precipitation of carbonate minerals including calcite and siderite. The surface water is undersaturated with respect to siderite with the exception of 14 cm (SI=0.8) and within the silt unit, siderite SIs increase to 2-3 suggesting the system favors precipitation of siderite, which will decrease alkalinity. Saturation indices indicate that the system is supersaturated with respect to calcite (Figure 2.8), however, the extent to which calcite is precipitating is unclear. Calcium concentrations are unusually high throughout the profile (highest concentrations observed in the upper water column near the aquatic grasses). These values may be explained by the high concentrations of organic carbon present in the system. Dissolved organic compounds and humic acids have been shown to inhibit calcite precipitation (Reynolds, 1978) and may explain the system being out of equilibrium.

Vegetation Effects

Aquatic plants floating in the wetland provide an oxygen source to the surface water via photosynthesis. Oxygen levels (~15.9 mg/L) within the top 10 cm of the surface water are supersaturated (theoretical saturation at 20ºC is 10.9 mg/L). Measurements were taken from waters in contact with the aquatic vegetation and high concentrations are attributed to active photosynthesis. Senescence of the thick layer of aquatic grasses leads to decomposition of organic matter coupled to the depletion of

oxygen and other electron acceptors. Jones et al. (2003) suggested that the redox gradient from oxic to anoxic conditions in the water column is influenced by the dynamic activity of aquatic plant cover. The random distribution of aquatic vegetation in the system resulted in microzones of reducing conditions within the water column as evidenced by 1) the increase in ammonium and decrease in sulfate at 20 cm above the sediment-water interface and 2) elevated sulfide and Fe^{2+} concentrations at 14 cm above the sediments.

The input of organic matter from decomposing plants provides abundant electron donors at the sediment-water interface for iron and sulfate reduction. Previous studies found an increase in sulfate reduction rates when a wetland was covered with vegetation (Hines et al., 1989; Koretsky et al., 2005) and demonstrated the influence on redox stratification in the sediments to be more pronounced in the summer than in the winter due to vegetation dynamics (Koretsky et al., 2005).

Calcium carbonate dynamics also appear to be linked to the vegetation in the wetland system. In the upper portion of the water column, where aquatic grasses are abundant, calcium concentrations and calcite SI were at their highest (~31.1mM and 2.4 respectively). This is consistent with the possibility that grasses are playing a role in the cycling of calcium carbonate in the system. Some aquatic grasses such as sago pondweed precipitate calcium carbonate on their leaves, stems and lacunae which can be released to the water upon senescence (Kantrud, 1990).

Scale Considerations

The potential effect of collecting samples at a larger spatial resolution than the cm scale used in this study was evaluated numerically using the acetate concentrations measured in peeper 2 as an example. The concentrations of acetate that would have been observed had samples been collected at intervals of 5 cm or 10 cm *(Cw)* were calculated by:

$$C_w = \frac{\sum Vk_i Ck_i}{\sum Vk_i}$$

where Ck_i is the actual acetate concentrations measured at 1 cm intervals and Vk_i is total volume associated with that concentration. Results show that if samples were collected at 5 cm intervals, the general trend would be the same but the maximum concentration observed would be ~78 % of that observed using 1 cm sampling (Figure 2.10). The use of an even larger sampling interval, 10 cm, results in a substantially different concentration profile with the location of the maximum concentration being shifted ~7 cm lower than the peak concentration shown in the 1 cm profile. In addition, at -30 cm depth, the acetate concentration predicted from the 10-cm sampling interval would be ~60% of that shown in the 1-cm profile (Figure 2.10).

This exercise illustrates the significant impact that the scale of the sampling interval has on the observable concentration profiles in heterogeneous system such as this. Sampling at discrete 0.5-1 centimeter intervals was sufficient to resolve steep gradients observed 1) within the water column (e.g., 0.5 cm peaks in Fe^{2+} and H_2S at 14 cm above the sediment-water interface), 2) at the sediment-water interface (e.g.,

decrease in SO_4^{2-} and increases in H_2S and Fe^{2+} over 4 cm), 3) at major lithologic boundaries within the sediment (e.g. decrease in organic acids in the transition zone to the coarse sand layer over 20 cm), and 4) within the sediment not associated with major lithologic contacts (e.g., ~20 cm peak in organic acids at 30 cm depth within the silt unit; oscillations of carbonate chemistry over 3-4 cm intervals). Although the microbiological processes controlling these gradients likely occur at a smaller (micron) scale, it is clear that resulting chemical dynamics can be resolved at the cm-scale in this system. This suggests that the combined use of small-scale peepers to collect discrete field samples and capillary electrophoresis to conduct complete geochemical analyses on limited sample volumes is a powerful technique for providing new insights into redox dynamics.

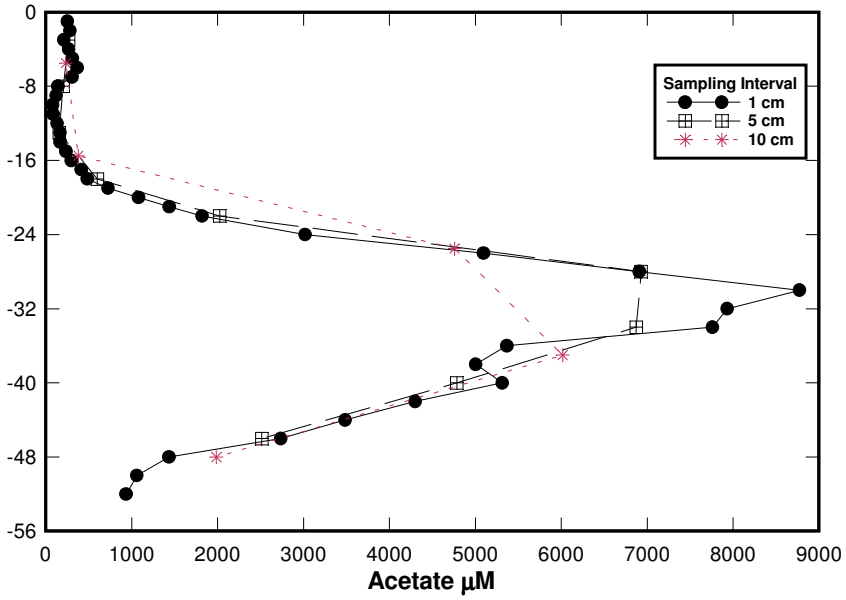

Figure 2.10. Model of acetate concentrations by increasing the sample scale (5 and 10 cm) compared to the acetate concentrations obtained from peeper 2 (1 cm).

CE technology is becoming popular in environmental studies due to the wide range of chemical compounds that can be analyzed even in complex matrices. Some of the applications of CE include: analysis of organic acids in water and air (Dabek-Zlotorzynska et al., 2005; Huang et al., 2005; Wu et al., 2003), analysis of pesticides and pollutants in environmental waters (Frías et al., 2004; Hsieh and Huang, 1996; Molina et al., 1999; Safarpour et al., 2004; Sanchez et al., 2003), analysis of minerals in hydrothermal veins (Voicu and Hallbauer, 2005), analysis of trace metals in water and air (Dabek-Zlotorzynska et al., 2003; Fung and Lau, 2001b; Shakulashvili et al., 2000; Yang et al., 2003), oxyanions in groundwater (Fung and Lau, 2001a), analysis of tracers in brine (Kleinmeyer et al., 2001), separation and quantification iron species (Rennert and Mansfeldt, 2005; Seidel and Faubel, 1998), bromide and nitrate in seawater (Mori et al., 2002), nitrogen species (Yao and Xu, 2002), sulfur species (Chen and Naidu, 2003). Given these advances, the combined use of peepers and CE have applications to a wide range of biogeochemical questions at small scales and can provide insights into linkages between microorganisms, minerals and aqueous solutions. Modifications to field sampling designs could allow resolution of gradients at even finer spatial resolution than presented here.

SUMMARY

Steep geochemical gradients indicating zones of significant biogeochemical cycling were observed at sediment interfaces within a wetland-aquifer system. Both the sediment-water and silt-sand interfaces appear to be contact zones between waters of different redox potential. At the sediment-water interface, the more oxidizing surface water is a source of electron acceptors to the anoxic wetland sediments while the wetland sediments supply organic acids to serve as electron donors. Similarly, the interface between the upper silt zone and less reducing coarse sand lens mark the contact between zones of differing redox potential. In these unique zones microbial metabolism is enhanced because it benefits from the mixing of electron donors and electron acceptors. Centimeter-scale sampling allowed for resolution of steep geochemical gradients (sulfate, iron, sulfide, ammonium, acetate, propionate, and butyrate) supporting the idea that increased microbial activity occurs over small spatial scales at mixing interfaces. This resolution was made possible by the use of capillary electrophoresis (CE) to analyze the majority of geochemical parameters on the low sample volumes available in cm-scale pore waters. Data provided in this paper indicate that CE is a powerful tool to quantify geochemical indicators in complex natural waters when sample volumes are limited and suggest that the combination of custom peepers and CE could be used to evaluate geochemical gradients at even finer spatial resolution.

At the sediment-water interface the dominant TEAPs, sulfate and iron reduction, were enhanced by the senescence of an aquatic grass cover. Both processes appear to be occurring at the same location or in reversed thermodynamic order (i.e., sulfate reduction

above iron reduction). These trends can be explained by the abundant electron donors present at the sediment-water interface and by the possible limited availability of reactive iron compared to the availability of sulfate. Below 18 cm, a change in the organic carbon distribution is evidenced by a sharp increases in the concentration of organic acids, loss of viable seeds, and enhanced sulfate reduction (likely of both free sulfate and barite). At ~30 cm, sulfate decreases to below detection limits allowing organic acids and ammonium to accumulate to high levels reaching 36,000 μM NH_4^+ and 9,000 μM acetate. Below this point, these electron donors decrease coincident with the transition to the coarse sand unit. Supersaturated conditions with respect to calcite were observed throughout the profile, and were highest in the water column where more calcium and higher pH were observed likely due to the presence of aquatic vegetation.

This study documents significant centimeter-scale biogeochemical gradients at various mixing interfaces between a wetland and aquifer contaminated with landfill leachate. These results suggest that quantifying the redox reactions occurring at these relatively small interface zones may be critical to assessing overall biogeochemical cycling in aquifer systems. Inclusion of these active zones in conceptual and numerical models of anaerobic systems would improve understanding of the controls on chemical fate and transport, including the ability of systems to naturally attenuate pollutants. To further quantify the importance of interface processes on system-scale biogeochemical cycling, more detailed knowledge of the spatial and temporal variability of these zones and the rates of various TEAPs should be acquired.

CHAPTER III

DETERMINATION OF DOMINANT BIOGEOCHEMICAL PROCESSES IN A CONTAMINATED AQUIFER-WETLAND SYSTEM USING MULTIVARIATE STATISTICAL ANALYSIS*

SYNOPSIS

Determining the processes governing aqueous biogeochemistry in a wetland hydrologically linked to an underlying contaminated aquifer is challenging due to the complex exchange between the systems and their distinct responses to changes in precipitation, recharge, and biological activities. To evaluate temporal and spatial processes in the wetland-aquifer system, water samples were collected using cm-scale multi-chambered passive diffusion samplers (peepers) to span the wetland-aquifer interface over a period of three years. Samples were analyzed for major cations and anions, methane and a suite of organic acids resulting in a large dataset of over 9,700 points, which was evaluated using multivariate statistics. Principal Component Analysis (PCA) was chosen with the purpose of exploring the sources of variation in the dataset to expose related variables and provide insight into the biogeochemical processes that control the water chemistry of the system. Factors scores computed from PCA were

*Reproduced with permission from Baez-Cazull, S.; McGuire, J.T.; Cozzarelli, I.M.; Voytek, M.A. Journal of Environmental Quality 2007 in press.

mapped by date and depth. Patterns observed suggest that 1) fermentation is the process controlling the greatest variability in the dataset and it peaks in May; 2) iron and sulfate were the dominant terminal electron accepting processes in the system and were associated with fermentation but had more complex seasonal variability than fermentation; 3) methanogenesis was also important and associated with bacterial utilization of minerals as a source of electron acceptors (e.g. barite $BaSO_4$); and 4) seasonal hydrological patterns (wet and dry periods) control the availability of electron acceptors through the reoxidation of reduced iron-sulfur species enhancing iron and sulfate reduction.

INTRODUCTION

Biogeochemical dynamics in sediments are controlled by linked biological, physical and chemical processes including hydrologic fluctuations, seasonal changes in temperature and biological activity, and rock-water interactions (Aller et al., 1998; Dahm et al., 1998; Donahoe and Liu, 1998; Eser and Rosen, 1999; Kemp et al., 1992; Koretsky et al., 2003; Neubauer et al., 2005). These factors interact to create different hydrochemical facies that change temporally and spatially (Thyne et al., 2004). Variability in type and concentration of organic matter, availability of electron acceptors, chemical composition of the lithology, biological activity, and hydrogeologic conditions of the system will determine fluctuations in the redox reactions occurring in situ (Koretsky et al., 2003) including aerobic respiration, nitrate reduction, iron/manganese

reduction, sulfate reduction and methanogenesis. These reactions occur in sequential order according to thermodynamic energy yields (Champ et al., 1979; Froelich et al., 1979; Megonigal et al., 2004), however, in dynamic environments such as wetlands and anaerobic aquifers these processes are linked and can coexist reflecting the complexity of the system. In biogeochemical studies, these processes are often interpreted from the analysis of geochemical parameters such as redox couples (e.g. H_2S and SO_4^{2-}). One caveat with this approach is that many geochemical parameters are affected by multiple hydro-bio-geo-chemical processes. Thus to interpret processes, it is important to determine the correlations between parameters to identify the contributing process(es) for each parameter. These correlations can then give insights into the dominant biogeochemical processes in space and time within a system.

In a wetland-aquifer system the distribution of redox processes responds to solute transport processes, biological activities, and solid phase composition which can vary on small spatial scales (Brune et al., 2000; Hunt et al., 1997; Kappler et al., 2005). Hydrologic fluctuations, such as aquifer recharge, provide a mechanism for the delivery of electron acceptors or electron donors to a discrete zone. The availability of these transported solutes (e.g., electron donors and acceptors) can enhance microbial activity and in turn result in microbial community shifts. Biological activities are also impacted by seasonal changes in vegetation growth, which exert an important control on redox processes, for example in root zones oxygen is introduced increasing the availability of electron acceptors (Neubauer et al., 2005). In addition vegetation is a primarily source of organic carbon to the wetland sediments. Heterogeneities in the solid-phase

composition (ex. distribution of Fe-oxide minerals) provide another source of heterogeneity in the distribution of redox processes. Superimposed on the spatial variability in redox processes are temporal fluctuations driven by seasonal dynamics and recharge events (Chapelle et al., 1995; Eser and Rosen, 1999; McGuire et al., 2000; Seybold et al., 2002). Therefore, gathering the necessary data to describe the controls on biogeochemical cycling at appropriate spatial and temporal scales generally results in large, complex datasets that are difficult to interpret (Hunt et al., 1997). Often expected relationships cannot be easily discerned in geochemical datasets due to the effects of multiple processes on a single geochemical indicator. Multivariate statistical analyses can provide details on the correlations between parameters often revealing obscured relationships between hydro-bio-geochemical parameters to potentially give new insights into the processes controlling the variability in the dataset.

Since 1901, when first introduced by Spearman, principal component analysis (PCA) has routinely been applied in a wide variety of fields in the natural and social sciences. Its primary function is to explore complex datasets of many dimensions, collapsing many variables, based on their correlations, to a few factors that explain the observed variability and thereby reveal underlying data structure and highlight relationships between the variables. Although the analysis does not provide a mechanism or demonstrate causality, it does provide a quantitative measure of relatedness of variables to one another that can be suggestive of the underlying processes controlling the variability in the dataset (Kumar et al., 2006; Mathes and Rasmussen, 2006; Thyne et al., 2004; van Helvoort et al., 2005). Recent studies that have used PCA

analysis to interpret geochemical datasets include: delineation of groundwater contamination potential (Mathes and Rasmussen, 2006; Xie et al., 2005), identification of hydrogeochemical processes (Kumar et al., 2006; Liu et al., 2003; Thyne et al., 2004), characterization of fluvial deposits (van Helvoort et al., 2005), identification of contaminated aquifer zones (McGuire et al., 2005; Suk and Lee, 1999), and hydrologic effects on trace metal geochemistry (Farnham et al., 2003; van Griethuysen et al., 2005). Generally, variability in water-chemistry parameters have been associated with linked biogeochemical processes such as microbiological reactions, abiotic reactions, macro-biological seasonal activities (e.g., vegetation growth in a wetland), groundwater contamination, hydrologic fluxes, mineral dissolution, anthropogenic influence, recharge area (precipitation), climate, and topography (Thyne et al., 2004). Knowledge of the extent to which these factors are important and the scale at which they occur is essential to understanding elemental cycling in natural systems, and multivariate statistical analysis is the preferred technique for discerning these controls. In addition, mapping of factors scores obtained from PCA is useful for describing the spatial and temporal components of the dataset (Mathes and Rasmussen, 2006; McGuire et al., 2005; Suk and Lee, 1999).

The system discussed in this paper consists of a seasonally submerged wetland hydrologically connected to a regional aquifer impacted by municipal solid-waste landfill leachate located in Norman, Oklahoma, USA. Wetlands (both natural and constructed) have been studied for their "water-quality function" specifically their ability to retain and transform nutrients and metals (Hunt et al., 1997). Understanding the

dominant biogeochemical processes in wetlands is critical to assess the water-quality function. The most biogeochemically active zone of a wetland is near the surface, where the system is susceptible to changes in temperature, precipitation, infiltration, and nutrient loading (Hunt et al., 1997). In addition, other interfaces with depth have been identified as important zones of biogeochemical cycling in a wetland-aquifer system (Baez-Cazull et al., 2007a). From the hydrochemical viewpoint, a wetland functions both as an interface zone for water exchange between groundwater and surface water, and as a biochemical filter through which water quality changes greatly (Dahm et al., 1998). Water from infiltration, migration, and the waste itself produces leachate as moisture passes through the waste in the landfill. Leachate can contain an undesirable mix of toxic organics and inorganic chemicals. Wetlands are complex sediment matrices that are organic-rich and provide chemical and biological conditions conducive to the removal of contaminants from the leachate plume as it moves into and through the system. The complex linkages between the wetland and the underlying leachate-contaminated aquifer make determining the dominant biogeochemical processes a challenge. A previous study on the spatial vertical variations in the system (Baez-Cazull et al., 2007a) found sharp geochemical gradients at small (centimeter) scale associated with lithological, hydrological, and chemical interfaces. Subsequent field studies to tease out these relationships have resulted in a large spatial and temporal dataset containing cm-scale depth profiles of water-chemistry parameters at a single location over 3 years. Complex and variable solute transport pathways, heterogeneous distribution of solid phase minerals (acting as electron acceptors, nutrients, etc.),

microbial growth and decay, and seasonal variations in temperature, recharge, and macrobiology are all linked controls on the biogeochemical cycling of the system (Baez-Cazull et al., 2007a; Breit et al., 2005; Cozzarelli et al., 1999b; Koretsky et al., 2003; Kostka et al., 2002; Scholl et al., 2005; Weiss et al., 2004).

This paper describes the dominant biogeochemical processes operating in a linked wetland-aquifer system over space (cm-scale depth profiles) and time (study duration of 3 years). Multivariate statistics were used in conjunction with traditional graphical and modeling techniques to explore the more than 8,000-point dataset to expose significant relationships among geochemical parameters and evaluate changing processes. The use of PCA for exploring parameter correlations and the mapping of factor scores improved the understanding and interpretation of processes controlling the surface water and groundwater composition affected by seasonal changes and hydrologic fluctuations. This study demonstrates the value of using multivariate statistics to reveal previously obscured biogeochemical relationships and enhance understanding of complex system dynamics.

MATERIALS AND METHODS

Site Description

The wetland (slough) is situated in the Canadian River alluvial plain in central Oklahoma (Figure 3.1), and formed in a previous location of the main channel of the Canadian River (Schlottmann, 2001). The geologic setting is characterized by

moderately permeable alluvial and terrace deposits with a shallow water table that overlies a Permian shale and mudstone confining unit known as the Hennessey Group (Scholl and Christenson, 1998). The slough acts as a surface expression of the local water table with some lateral flow during the wet season due to minor inputs upstream. It is fed by groundwater discharge, runoff, and precipitation. Water levels vary seasonally ranging from approximately 1 m deep in the spring to dry in the summer (Figure 3.2). Upper sediments have been variably saturated during the summer months. The area surrounding the wetland is densely vegetated, dominated by *Phragmites*, *Leersia* and *Phalaris* and with at least three species of phreatophytes (willow, cottonwood, and tamarisk) (Christenson et al., 1999). The growing season is from mid-April through October. The wetland is approximately 700 m long and 15-25 m wide and is downgradient from the Norman municipal landfill (50-100 m from the edge).

The surficial sediments of the wetland consist of alternating units of fluvial silt and sand described in Baez-Cazull et al. (2007a). A cross section of the wetland (slough) is shown in Figure 3.3. The upper 40 cm consist of an organic-rich silt unit. Particulate organic matter, such as plant fibers, seeds and insect parts is most abundant in the upper 10 cm and generally decreases with depth. Underlying the silt unit (41-44 cm) is a transitional zone containing medium to coarse-grained sand interbedded with organic-rich silt lenses. Below the transitional zone is a distinct coarse sand unit located 45 to 60 cm below the sediment-water interface, which is underlain by a 7 cm thick organic-rich silt unit. Below this silt unit there is another coarse grained sand layer. The silt/sand couplets in these cores record three depositional sequences. The coarse sand

layers are flood deposits and the overlying organic-rich silts originate from wetland sediments.

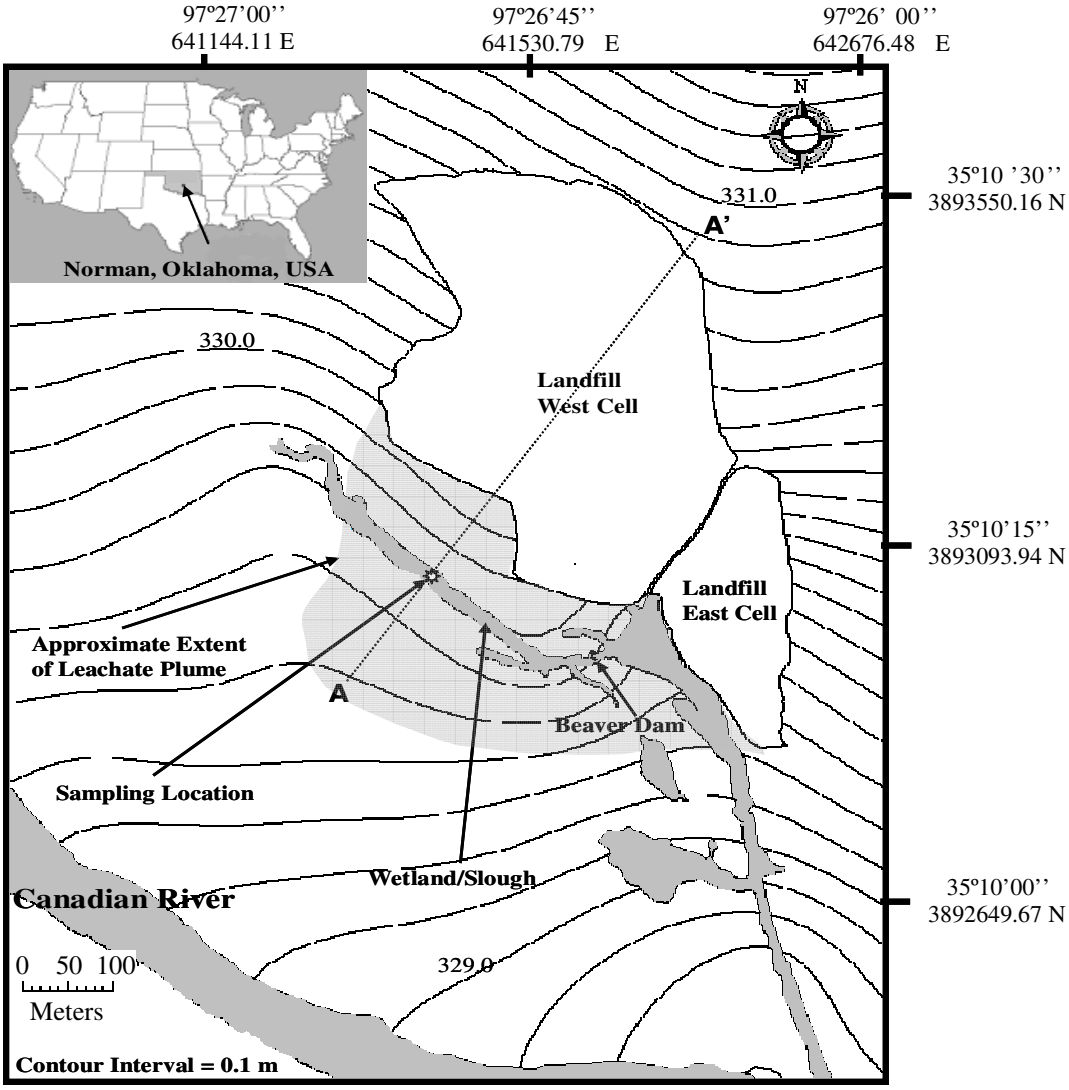

Figure 3.1. Map of the Norman Landfill site in Oklahoma, U.S., showing sample location for 2003-2005. Star symbol indicates approximate location of USGS (U.S. Geological Survey) well SI 102. Potentiometric lines shown. Modified from Scholl and Christenson (1998). Coordinates projected in UTM, zone 14 N, datum NAD 1983.

a.

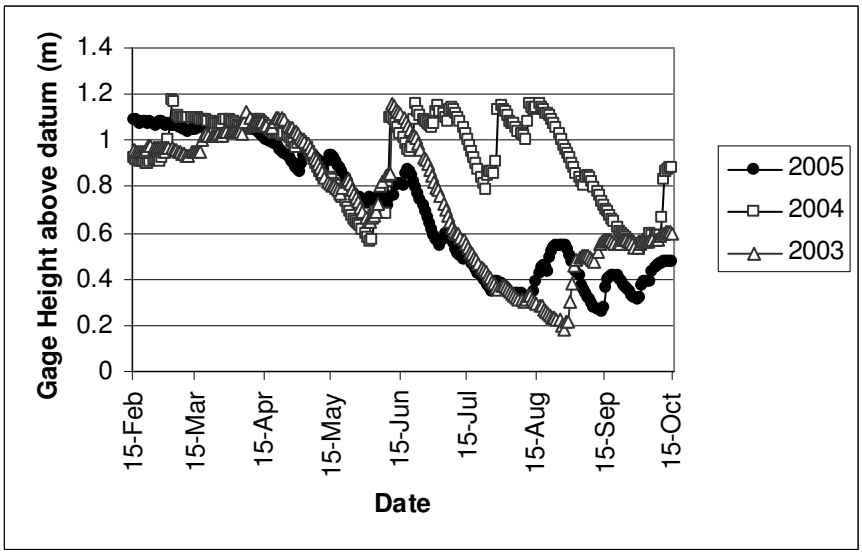

b.

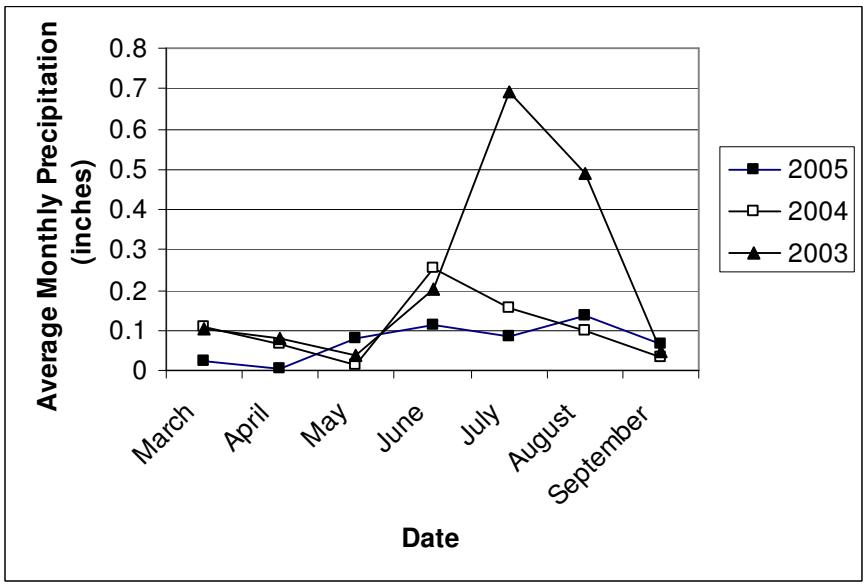

Figure 3.2. a. Water levels recorded for the three years when the peepers were collected. b. Average monthly precipitation data collected from March through September during 2003, 2004, and 2005. Data obtained from USGS Water Resources of Oklahoma (2007).

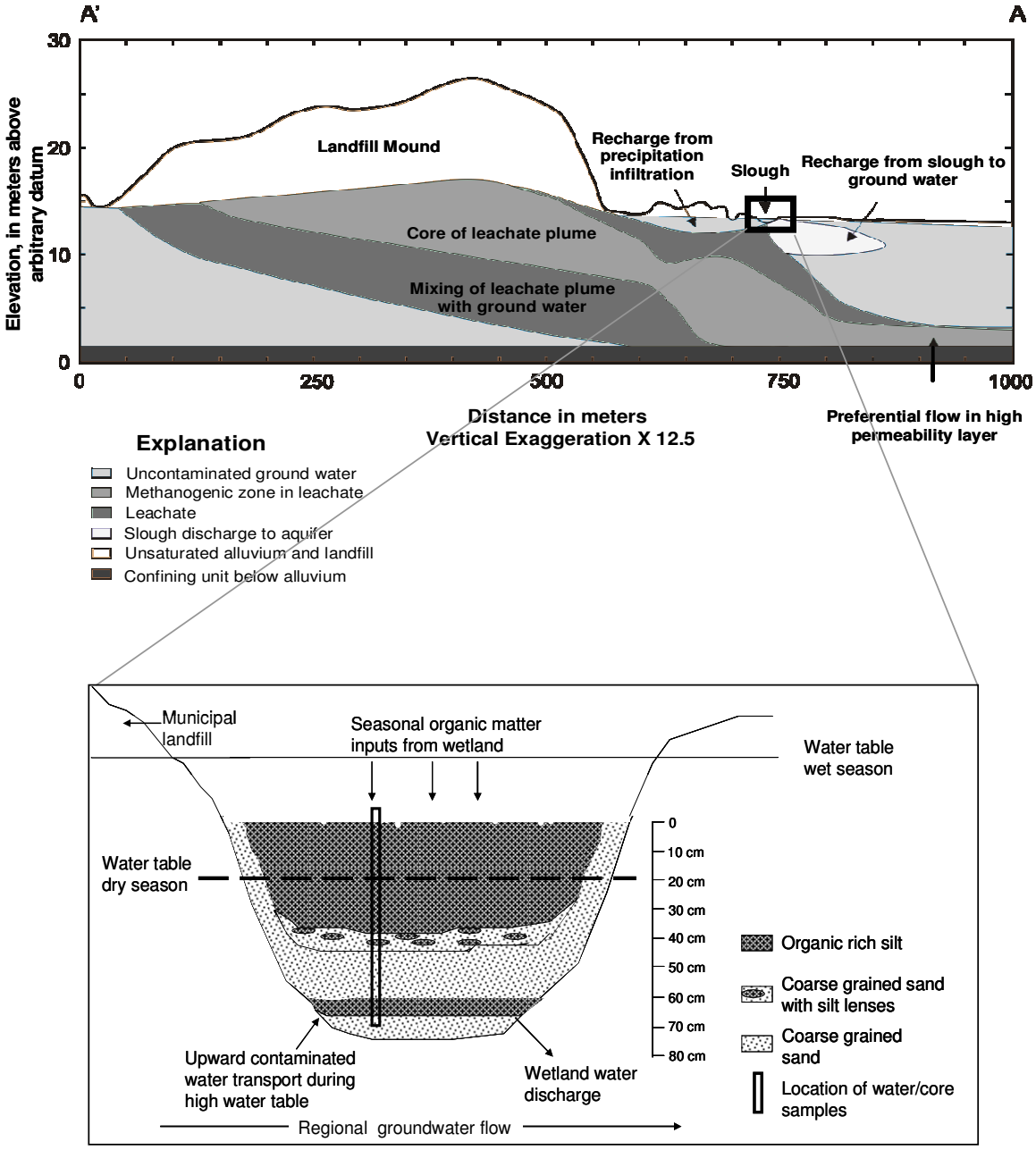

Figure 3.3. Cross-sectional view of the Norman Landfill along section A-A' (as shown in Figure 3.1) and larger cross sectional view of the wetland's conceptual model. The leachate plume and recharge zones are drawn on the basis of chemistry measurements made in the aquifer between 1997 and 2002 (from Scholl et al., 2005).

The Norman Landfill was a municipal non-restricted solid-waste landfill that operated from 1922 to 1985 in the city of Norman, OK. Leachate from the unlined landfill resulted in a groundwater plume that extends downgradient approximately 250 m from the landfill toward the Canadian River. The hydraulic conductivity is estimated to range from $7.3x10^{-2}$ to $2.4x10^{1}$ meters per day and the plume flows directly beneath the wetland (Scholl and Christenson, 1998). Since 1995, the Norman Landfill has been the site of active, ongoing investigations into the biogeochemistry of the plume as part of the U.S. Geological Survey Toxic Substances Hydrology Program. Recent studies at the site have reported evidence that the wetland sediments provide an interface between the underlying contaminated aquifer and the wetland surface water. With access to a supply of electron donors and acceptors the system can provide loci for enhanced degradation of contaminants. Lorah et al. (2007) demonstrated the spatial and temporal link between redox conditions in the wetland sediments and fluctuations in groundwater/surface-water levels. Generally, during periods of high recharge, the upgradient bank of the slough had higher concentrations of leachate constituents including ammonium, dissolved organic carbon, iron, and bicarbonate which were found in the top 60 cm of the wetland-sediment pore water compared to low recharge periods, indicating that leachate contaminated groundwater discharged into the wetland. Scholl et al. (2005) also observed that exchange between the wetland and shallow groundwater was episodic and that shallow groundwater downgradient from the wetland contained, on average, 29 percent wetland water during periods of high recharge. An additional study by Bruner et al. (1998) supports the connection between the contaminated aquifer and the wetland

surface water. In the study, Bruner et al. (1998) used FETAX (Frog Embryo Teratogenesis Assay-Xenopus) to evaluate the developmental toxicity of ground water collected from a network of wells in the shallow unconfined aquifer downgradient from the landfill and in surface water from the wetland. Groundwater samples were highly toxic in the area near the landfill and surface water samples from the wetland demonstrated lower but still elevated developmental toxicity. This toxicity was temporally variable and was significantly correlated with weather conditions. A generalized conceptual model showing the connection between the wetland (slough) and surrounding aquifer is shown in Figure 3.3.

In Situ Measurement

Surface and pore-water samples were collected from the wetland (slough) adjacent to the Norman Landfill site in May 2003 (*P1-May-03 and P2-May-03*), March 2004 (*P1-Mar-04, and P2-Mar-04*), April 2005 (*Pa-Apr-05, Pi-Apr-05*), May 2005 (*P-May-05*), and September 2005 (*P-Sept-05*) (Figure 3.4). Water samples were collected using multi-chambered equilibrium dialysis frames (‘‘peepers’’) (Hesslein, 1976). Custom peepers were designed to span a vertical profile of 75 cm capturing the sediment-water interface as well as interfaces across the wetland- aquifer transition zone with a total of 75 horizontal ports with apertures and spacing of 0.5 cm covered by a Millipore® membrane with a pore size of 0.45 μm.

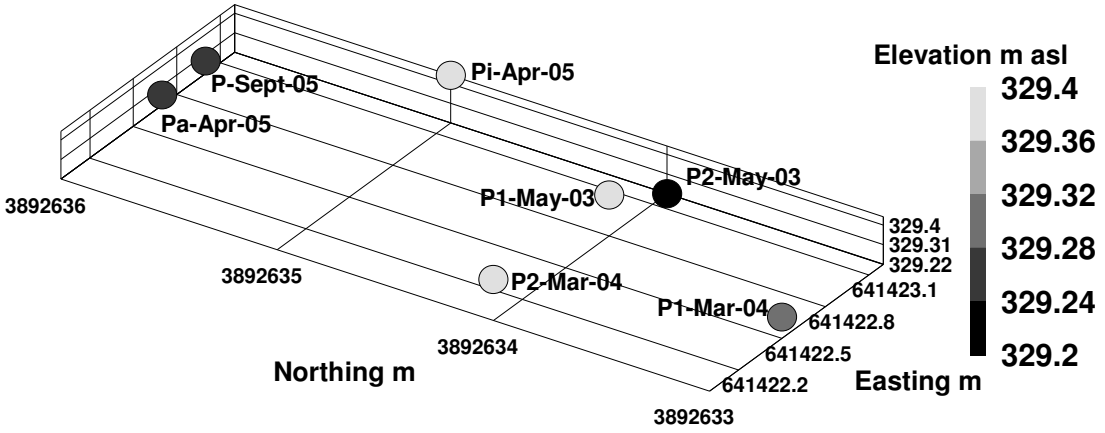

Figure 3.4. Location of peeper deployment (all near USGS well SI 102, see figure 3.1). Exact peeper location in May 05 was not surveyed but was deployed very near P-Sept-05. Coordinates projected in UTM, zone 14 N, datum NAD 1983, vertical datum GEOID 99.

The peeper design allowed us to obtain discrete water samples at small spatial resolution by limiting the vertical mixing of adjacent water masses during sampling. Peeper ports were filled with nanopure water (18 mΩ) and deoxygenated with nitrogen for three days to remove oxygen from the water and plastic samplers. Peepers were transported in an anaerobic PVC-constructed chamber to the site and maintained under deoxygenated conditions until deployment into the wetland sediments. The peepers were positioned in the center of the wetland parallel to groundwater flow near the USGS well SI 102 (Figure 3.1) and were left in place for approximately 2 weeks to allow

equilibration and diffusion of solutes between the nanopure water and surrounding pore water (Azcue et al., 1996; Jacobs, 2002; Webster et al., 1998). After two weeks of equilibration, the peepers were retrieved and processed immediately after collection in an anaerobic glove bag filled with an N_2 atmosphere.

Geochemical Analysis

Geochemical parameters collected during the three year sampling period represent indicators of biotic and abiotic redox process, as well as indicators of landfill leachate measured with the purpose of understanding biogeochemical process in the wetland-aquifer system. Dissolved oxygen, pH, conductivity, temperature, and redox potential were measured using a 600 XLM YSI Hydrodata multiparameter meter* (Yellow Springs, OH USA). Alkalinity, was measured in the field using electrometric titration. Fe^{2+} and H_2S were also measured in the field using a modified phenanthroline and methylene blue photometric methods (APHA et al., 2005). Cations (Na^+, K^+, Ca^{2+}, Mg^{2+}, NH_4^+) were preserved in 1% metal grade hydrochloric acid, except for ammonium which was flash frozen with dry ice, and analyzed by capillary electrophoresis (CE) (Agilent Technologies, Germany) (Baez-Cazull et al., 2007a).

Some elements were also measured by inductively coupled plasma – mass spectrometer (ICP-MS); these included Mn, Ba, Fe, and Na, K, Ca, Mg collected in 2005. The ICP-MS does not distinguish between species; therefore, cations analyzed by ICP-MS are expressed as elements. Anions (SO_4^{2-}, Cl^-, and NO_3^-) were preserved in 0.5% formaldehyde and analyzed by CE. Organic acids such as propionate, acetate,

butyrate, oxalate and lactate were flash-frozen with dry ice and analyzed in the laboratory by CE. Water samples for measurement of CH_4 concentrations were collected in Glasspak syringes that were connected directly to the sample-pump outlet (Baedecker and Cozzarelli, 1992). The water samples were transferred from the syringe into 25-mL serum bottles flushed with He. Water samples for dissolved organic carbon (DOC) analyses were filtered in line through a 0.45 µm filter, collected in a baked glass bottle, and acidified with H_3PO_4 to a pH of 2. DOC was measured by high temperature combustion techniques following the method of Qian and Mopper (1996). Formate and benzoate were determined on samples collected raw and kept frozen until analyzed by ion chromatography.

Data Analysis

The data were analyzed with multivariate factor analysis using SAS software JMP® (SAS Institute, 1999). The geochemical data arranged in R-mode factor analysis included: acetate, propionate, methane, ammonium, sulfate, pH, Na, K, Ca, Mg, Fe^{2+}, Cl^-, HCO_3^-, H_2S, butyrate, Mn, Ba, Fe^{3+}(Total iron – Fe^{2+}), and DOC. Because the data collected for 2003 and 2004 did not include DOC, CH_4, Ba, Fe^{3+} and Mn, these parameters were excluded from the first PCA, which includes all sampling periods. Nitrate, formate, and benzoate were not included in any of the analyses because over 90% of the data were below detection limits (Farnham et al., 2003; Güler et al., 2002; van Helvoort et al., 2005). The complete dataset was tested for normality using various mathematical transformations, such as the natural logarithm, square root, inverse and

power transformations. For each of the transformations, the data were tested for normality by evaluating boxplots, normal quantile plots (Q-Q plots of expected normal value vs. observed value), and Kolmogorov-Smirnov (K-S) tests for goodness of fit. The K-S tests resulted in *p* values less than 0.0001 for all the parameters except for alkalinity, which fit a normal distribution with the natural log transformation. For all the other parameters, the null hypothesis for the K-S test (data exhibiting a normal distribution) had to be rejected. As a result of the non-normal distribution, conservative nonparametric statistical tests were chosen. In order to avoid problems with the differences in scale among the chemical parameters, the data were standardized using z-scores (Güler et al., 2002; Thyne et al., 2004). A nonparametric Spearman's Rho correlation analysis was performed on the standardized data. A pairwise correlation matrix was selected to exclude cases with missing data. A factor analysis was performed on the correlation matrix using the standardized dataset.

Factor Analysis

A principal component analysis was performed to determine the factors that best explain the variation in the dataset. Factors were rotated using varimax orthogonal rotation to maximize the relationship between the variables and some of the factors. Factor scores were computed from the selected factors for each case and the variability was plotted by location (depth below surface) and season. Centimeter-scale data were divided into five intervals selected according to previous knowledge of important interfaces and sedimentary layers in the profile (Figure 3.3) (Baez-Cazull et al., 2007a).

For example, an interval comprised of data from the uppermost 9 cm of sediment (0-9 cm) was grouped to represent processes occurring in the portion of the organic-rich silt layer that contained the greatest concentration of particulate organic matter. Similarly, data from the surface water were grouped together as a separate interval. Grouping depth data into smaller intervals based on site characteristics allowed for a simple graphical output to contextualize the factor analysis. Bars shown in the variability plots indicate the range of the factor scores for that depth interval and each of the dots indicates the factor score for a particular depth from within the group.

RESULTS AND DISCUSSION

Descriptive Statistics and Correlation Matrix

Table 3.1 shows the range of values, medians and means for each of the parameters used in the descriptive analysis. Spearman's Rank Order Correlation test was chosen as a non-parametric method to estimate the degree to which two variables vary together. In this analysis, the assumption is that correlated variables are affected by a common cause. The resulting correlation matrix is plotted in Figure 3.5 and only includes correlations that had a significant $p<0.0001$. Because large sample sets can result in low p-values, suggesting a significant correlation when the actual correlation is low, only values having a Rho value larger than 0.5 were considered significant.

Table 3.1. Distribution analysis for the complete dataset. Data are given in µmoles/L except dissolved organic carbon (DOC), which is reported in mg/L.

Variable	Maximum	Minimum	Median	Mean	N
Acetate	8773	0	0	192	511
Propionate	1706	0	0	53	512
pH	8.7	6.7	7.5	7.5	519
Na	21768	6592	11355	11495	519
K	2853	0	463	557	510
Ca	32009	1004	8250	9813	520
Mg	8738	1553	2561	2619	520
Fe^{2+}	869	0	267	283	519
Cl^-	14530	1766	6982	6732	519
HCO_3^-	48383	6265	20283	20979	522
SO_4^{-2}	24456	0	13	683	524
H_2S	1004	0	6.1	38.1	515
NH_4^+	36349	0	1042	2211	506
CH_4	423	0.16	22	58	296
Mn	185	18	43	46	298
Ba	21	2.2	13	12	298
Total Iron	3971	0	303	362	298
Fe^{3+}	3849	0	50	95	296
DOC	110	1.4	11.4	13.5	294

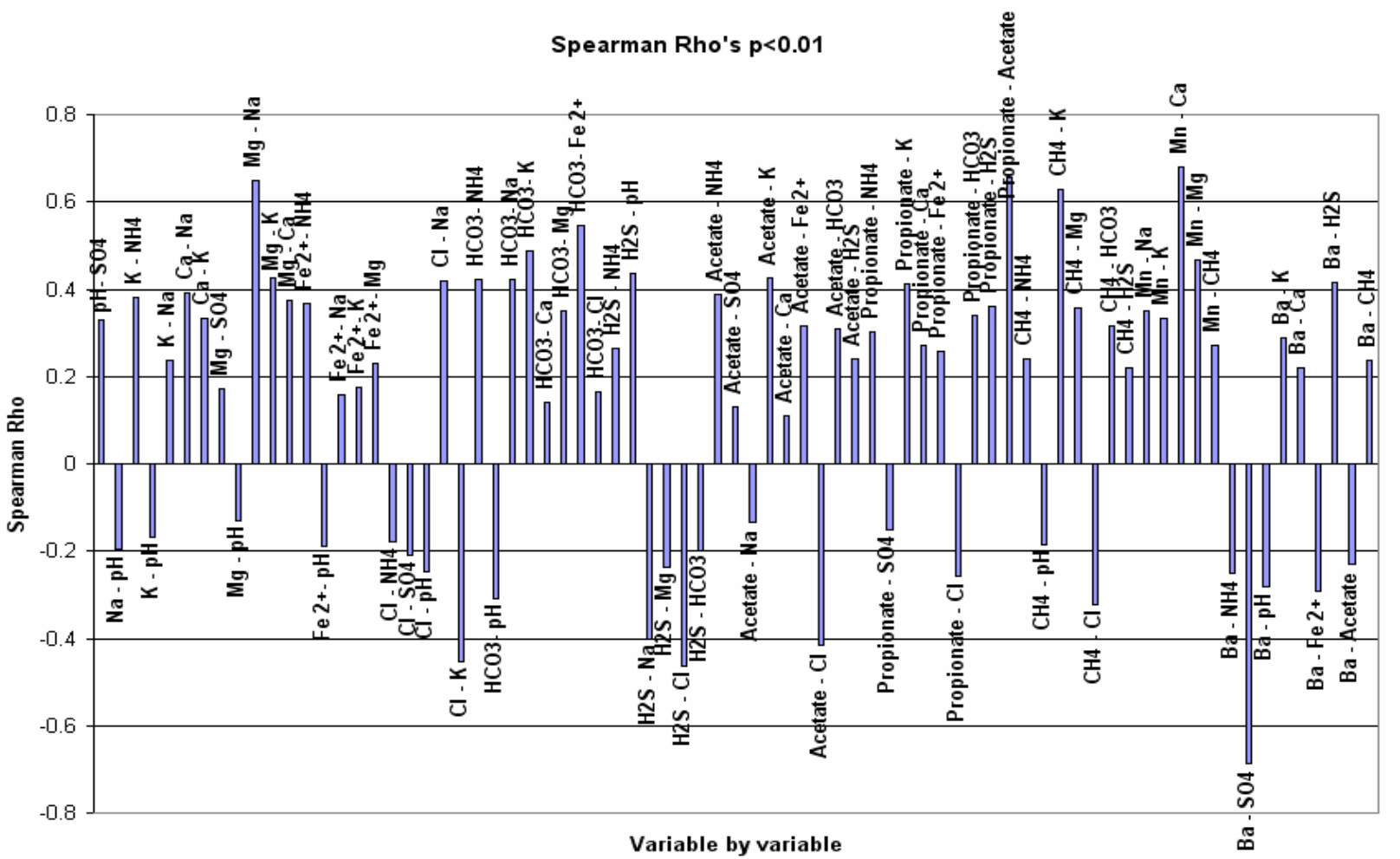

Figure 3.5. Spearman's Rho correlation analysis for correlations with a probability less than 0.0001 for all the sampling periods.

The Spearman's Rho correlation analysis revealed that Ca was significantly correlated with Fe^{3+} (rho = 0.71), Mn was significantly correlated with Ca (rho = 0.68), Mn with Fe^{3+} (rho = 0.67), propionate with acetate (rho = 0.66), Mg with Na (rho = 0.65), CH_4 with K (rho = 0.63), Mg with Fe^{3+} (rho = 0.59), alkalinity with Fe^{2+} (rho = 0.55), and NH_4^+ with DOC (rho = 0.54). All these variables exhibit a positive correlation suggesting that they could be related by similar process(es). Most of the positive correlations could be generally explained by processes of mineral equilibrium dynamics and organic matter degradation processes. There was only one negative correlation; Ba covaried negatively with SO_4^{-2} (rho = -0.69). This negative correlation reflects opposite interdependence of these variables and suggests a common cause that results in high concentrations in one and lower concentrations in the other. A possible mechanism would be barium solubilization by sulfate-reducing bacteria, which can use barite as a sulfate source for anaerobic respiration (Bolze et al., 1974). At the Norman Landfill site, barite rose rock from the Garber Sandstone occurs naturally in the sediments and barium-sulfate dissolution has been demonstrated in groundwater collected from the underlying aquifer (Ulrich et al., 2003).

Multivariate Factor Analysis

The first 13 variables listed in Table 3.1 were used in the first factor analysis. Principal Component Analysis (PCA) was the method chosen for extraction of factors explaining most of the variability and it was performed on standardized variables. Table 3.2 includes the eigenvalues, which are a measure of the variability of a factor, the

percent of the total variance attributed to each factor, and the cumulative percent variance. According to the Kaiser criterion (i.e. those factors that have an eigenvalue larger than unity (Kaiser, 1960)), four factors were determined significant and they account for 75% of the variability in the dataset.

Table 3.2. Principal Component Analysis (PCA) on the standardized correlated variables for all sampling periods. Parameters that were not collected in May 2003 and March20 04 (CH_4, Ba, Mn, DOC, and Fe^{3+}) were not included in the analysis.

Eigenvalue	Percent	Cumulative percent
3.64	28.0	28.0
2.62	20.2	48.1
2.16	16.6	64.8
1.27	9.78	74.6
0.95	7.34	81.9
0.62	4.77	86.7
0.52	4.02	90.7
0.33	2.57	93.3
0.31	2.35	95.6
0.20	1.54	97.2
0.18	1.39	98.6
0.14	1.11	99.8
0.04	0.33	100

The factor matrix was then rotated using varimax orthogonal rotation on the four significant factors. Factor loadings indicating the correlation coefficient between a variable and a factor are shown in Table 3.3 and include both positive and negative correlations. Loadings approaching ±1 indicate a strong correlation of a variable with a factor, whereas loadings approaching 0 indicate weak correlations. Loadings higher than ±0.75 are considered strong correlations, and loadings between ±0.5 and ±0.74 are considered to be moderately correlated (McGuire et al., 2005; Wayland et al., 2003). Based on the loadings, each factor was assigned a process likely to be associated with the significant variables within each factor.

In Factor 1 (F1) the variables with the strongest loadings were all negative and included propionate, ammonium, and acetate. K was also negative but had a moderate loading value. This factor explained 28% of the variability in the dataset. The process assigned to this factor was fermentation or the degradation of organic matter. Organic acids, such as acetate and propionate, are the products of fermentation and high concentrations of organic acids are commonly observed in wetland sediments (Duddleston et al., 2002; Hines et al., 1994; Kostka et al., 2002; Shannon and White, 1996; Wellsbury and Parkes, 1995) and throughout sediment profiles in other studies (Capone and Kiene, 1988; Chapelle and McMahon, 1991). Many fermentation products have been studied as indicators of organic carbon decomposition (Ho et al., 2002) and microbial activities (Boschker et al., 1998; Kleikemper et al., 2002). The correlation between K and fermentation may be explained by decomposition of organic material in

anaerobic environments resulting in the release of ammonium, which can exchange with K^+ from the solid phase.

Table 3.3. Varimax Orthogonal Factor Rotation obtained from the Principal Component Analysis of the complete dataset. Parameters that were not collected in May 2003 and March 2004 (CH_4, Ba, Mn, DOC and Fe^{3+}) were not included in the analysis. Four factors were selected explaining 75% of the variability. Shaded numbers highlight loadings higher than ±0.75, considered strong correlations, and loadings between ±0.5 and ±0.74, considered to be moderately correlated.

Parameter	**Factor 1 (28%)**	**Factor 2 (20%)**	**Factor 3 (17%)**	**Factor 4 (10%)**
Std Propionate	-0.94	-0.01	0.00	0.01
Std NH4	-0.93	-0.07	-0.03	0.02
Std Acetate	-0.92	0.02	0.07	0.03
Std K	-0.60	0.33	-0.52	-0.13
Std HCO3	-0.45	-0.49	-0.39	0.26
Std Fe 2+	-0.40	-0.59	-0.19	-0.14
Std Ca	-0.15	0.14	-0.69	-0.07
Std H2S	-0.13	0.82	-0.26	0.01
Std pH	0.01	0.76	-0.06	0.01
Std Mg	0.07	0.14	-0.78	-0.45
Std SO4	0.10	-0.11	-0.09	-0.90
Std Na	0.17	-0.22	-0.85	0.23
Std Cl	0.29	-0.59	-0.04	0.53
Interpretation	**(-)Organic matter degradation/ Fermentation**	**(+)Sulfate reduction (-) Fe reduction/ plume advection**	**(-) Mineral dissolution**	**(-) Oxidation (+) plume advection**

Factor 2 (F2) explained 20% of the variability and is highly correlated with H_2S and pH, and moderately correlated to Fe^{2+} and Cl^- in opposite dimensional space. Sulfide and Fe^{2+} are products of sulfate and iron reduction in anoxic sediments and are attributed to microbial reduction. Sulfate is considered chemically to be metastable at standard Earth-surface temperatures (Nealson, 1997); thus, its reduction to H_2S under these conditions suggests a microbial pathway. At circum-neutral pH, microbial iron reduction is more important in the reduction of iron (III) than abiotic reduction (Lovley et al., 1991). Therefore, F2 was interpreted as anaerobic respiration, specifically, sulfate and iron reduction. The opposite relationship of H_2S and Fe^{2+} suggests that the processes may be occurring in separate locations or, if simultaneous, the products may be precipitating into iron sulfides due to sulfide's high reactivity with Fe^{2+}. The Fe^{2+} and Cl^- association may indicate that iron reduction may be happening elsewhere in the system and the Fe^{2+} produced is simply transported to this location along with other landfill-leachate components because these constituents are both present in high concentrations in the Norman Landfill leachate (Cozzarelli et al., 1999b). Because of the multitude of processes affecting the Fe^{3+}/Fe^{2+} redox couple, determining iron cycling in the system is complex.

Factor 3 (F3) accounts for 17% of the variability and contains the variables Na, Mg, Ca, and K with negative loadings. Na and Mg had the highest loadings on F3, whereas Ca and K exhibit moderate correlations on this factor. This factor was interpreted as a mineral dissolution factor. Other studies have interpreted these parameters as a weathering process (Puckett and Bricker, 1992; Schot and van der Waal,

1992; Wayland et al., 2003) from the dissolution of calcite, dolomite and potassium feldspar minerals. At the Norman Landfill research site, the alluvial sediments contain potassium feldspars, calcite, dolomite and clay minerals and the silts have distinct increased abundances of clay and calcite minerals (Breit et al., 2005).

Factor 4 (F4) accounts for 10% of the variability and is highly correlated with SO_4^{2-} and moderately correlated with Cl^-. Two distinct processes with opposite loadings are interpreted from this factor, plume advection and sulfide oxidation. Chloride, often used as a proxy for leachate transport in this and other systems (Grossman et al., 2002; Röling et al., 2001; van Breukelen and Griffioen, 2004), has a positive loading in this factor, which is interpreted as plume advection process, where contaminated aquifer water containing a high concentration of Cl^- is being transported upward into the wetland sediments. Sulfate has a strong negative loading on F4 and is interpreted to be a result of oxidizing conditions. During wet conditions, sulfate is primarily observed in the surface water and has a low concentration in the sediments where microbial respiration depletes it (Baez-Cazull et al., 2007a). However, when the water table drops, iron sulfide minerals can be reoxidized, providing a new source of SO_4^{2-} to the system.

Interpretation of Factor Scores

Factor scores were assigned to each case (depths). Scores on each factor were plotted by sampling date and depth to determine the variability associated with the factors (Figure 3.6) and aid in the interpretation of factors.

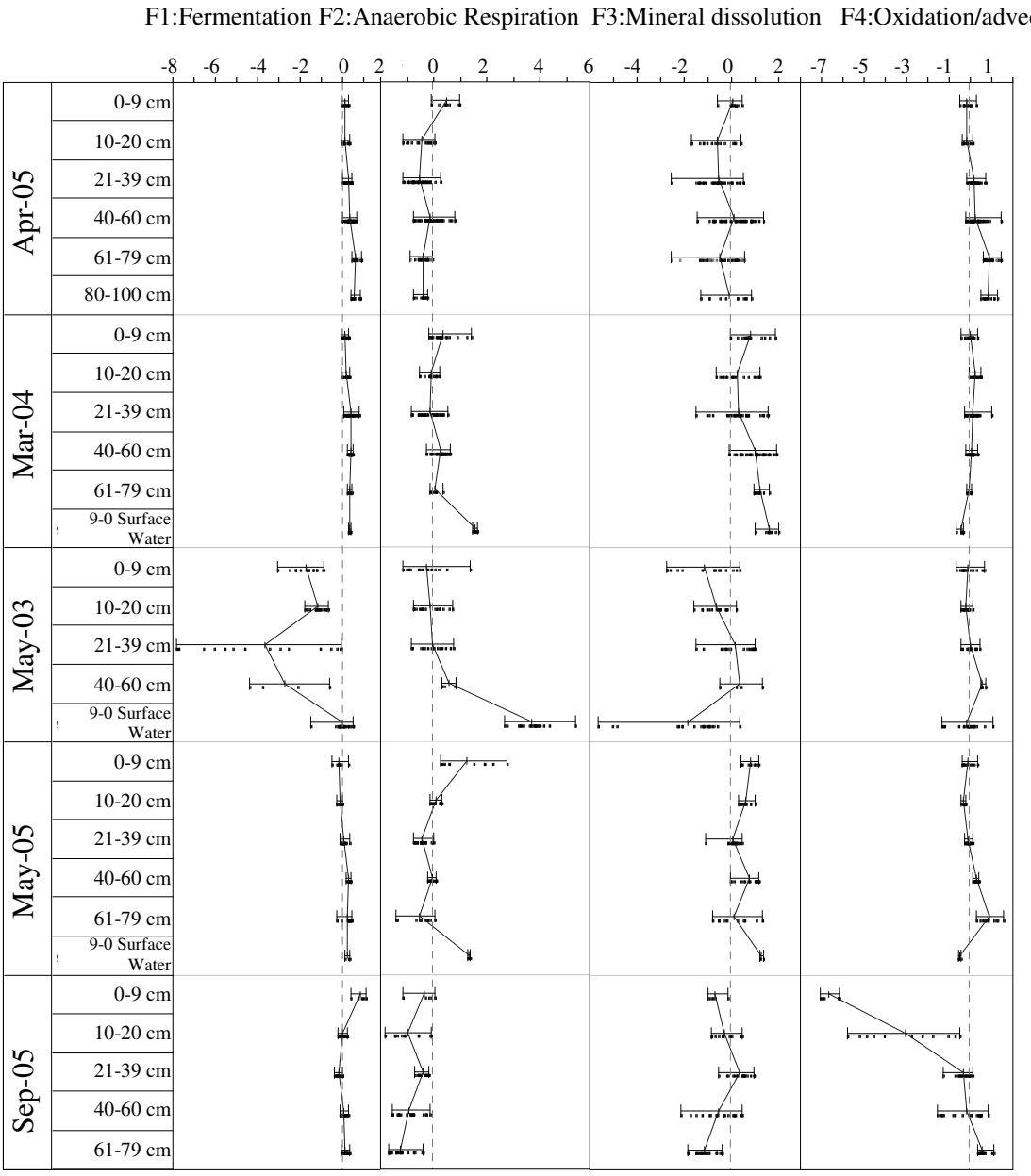

Figure 3.6. Variability chart of rotated factors by sampling date and depth. Factor scores were computed from the Principal Component Analysis (PCA) results in Tables 3.1-3.3. The bars indicate the range in the factor scores data, the solid lines indicate the mean for each peeper, and the dashed line represents the true mean (0). Depths are reported in cm below the sediment-water interface.

The variability chart in Figure 3.6 shows the factor scores by month and depth for F1 in the first column. In this chart, the fermentation/organic degradation process is mapped on the negative side of the factor scores because the factor loadings were negative. According to the variability chart, the fermentation process was dominant in May 2003 throughout the profile with a stronger signal in the middle section of the sediments (21-39 cm). Concentrations of organic acids for May 2003 were very high and are explained in detail in a previous study (Baez-Cazull et al., 2007a). The source of fermentation products in the upper sediments was attributed to decomposition of organic material deposited from wetland detritus; whereas the source of fermentation products in the 21-60 cm depth was attributed to two sources, localized decomposition of organic matter and/or fluxes of DOC from the aquifer plume. The high concentrations of organic acids and ammonium observed in May 2003 were much higher than the other sampling periods; as a result, this factor is not expressed strongly in any of the other months (Figure 3.6). To evaluate this factor for the other sampling periods, a separate analysis was performed which excluded the May 2003 and is discussed in the next section.

Figure 3.6 shows the F2 scores loaded on the positive side to indicate sulfate reduction and on the negative side to indicate iron reduction. The plot of factor scores by depth and date indicate that sulfate reduction is higher in May (Figure 3.6) than other times in the year. High factor scores for F2 found in the surface water for May are a product of either sulfate reduction occurring in the surface water or fluxes of sulfide produced in the first 9 centimeters in the sediments. Though a lesser signal, in March

2004 sulfate reduction is also observed in the upper sediments. Another location where sulfate reduction seems to be occurring throughout different time periods (May, March and April) is at the depth of 40-60 cm. In September 2005, sulfides are not observed suggesting either decreased sulfate reduction, rapid oxidation of sulfide in this drier month, or precipitation of iron sulfides with the increased levels of Fe^{2+} found in the upper sediments in September.

Iron reduction is most strongly indicated in April 2005, peaking at the depths of 10 to 39 cm below the sediment-water interface. In May 2003, iron reduction and sulfate reduction are indicated in the first 30 cm. The bars in Figure 3.6 show an equal distribution of factor scores on the positive side as in the negative side, indicating an equal importance for iron reduction and sulfate reduction in the first 30 cm. This finding indicates spatially simultaneous terminal electron-accepting processes (TEAPs) occurring this month, supporting prior observations (Baez-Cazull et al., 2007a). Due to the elevated concentrations of organic acids (data not shown), it is possible that both reactions can be microbially competitive given the availability of electron donors. In addition, our samples integrate conditions at a scale (cm) greater than the scale (μm) of documented heterogeneities in microbial processes which result in microzones of competing anaerobic respirations (Kappler et al., 2005). In March 2004, the same situation occurs at a depth of 10-39 cm where the two processes have an equal significance in the distribution of factor scores, indicating simultaneous processes. In May 2005, the Fe^{2+} suggested by F2 found at depths of 21-39 cm and 61 to 79 cm may be an indication of iron reduction and/or leachate plume advection. Similarly, in Sept.

2005, iron reduction is suggested at 10-20 cm depth although the gradual increase with depth below 39 cm of factor scores on F2 suggests that transport of the leachate plume is the dominant control deeper in the profile.

Mineral dissolution interpreted from a negative factor score in F3 was not significant in March 2004 and May 2005 (Figure 3.6). April 2005 and May 2003 exhibit greater mineral dissolution. Mineral dissolution in April is strongly observed throughout the sediment profile except for the 40-60 cm depth. In May 2003 mineral dissolution is greater at the surface water and the upper sediments, and a decrease is also observed at the 40-60 cm interval. In September 2005, mineral dissolution is observed in the upper and lower sediments. Note that the trend observed in F3 is the same trend as F2. This suggests that mineral dissolution varies with the anaerobic respiration processes. The exception is the surface water in May 2003 in which mineral dissolution is not associated with anaerobic respiration. In May 2003, mineral dissolution is higher in the surface water and upper sediments and decreases with depth. The parameter likely contributing most to this factor is the high calcium concentrations (~1000 ppm) in the surface water and upper sediments. May 2003 exhibited different conditions in the surface water than the other months, which contributed to different water chemistry. The water was stratified in respect to redox potential and dissolved oxygen and a dense blanket of senescing aquatic grass vegetation covered the wetland. A previous study (Baez-Cazull et al., 2007a) suggests that the dying vegetation in this month contributed to the dissolution of minerals in the surface water.

In F4, the oxidation process plotted as a negative factor score was significant in the upper 39 cm in September 2005. This oxidative condition is expected in this region due to a lower water table. The other months did not exhibit an oxidation component. The plume advection component, indicated by Cl^- concentrations, was significant at depths, suggesting a diffusion-gradient component increasing with depth on all sampling periods except for March 2004.

PCA Results Eliminating May 2003

In May 2003, data suggest that a unique incidence of elevated fermentation, as indicated by high concentrations of acetate, ammonium, and propionate, occurred at ~30 cm depth and was likely due to localized decomposition of organic matter (Baez-Cazull et al., 2007a). To evaluate the effect this event had on the overall variability of the dataset, the May 2003 data were removed and a separate PCA performed on the other months to explore whether or not this event was obscuring significant processes that might be dominant in other periods. Generally, dominant processes remain the same but the relative importance of these processes changed. Most notably, fermentation no longer accounted for the greatest variability but rather was associated with other processes (sulfate reduction) in the second factor and other processes that once grouped together (oxidation and plume advection) were teased apart. This discrimination allowed for a better evaluation of the linkages between dominant processes.

Five factors that explain 74% of the variability were selected for the factor rotation according to the Kaiser criterion (Kaiser, 1960). The factor loadings for each

parameter are shown in Table 3.4. Five processes were attributed to the grouped parameters and are discussed below. Figure 3.7 presents the variability of factors scores for each factor by date and depth, obtained from the rotated factor model.

Table 3.4. Varimax Orthogonal Factor Rotation obtained from the Principal Component Analysis of the dataset excluding May 2003. Five factors were selected explaining 74% of the variability. Parameters that were not analyzed for March 2004 (CH_4, Ba, Mn, DOC, and Fe^{3+}) were not included in the analysis. Shaded numbers highlight loadings higher than ±0.75, considered strong correlations, and loadings between ±0.5 and ±0.74, considered to be moderately correlated.

Parameter	**Factor I (25%)**	**Factor II (16%)**	**Factor III (13%)**	**Factor IV (12%)**	**Factor V (8.0%)**
Std pH	-0.67	-0.13	0.01	0.20	-0.07
Std Cl	-0.20	0.18	0.25	-0.84	0.01
Std SO4	-0.05	0.06	-0.88	0.27	-0.03
Std Propionate	-0.04	-0.64	-0.02	-0.08	0.02
Std Fe 2+	-0.03	0.09	-0.43	-0.34	0.65
Std H2S	-0.03	-0.83	0.12	0.25	-0.05
Std Acetate	0.02	-0.93	0.01	0.08	-0.05
Std Ca	0.25	0.08	-0.36	-0.43	-0.60
Std Na	0.26	0.01	-0.19	-0.84	-0.03
Std Mg	0.33	0.02	-0.84	-0.27	0.01
Std NH4	0.42	0.05	0.07	0.08	0.67
Std HCO3	0.47	0.04	0.03	-0.52	0.49
Std K	0.87	-0.09	-0.23	0.12	0.05
Interpretation	**(+) Mineral Dissolution (K)**	**(-) Fermentation (+) Sulfate reduction**	**(-) Oxidation**	**(-) Plume advection**	**(+) Iron reduction (-) Ca dissolution**

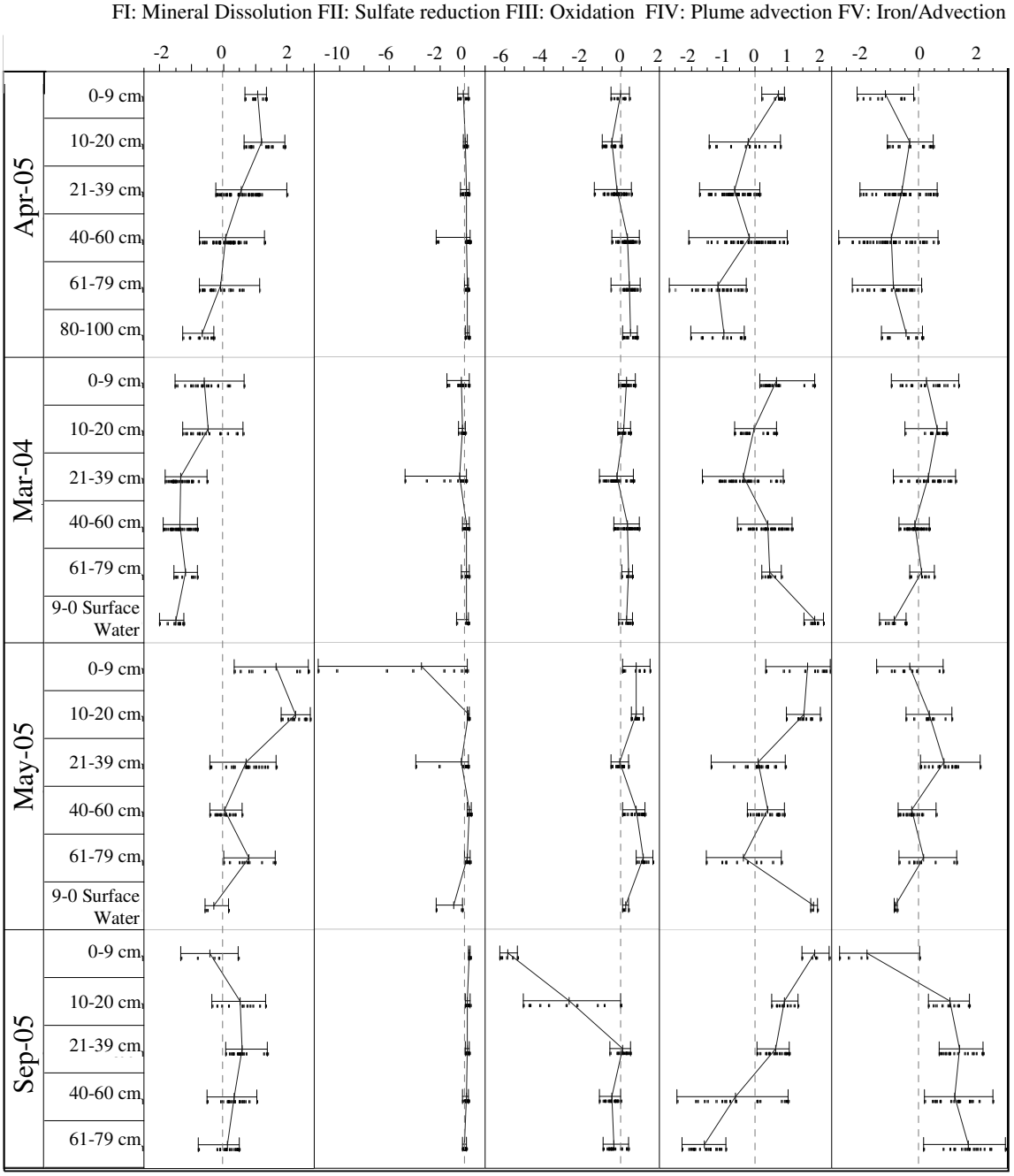

Figure 3.7. Variability chart of rotated factors by sampling date and depth excluding May 2003. Factor scores were computed from the PCA results shown in Table 3.4. The bars indicate the range in the factor scores data, the solid lines indicate the mean for each peeper, and the dashed line represents the true mean (0).

The first factor, Factor I (FI), explains most of the variability (25%) and has negative loadings for pH and a positive loading for potassium. This factor was interpreted to represent release of potassium (K) at lower pH. Analyzing the factor scores by depth and month (Figure 3.7), the release of K is dominant in May 2005 and April 2005 with similar trends of high loadings near the surface that generally decrease with depth.

The source of potassium in the months of April and May 2005 was explored. Cation exchange was evaluated as a possible process for the changes in K concentration. The exchange capacity of the soil was determined at depths of 10 and 30 cm using the equation of Breeuwsma (Amini et al., 2005) where, Cation Exchange Capacity ($cmol_C/kg$) = 0.32 (% clay) + 3.1 (2.7% carbon). The clay and organic carbon content of the sediments was determined from cores described in a previous study (Baez-Cazull et al., 2007a). At 10 cm the clay content was less (2.9%) than at 30 cm (3.9%) but the organic carbon content was higher at 10 cm (2.7%) than at 30 cm (0.3%). The exchange capacity at depths of 10 and 30 cm was determined using PHREEQC-2 (Parkhurst, 1995) with the solution at these depths for April and May 2005. The results indicate that the soil K exchange composition is 1.3×10^{-3} moles at 10 cm for April 2005 and 1.6×10^{-3} moles in May 2005. At 30 cm, the exchange composition is 1.4×10^{-4} moles and 3.3×10^{-4} moles for April and May 2005, respectively. This indicates that in the upper sediments, K will have a greater affinity to the particles than in the deeper sediments due to higher concentrations in the upper sediments. However, cation exchange capacity could not be a major control because K exchange capacity was lower than for other

cations that were found throughout the sediment profile, such as Ca, Mg, Na, and NH_4^+, and high concentrations of these cations are often found in the system. This suggests that another process is controlling the K cycle to explain the shifts in concentrations in the sediments. In the first PCA (Figure 3.6) it was noted that the anaerobic respiration factor (F2) mimicked the mineral dissolution factor (F3), suggesting that mineral dissolution is linked to anaerobic respiration.

The second factor, Factor II (FII), includes high positive factor loadings for acetate, sulfide and propionate (Table 3.4) and explains 16% of the variability. These associations suggest that the underlying processes controlling this factor are fermentation and sulfate reduction. In the first PCA (including May 2003 data) the factor interpreted as fermentation was the first factor, F1 (explaining 28% of the variability). However, the strength of the signal in the May 2003 dataset obscures the importance of this process in time and space, as well as the relationship between fermentation and sulfate reduction. Once the May 2003 data were removed, it becomes evident that fermentation and sulfate reduction were dominant in May 2005 in the first 9 cm and at the transition zone at 21 to 39 cm. It is also observed in April 2005 at 40-60 cm and in March 2004 in the transition zone (21-39 cm) but not in September 2005.

The third factor, Factor III (FIII), with a variability of 13%, includes sulfate and magnesium with high negative loadings and was interpreted as an indication of oxidation. This factor was dominant in September 2005 in the first 20 cm, just as in F4 in the first PCA.

The fourth factor, Factor IV (FIV), with a 12% variability, contains the variables Cl^-, Na, and alkalinity and was interpreted as an indication of plume advection. With the exception of March 2004, the variability in FIV scores plotted with depth and season show that the trend for this factor increases with depth, suggesting a diffusion gradient of plume components. This pattern is consistent with previously determined hydrologic flow paths between the aquifer and wetland sediments which have documented landfill-leachate water moving upward into the wetland sediments (Lorah et al., 2007). Toxicology studies have also demonstrated leachate-plume discharge to the slough resulting in elevated developmental toxicity levels (Bruner et al., 1998).

The fifth factor, Factor V (FV), has a variability of 8% and includes positive loadings for Fe^{2+} and NH_4^+, and a negative loading for Ca. This factor was interpreted as an indicator of iron reduction and organic matter degradation either in the direct vicinity of the profile or elsewhere in the system. This factor is dominant in September 2005 below 10 cm and continues throughout the sediments. This indication of iron reduction at depth may be the result of in situ processes (including respiration and mineral precipitation/dissolution) or may reflect the upward transport of Fe^{2+} into the wetland sediments via advection from the aquifer. It is also observed in the middle sediments (silt layer-transition zone) in May 2005 and observed in the upper sediments in March 2004. This indicates that the activity of iron reduction changes in space, with active iron reduction having likely occurred in the upper sediments early in the season and throughout the profile in September when oxidizing conditions enhance the availability of iron(III) minerals. However, this factor (FV), and indeed iron reduction

itself, are difficult to interpret because the indicators are affected by multiple processes, including transport and phase changes between solid and dissolved forms.

PCA Including Additional Data from 2005

To further explore the relationships among processes illuminated by these first two PCAs, a third PCA was performed on a subset of the data (April, May and September 2005) because additional geochemical parameters were only collected in 2005 and indicators including CH_4, DOC, Ba, Mn, and Fe^{3+} could be included. A Spearman Rho's correlation analysis was evaluated for 2005 and compared to correlations on the entire dataset (Figure not shown). Unlike PCA for the whole dataset (Figure 3.5), PCA for 2005 data, yield the highest positive correlation for Cl^- and Na with a rho = 0.76. All the other positive correlations remain similar and were discussed previously and include Fe^{3+} and Ca; Mn and Ca; Fe^{3+} and Mn; CH_4 and K; and DOC and NH_4^+. The correlation matrix for the whole dataset showed significant negative correlations only between Ba and SO_4^{2-} (Figure 3.5), although the correlation matrix for the 2005 dataset showed additional significant negative correlations for Na and H_2S (rho = -0.52), and Cl^- and K (rho = -0.50). The negative correlation between sulfate and barium is an indication of barite utilization as described in the first PCA. The negative correlation between K and Cl^- indicates that the potassium observed in the system is not controlled by the same mechanism as Cl^- in the system, which is attributed to plume advection.

To better understand the relationships from the PCA, the six factors with eigenvalues higher than 1 (Kaiser, 1960) and explaining 76% of the variability were rotated using Varimax Orthogonal rotation. The factor loadings obtained from the rotation are shown in Table 3.5.

Factor A (FA) explains 19.6% of the variability and included the variables acetate, H_2S, DOC, and propionate. This factor is interpreted as an indicator of fermentation and sulfate reduction processes. In all of the PCA analyses, these two processes have been consistently identified in the top factors explaining most of the variability in the dataset. This control of the overall structure of the data suggests that these processes are dominating the system. In May 2005, these processes are dominant (Figure 3.8) in the upper 10 cm and at 21-39 cm as it was observed in May 2003 in F1 (Figure 3.6). Fermentation was not dominant in April and September 2005.

The second factor, Factor B (FB), which explains 17.3% of the variability, included high positive loading values for the variables Mg, SO_4^{-2} and a moderate loading value for Fe^{2+}. This factor was interpreted as an oxidation/Fe^{3+} and $SO4^{2-}$ reduction factor. Oxidation was represented in the fourth factor (F4-explaining 10% variability) in the first PCA and the second factor (FB) in the PCA on the 2005 dataset. The oxidation factor is dominant in September 2005 when the water table dropped and additional electron acceptors (e.g., SO_4^{2-} and Fe^{3+}) are available. The concentrations of sulfate and Fe^{2+} were highest in September 2005 after exposure of previously reduced sediments to oxygen supporting active iron and sulfate reduction. In this PCA, when the dataset was reduced to only April, May and September 2005, indicators of oxidation explained more

Table 3.5. Varimax Orthogonal Factor Rotation obtained from the Principal Component Analysis of the dataset in 2005 to include parameters CH_4, Ba, Mn, DOC and Fe^{3+}. Six factors explained 76% of the variability. Shaded numbers highlight loadings > ±0.75, considered strong correlations, and between ±0.5 and ±0.74, considered to be moderately correlated.

Parameter	Factor A (20%)	Factor B (17%)	Factor C (12%)	Factor D (11%)	Factor E (10%)	Factor F (5.7%)
Std NH4	-0.02	0.02	0.25	-0.79	0.00	-0.03
Std SO4	0.03	0.82	-0.20	0.04	0.34	-0.14
Std pH	-0.24	0.02	-0.57	0.07	0.05	-0.03
Std Na	0.03	0.13	-0.16	0.03	-0.88	-0.17
Std K	-0.16	0.36	0.69	-0.13	0.24	-0.08
Std Ca	0.07	0.30	0.16	0.59	-0.43	-0.37
Std Mg	-0.03	0.89	0.18	0.07	-0.15	-0.16
Std Fe 2+	0.17	0.59	-0.04	-0.47	-0.32	0.01
Std Cl	0.18	-0.22	-0.30	0.05	-0.80	0.05
Std HCO3	0.04	0.07	0.18	-0.54	-0.60	0.03
Std H2S	-0.89	-0.14	0.08	0.00	0.22	-0.07
Std Acetate	-0.93	-0.05	-0.07	0.05	0.10	-0.02
Std Propionate	-0.52	0.03	0.06	0.18	-0.06	0.19
Std CH4	-0.25	-0.08	0.76	-0.23	0.30	-0.08
Std Mn	-0.09	0.44	0.18	0.07	-0.17	-0.78
Std Ba	0.00	-0.49	0.64	0.47	0.00	0.04
Std Fe 3+	0.08	0.01	-0.07	-0.01	0.01	-0.91
Std DOC	-0.82	0.13	-0.06	-0.33	0.00	-0.07
Interpretation	**(-) Fermentation/ Sulfate Reduction**	**(+) Oxidation/ Fe Reduction**	**(+) Methanogenesis / Mineral diss./ Ba utilization**	**(-) Organic degradation**	**(-) Plume advection**	**(-) Electron acceptors**

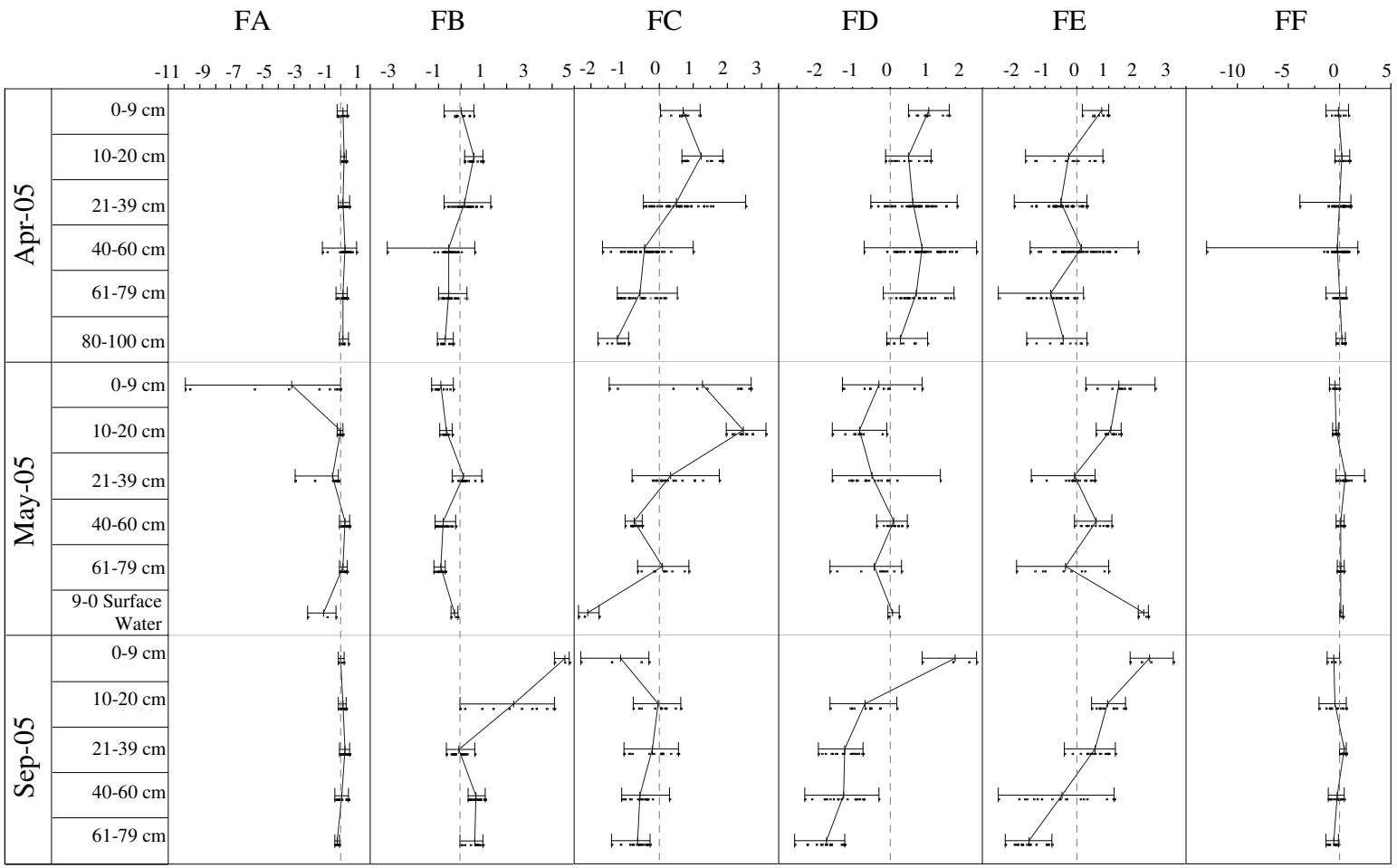

Figure 3.8. Variability chart of factor scores by sampling date and depth of six factors obtained from the PCA including only data for 2005 (Shown in Table 3.5). The bars indicate the range in the factor scores data, the solid lines indicate the mean for each peeper, and the dashed line represents the true mean (0).

of the variability (second factor versus fourth factor in the first PCA). In the third PCA, the oxidation (wet/dry cycle) in September 2005 represents a greater proportion of the dataset. Because our dataset is biased in terms of "wet" seasonal measurements, this representation is probably more representative of the actual importance of oxidation processes in an annual cycle. It should also be noted that barium is negatively loaded (-0.49) on this factor (FB), opposite to the loading of SO_4^{2-} (0.82). This supports our hypothesis that when sulfate concentrations are low, microorganisms will use barite as a source of sulfate for metabolism.

Factor C (FC) includes the variables CH_4, K and Ba as positive loadings and pH as a negative loading and explains 12.2% of the variability. The variables expressed in this factor were not collected for the sampling periods 2003 and 2004 and demonstrate important redox processes that could not be determined in previous years but were probably present. The processes interpreted for FC are methanogenesis and bacterial mineral utilization, such as utilization of barite ($BaSO_4$) as a source of sulfate by sulfate-reducing bacteria. In addition, K associated with this factor with 72% communality and exhibited a strong Spearman's correlation with methane. This is an indication that the concentration of K in the system is associated with reducing conditions, such as a methanogenic environment, with K concentrations increasing with the increase of methane in the system. A plausible hypothesis for the release of K is the dissolution of silicate minerals by bacteria seeking electron acceptors (Fe^{3+}) or nutrients (e.g., K^+, P).

It has been demonstrated in other studies that microorganisms are capable of utilizing crystalline minerals to obtain electron acceptors for their metabolic activities

and release mineral components to solution. One example is sulfate bacteria harvesting sulfate from minerals such as barite in dissolved sulfate-limited environments (Bolze et al., 1974; Ulrich et al., 2003). Barium strongly associated in this factor supports the hypothesis that in methanogenic conditions, sulfate reducers can utilize sulfate from barite as an electron acceptor. Iron reducers have also been documented to utilize mineral forms as a source of oxidized iron for their metabolic activities. Some studies even recognize the importance of this pathway in the release of K through the dissolution of minerals. Clay minerals such as illites and smectites are potassium-bearing phyllosilicates that have been studied for their implications on potassium availability as a result of microbial activity. At the Norman landfill site, illites and smectites are abundant comprising most of the clay minerals (Breit et al., 2005). In other studies, these minerals have shown significant reactivity with iron reducers and have been documented to have an impact in soil and physicochemical properties of sediment (Kostka et al., 1999; Stucki and Kostka, 2006). Stucki and Shen (1993) determined that potassium fixation occurs when microbial iron reduction causes the smectite minerals to collapse and trap ions such as NH_4^+ and K^+. Conversely, they observed a release of K to solution during microbial iron reduction of illites. In their study they attribute the release of K^+ to exchange with Fe^{2+} produced from the reaction (Stucki and Shen, 1993). There have also been other studies that report dissolution of potassium-bearing minerals such as jarosite by iron reducers in which K^+ and Fe^{2+} are released to solution at neutral pH (Jones et al., 2006).

The finding that in this system K is linked to reducing conditions has implications for studies relating to nutrient availability in redox sensitive systems (Babu et al., 2006; Chen et al., 1997). Because K^+ has a lower exchange capacity affinity and will remain in solution, it could be used as an indicator of mineral utilization by bacteria and/or methanogenesis in systems lacking vegetation, such as aquifers. A previous study by McGuire et al. (1999) observed important correlations between K^+ and high levels of H_2, indicating methanogenic processes in a contaminated aquifer. Further studies will be needed to support this hypothesis.

The variability of FC by depth and season is shown in Figure 3.8. Positive factor scores in FC indicate greater methanogenesis and mineral utilization and were observed in both April and May 2005 at a depth of 10-20 cm. In September 2005, this factor was not significant, which was likely due to the oxidizing conditions in this month. This suggests that the system presents more reducing conditions in May, which is a warm and wet month.

The fourth factor, Factor D (FD), explains 11.3% of the variability and contains the variables NH_4^+, Ca, and HCO_3^- (Table 3.5). This factor was interpreted as organic matter degradation (negative factor scores). The high levels of ammonium together with higher alkalinities suggest significant organic matter degradation (Bally et al., 2004). This process is observed throughout May 2005 except in the 40-60 cm zone (Figure 3.8). This is expected because May presents the most reducing conditions, indicating enhanced microbial activities. The trend in FD is similar to the trend in FC, suggesting that the concentrations of NH_4^+ and alkalinity in this factor may also be related to the

methanogenic and mineral utilization activity discussed for FC. For example, organic degradation fuels the progression of TEAPs and provides substrates for methanogenesis. The one exception is in September 2005 below 10 cm depth where this factor (FD) does not appear to be related to the methanogenic activities observed in FC. However, the higher NH_4^+ and alkalinities may be attributed to organic degradation by iron reduction combined with transport of ammonium and alkalinity from the contaminated aquifer, which has high ammonium concentrations and high alkalinity (Christenson and Cozzarelli, 1999; Cozzarelli et al., 1999b).

Factor E (FE), explaining 9.99% of the variability, was interpreted as a plume advection process because it contains geochemical parameters that are associated with landfill-contaminated water. Chloride, which has been used as a conservative tracer for landfill contamination, is highly correlated in this factor together with its common counter ion, Na. High alkalinity is also characteristic from the aquifer plume (Cozzarelli et al., 1999b) and it has a moderate negative loading on this factor. In September and April 2005, the general trend for this process increases with depth. In May 2005, the trend is markedly disrupted at 40 to 60 cm, suggesting that the water contained in this sandy layer has a source other than direct flow from the contaminated aquifer. This finding helps to understand why this zone consistently presents an opposite process for all the factors in April and May. It is suspected that the composition of the water in this zone is affected by the water level or recharge conditions because the pattern is different for September. This is consistent with hydrologic patterns discerned by other studies (Lorah et al., 2007; Scholl et al., 2005).

The sixth factor, Factor F (FF), only explains 5.66% of the variability. It includes Fe^{3+} and total Mn and was interpreted as available electron acceptors. These electron acceptors are dominant in April 2005 in the 21-60 cm depth. April 2005 had the highest recharge and the lowest microbial activity, and therefore it is not surprising to observe higher concentrations of electron acceptors during this month. Moreover, the location where these are found (the sandy layer) confirms the disconnection of this layer from the deeper sediments and suggests that this oxidized layer may be connected to the surface.

SUMMARY

Biogeochemical cycling is complex and is controlled by linked geochemical, biological and hydrogeological processes that vary in space and time. Establishing significant relationships between linked geochemical parameters could not be accomplished by graphical and numerical techniques alone. Multivariate statistics were used to illuminate relationships between (bio)geochemical parameters to determine dominant biogeochemical processes occurring in a wetland-aquifer system impacted by landfill leachate. For example, determination of iron redox cycling and its spatial and temporal controls cannot be teased out from plots of the Fe^{2+} concentrations in the system alone because Fe^{2+} concentrations are affected by many processes in the system, including transport and solid phase precipitation/exchange reactions. Factor analysis determines correlations among geochemical parameters allowing for interpretation of

processes. Results show that Fe^{2+}, at various points in time and space, associates with indicators of transport in the aquifer (e.g., Cl^-), with indicators of anaerobic respiration, and with indicators of mineral precipitation/dissolution reactions. Spatial patterns of geochemical associations as calculated using PCA (factor scores) provide a robust means of interpreting Fe^{2+} concentrations in the system throughout time. The greatest variability in the dataset was explained by fermentation and it is thus considered to be the primary process governing biogeochemical cycling in the system. Sulfate and iron reduction were found to be the dominant TEAPs followed by methanogenesis and sulfate reduction via utilization of barite ($BaSO_4$). Seasonal hydrological patterns (wet and dry periods) are an important control on the availability of electron acceptors through the reoxidation of reduced iron-sulfur species, enhancing iron and sulfate reduction.

The combined use of PCA and spatial representation of factors was a powerful technique to explore the linked biogeochemical variability in a large dataset containing spatial and temporal data and to expose underlying relationships as well as evaluate the importance of various processes in the system. Though exploratory in nature, this application of PCA provides a mechanism to formulate hypotheses regarding process that may not have been observed previously that can then be tested with further experimentation.

CHAPTER IV

SEASONAL HYDROLOGICAL CONTROLS ON BIOGEOCHEMICAL PROCESSES AT A WETLAND-AQUIFER INTERFACE

SYNOPSIS

Seasonal and hydrological changes may significantly influence biogeochemical cycling in a wetland-aquifer system. Spatial and seasonal variation of geochemical indicators including sulfate, sulfide, methane, Fe^{2+}, Fe^{3+}, NH_4^+, and alkalinity were evaluated. Pore water samples were collected with depth at centimeter spaced intervals capturing a wetland-aquifer interface during a wet period in the spring (May) and a dry period in the fall (September). Sampling locations exhibited 1) upward, 2) downward, and 3) negligent flow between the aquifer and wetland. Biogeochemical processes were interpreted from data reduction of geochemical indicators via Principal Component Analysis (PCA). Analysis of Variance (ANOVA) was performed on factors obtained from PCA to test significant differences in the processes identified attributed to seasonal hydrological conditions. Seasonal differences in biogeochemistry were dominated by changes in water table levels and water flow paths. In May the dominant process is methanogenesis attributed to a high water table and strongly associated with negligible water flow. In September, lowering of the water table oxidizes previously reduced

sediments rich in iron sulfide minerals which contribute to the availability of electron acceptors, enhancing iron reduction. Fermentation and sulfate reduction processes were not affected by season or hydrologic regime. The results illustrate the effects of seasonal hydrological changes on biogeochemical cycling in a linked wetland-aquifer system.

INTRODUCTION

Understanding biogeochemical processes in aqueous systems have been of interest for their function in controlling the fate and transport of contaminants. Biogeochemical cycles in wetland environments have been studied for their function in global carbon cycling and as a sink or source of pollutants such as trace metals, methane, carbon dioxide, and N_2O. In aquifer systems, biogeochemical cycling has focused mainly on understanding contaminant fate and transport since aquifers are a main source of freshwater for agricultural, residential and industrial purposes. Most studies approach these systems separately targeting biogeochemical processes occurring in either the wetland or aquifer. However, shallow unconfined aquifer systems are often connected hydrologically to surface wetland systems resulting in linked biogeochemical processes. The complex hydrology and seasonal changes that these systems share are evident in the spatially heterogeneous and temporally changing biogeochemistry (Baez-Cazull et al., 2007a; Baez-Cazull et al., 2007b). Seasonal hydrological changes in aquifer-wetland systems are an important control on biological, physical and chemical processes but currently these linkages are poorly understood.

Biogeochemical processes in aqueous sedimentary environments are the result of reduction-oxidation reactions which occur in the following thermodynamic sequence, aerobic respiration, nitrate reduction, iron/manganese reduction, sulfate reduction and methanogenesis (Champ et al., 1979; Froelich et al., 1979; Megonigal et al., 2004). These terminal electron accepting processes (TEAPs) will determine the rates for decomposition of organic matter, nitrogen fixation, production of sulfide and methane. However, in wetland systems, the heterogeneous composition of sediments and abundant supply of organic matter due to vegetation dynamics may cause the sequential order of these processes to vary spatially and allow TEAPs to coexist, particularly at the sediment-water interface (Baez-Cazull et al., 2007a; Kostka et al., 2002). Complexities observed in other studies are the result of the heterogeneous distribution of organic matter, electron acceptors, minerals, and biology, which is controlled by seasonal and hydrological conditions (Koretsky et al., 2003).

Other factors affecting the distribution of biogeochemical processes in the wetland are environmental conditions such as temperature and precipitation. Temperature controls biological production in the wetland; increasing temperature generally increases microbial activity and vegetation growth. Warmer temperatures increase anaerobic microbial metabolism in peat wetlands, depleting nitrate and sulfate and releasing methane to the environment (Fenner et al., 2006). Some studies have demonstrated the relationship of strong seasonal fluctuation in rates of organic carbon and sulfate reduction with warmer months in saltmarsh wetlands (Koretsky et al., 2003; Kostka et al., 2002). Increased rates of anaerobic respiration correlate positively with

increases in temperature and in primary productivity in wetlands (Hines et al., 1989; Kostka et al., 2002). Precipitation events control TEAPs by introducing favorable electron acceptors, such as nitrate and sulfate as well as altering the physical hydrological conditions.

Changes in hydrological flowpaths and water table levels change the supply of electron acceptors and nutrients to systems such as wetlands, rivers, streams, and lakes (Clément et al., 2003; Malard et al., 2002). Spatially and temporally variable flowpaths that bring waters with limiting solutes (ex., nutrients, electron donors, or electron acceptors) into contact enhance microbial activities and organic matter mineralization. For example, one important zone where electron acceptors and electron donors come into contact is the interface between surface water and anaerobic groundwater (Baez-Cazull et al., 2007a). Previous studies have recognized the importance of seasonal hydrologic changes on biogeochemical processes at surface water and groundwater interfaces (Clément et al., 2003; Crowe et al., 2004; Dahm et al., 1998; Dempster et al., 2006; Drexler et al., 1999; van Griethuysen et al., 2005).

The system discussed in this paper consists of a wetland system hydrologically connected to a regional aquifer impacted by municipal solid waste landfill leachate located in Norman, Oklahoma, USA. The most biogeochemically active zone of the wetland is near the surface, where the system experiences changes in temperature, precipitation, infiltration, vegetation, and nutrient loading (Hunt et al., 1997). However, other interfaces with depth have shown evidence for enhanced biogeochemical activity such as the contact of wetland pore water with underlying aquifer water (Baez-Cazull et

al., 2007a). A previous study on the vertical variations of processes in the system (Baez-Cazull et al., 2007a) found sharp geochemical gradients at small (centimeter) scale associated with lithological, hydrological and chemical interfaces. From the hydrochemical viewpoint, a wetland functions as a complex interface zone for water exchange between groundwater and surface water. The exchange between groundwater and surface water is determined by water flow rates which are driven by diffusion or advection. The direction of the flow, from aquifer to wetland or from wetland to aquifer, impact the redox conditions found in this system. Lorah et al. (2007) demonstrated the link between redox conditions in the wetland sediments and fluctuations in groundwater/surface-water levels, finding that during periods of high recharge, aquifer water discharged into the wetland. They found high concentrations of leachate constituents normally found in the aquifer, including ammonium, dissolved organic carbon (DOC), iron, and bicarbonate, in and upgradient location (closer to the landfill mound) of the wetland-sediment pore water. In a location downgradient, Scholl et al. (2005) observed that exchange between the wetland and shallow groundwater was episodic and that shallow groundwater contained, on average, 29 percent wetland water during periods of high recharge. Both of these studies demonstrate the effect of mixing aquifer water and wetland surface water in locations exhibiting opposite water flow. One significant implication of these findings is that upward flow in this system could potentially enhance degradation of recalcitrant DOC transported from the aquifer into the wetland sediments via cometabolism of labile DOC available in the wetland pore water. Similarly, downward flow in the system can supply electron acceptors and/or

labile electron donors to the aquifer providing loci for enhanced degradation of contaminants.

The purpose of this study was to determine the dominant biogeochemical reactions in the sediments of a wetland-aquifer system resulting from changes in seasonal hydrologic conditions. Seasonality was evaluated in Spring (May) and Fall (September) 2005 using geochemical data from vertical profiles spanning the wetland-aquifer interface. The wetland's water levels and vegetation growth are high in May. In September, water levels drop, in some instances below the wetland sediment surface, causing biogeochemical conditions in the wetland to change. The hydrologic controls were studied by selecting three locations that exhibited different aquifer seepage rates: 1) high discharge to the wetland system, 2) high recharge to the aquifer system, and 3) low/negligible discharge rate. Multivariate statistics were used to explore significant relationships among geochemical parameters and evaluate changing processes. The use of PCA (Principal Component Analysis) for exploring parameter correlations and the Analysis of Variance (ANOVA) on factor scores allowed for interpretation of processes controlling the surface water and groundwater composition affected by seasonal hydrologic fluctuations.

MATERIALS AND METHODS

Site Description

The wetland is situated in the Canadian River alluvial plain in central Oklahoma (Figure 4.1), and formed in a previous location of the main channel of the Canadian River (Schlottmann, 2001). The geologic setting is characterized by moderately permeable alluvial and terrace deposits with a shallow water table that overlies a Permian shale and mudstone confining unit known as the Hennessy Group (Scholl and Christenson, 1998). The wetland acts as a surface expression of the local water table. It is fed by groundwater discharge, runoff, and precipitation and water levels vary seasonally ranging from approximately 1 m deep in the spring to dry in the late summer. Upper sediments have been variably saturated during the summer months. The area surrounding the wetland is densely vegetated, dominated by *Phragmites*, *Leersia* and *Phalaris* and with at least three species of phreatophytes (willow, cottonwood, and tamarisk) (Christenson et al., 1999). Seeds found in the wetland sediments include: southern nymph (*Najas guadalupensis* (Spreng.) Magnus), barnyard grass or cockspur (*Echinochloa crus-galli* (L.) Beauv.), and rough cocklebur (*Xanthium strumarium* L.) (Welsh et al., 2007). The growing season is from mid-April through October. The wetland is approximately 700 m long and 15-25 m wide and is downgradient from the Norman municipal landfill (50-100 m from the edge).

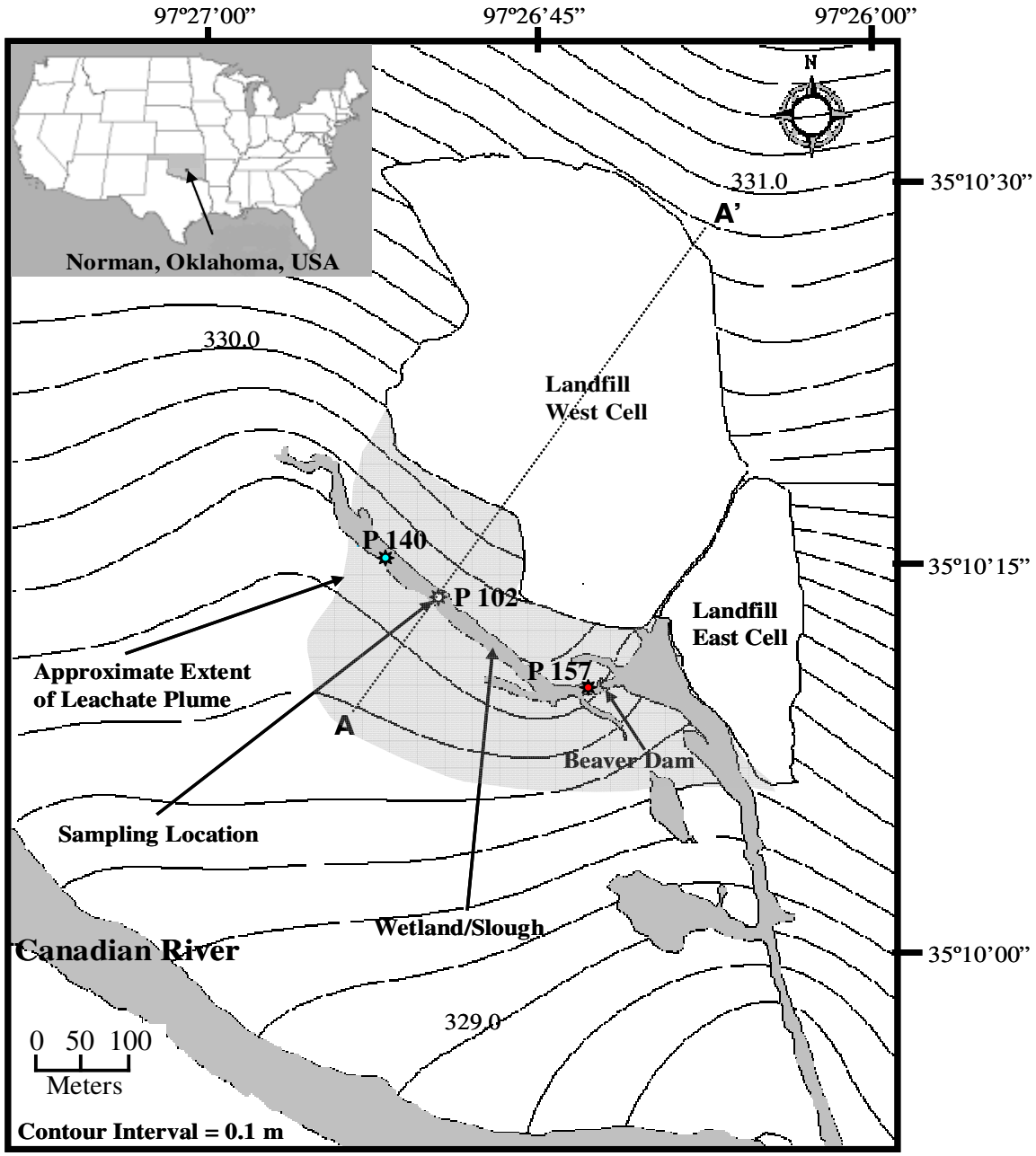

Figure 4.1. Map of the Norman Landfill site in Oklahoma, U.S., showing sample locations indicated by a star. Modified from Scholl and Christenson (1998). Locations selected according to water flow. Location 140 exhibited upward flow, location 157 exhibited downward flow and location 102 exhibited negligible flow. Potentiometric lines shown.

The shallow aquifer underlying the wetland has been geochemically characterized as part of the efforts of the U.S. Geological Survey Toxics Hydrology Program which have been monitoring a leachate plume originated from an unlined landfill site in Norman, Oklahoma, USA. The leachate plume extends downgradient approximately 250 m from the landfill toward the Canadian River. The hydraulic conductivity is estimated to range from $7.3x10^{-2}$ to $2.4x10^{1}$ meters per day and the plume flows directly beneath the wetland (Scholl and Christenson, 1998).

In Situ Measurement

Surface and pore-water samples were collected from the wetland (slough) adjacent to the Norman Landfill site in May 2005 (P102M, P140M, and P157M), and September 2005 (P102S, P140S, and P157S). Locations 102, 140, and 157 were selected according to seepage rates shown in Table 4.1. Seepage rates were collected by the U.S. Geological Survey Oklahoma Water Science Center using seepage meters with an area of 2,573.14 cm^2. Each bag in the seepage meter was filled with 3,000 mL of distilled water and seepage rates were calculated from average measurements of water lost or gained in the bags taken in 2004 and 2005. Seepage data for location 157, which is characterized by a beaver dam, were not measured but previous exploratory measurements indicate great water losses from a seepage bag and the elevation of the water is always higher than the elevation of water outside the wetland, indicating that water flow is downward.

Table 4.1. Discharge rates obtained from seepage measurements.

Location	Average Discharge Rate cm/day
147 (near 102)	0.00400
157	Recharge
140	0.133

Water samples were collected using passive diffusion samplers (‘‘peepers’’) (Hesslein, 1976). Custom peepers were designed to span a vertical profile of 75 cm capturing the sediment-water interface as well as interfaces across the wetland-aquifer transition zone with a total of 75 horizontal ports with apertures and spacing of 0.5 cm covered by a Millipore® membrane with a pore size of 0.45 μm. An additional shorter peeper consisting of 21 ports over two centimeter intervals was used for P140 S and P157 M. Peeper ports were filled with nanopure water (18 mΩ) and deoxygenated with nitrogen for three days to remove oxygen from the water and plastic samplers. Peepers were transported in an anaerobic PVC-constructed chamber to the site and maintained under deoxygenated conditions until deployment into the wetland sediments and were left to equilibrate in the sediments for two weeks (Azcue et al., 1996; Jacobs, 2002; Webster et al., 1998). The samples were processed immediately after collection in an anaerobic glove bag filled with an N_2 atmosphere.

Geochemical Analysis

Geochemical parameters collected represent indicators of biotic and abiotic redox processes, as well as indicators of landfill leachate measured with the purpose of understanding biogeochemical process in the wetland-aquifer system. Dissolved oxygen, pH, conductivity, temperature, and redox potential were measured using a 600 XLM YSI Hydrodata multiparameter meter* (Yellow Springs, OH USA) to describe surface water conditions in the wetland when the peepers were inserted and when they were removed. From each peeper port, water samples were measured for alkalinity, Fe^{2+} and H_2S immediately in the field using electrometric titration and colorimetric spectroscopy according to standard methods (APHA et al., 2005). Water samples for the analysis of elements that participate in mineral dissolution and biogeochemical reactions such as Na, K, Ca, Mg, Mn, Ba, and Fe were preserved in 1% metal grade hydrochloric acid, stored on ice, and refrigerated to be analyzed by inductively coupled plasma – mass spectrometer (ICP-MS). Samples analyzed for NH_4^+ and organic acids (acetate and propionate) were flash frozen with dry ice and analyzed by capillary electrophoresis (CE) (Agilent Technologies, Germany) in the laboratory (Baez-Cazull et al., 2007a). Water samples preserved with 0.5% formaldehyde, stored on ice and refrigerated, were analyzed to measure concentrations of anions (SO_4^{2-} and Cl^-) by CE. Water samples for CH_4 analyses were collected in Glasspak syringes that were connected directly to the sample-pump outlet (Baedecker and Cozzarelli, 1992). These water samples were transferred to 25-mL serum bottles flushed with He.

Data Analysis

The data were analyzed using multivariate factor analysis using SAS software JMP® (SAS Institute, 1999). The data arranged in R-mode factor analysis included the following geochemical variables: acetate, propionate, methane, ammonium, sulfate, pH, Na, K, Ca, Mg, Fe^{2+}, Cl^-, HCO_3^-, H_2S, butyrate, Mn, Ba, and Fe^{3+}(Total iron – Fe^{2+}). The complete dataset was tested for normality using various mathematical transformations, such as the natural logarithm, square root, inverse and power transformations. For each of the transformations, the data were tested for normality by evaluating boxplots, normal quantile plots (Q-Q plots of expected normal value vs. observed value), and Kolmogorov-Smirnov (K-S) tests for goodness of fit. The transformations tested did not help in fitting the dataset to a normal distribution using a uniform equation for all the parameters. As a result, conservative nonparametric statistical tests were chosen to avoid assumptions of the data being normally distributed. To parameterize large differences in scale among the chemical parameters, the data were standardized using z-scores (Güler et al., 2002; Thyne et al., 2004). A nonparametric Spearman's Rho correlation analysis was performed on the standardized data. A pairwise correlation matrix was selected to exclude cases with missing data. A factor analysis was performed on the correlation matrix using the standardized dataset.

Factor Analysis and ANOVA

A principal component analysis was performed to determine the factors that best explain the variation in the dataset. Factors were rotated using varimax orthogonal

rotation to maximize the relationship between the variables and some of the factors. Factor scores were computed from the factor analysis (PCA) and were used as input for Analysis of Variance (ANOVA). ANOVA is a common test used to determine if multiple means are significantly different. The statistical analysis is designed to test the null hypothesis that separate sets of data have the same mean, by testing if the variation within groups is the same as the variation between groups. A one-way ANOVA was evaluated for factors 1 through 5, with each factor containing multiple levels (P102M, P102S, P140M, P140S, P157M, and P157S) corresponding to the different hydrological locations measured in May and September. This test was performed to determine significant differences among hydrologic regimes and seasons using multiple comparisons tests. Factor scores were not normally distributed therefore a non-parametric Wilcoxon/Kruskall Wallis test was considered for ANOVA results. An all pairs Tukey-Kramer test was performed to determine difference in means from multiple comparisons (P102M, P102S, P140M, P140S, P157M, and P157S) when the probability resulting from Levene's test on homogeneity of variances was less than 0.01.

PCA on Each Location

An individual PCA was performed for each sampling location for May and September to determine the processes that best explain the variability in the dataset and infer the dominant biogeochemical processes. Factors were rotated using varimax orthogonal rotation to maximize the relationship between the variables and some of the

factors. Biogeochemical processes were interpreted from the parameters factor loadings on the factor that explained most of the variability (factor 1 for each PCA).

RESULTS AND DISCUSSION

Correlation Matrix and PCA

Spearman's Rank Order Correlation test was chosen as a non-parametric method to estimate the degree in which two variables vary together. Outliers were evaluated but were not discarded since they represent important maximum and minimum gradients in the profile concentrations. The resulting correlation matrix is plotted in Figure 4.2 and only includes correlations that had a significant $p<0.0001$. Since large sample sets can result in low p-values suggesting a significant correlation when the actual correlation is low, only values having a Rho value larger than 0.5 were considered significant. Among the highest positive correlations is Cl^- and Na (rho = 0.85), Fe^{3+} and Ca (rho = 0.71), and Mg and Ca (rho = 0.70). Among the negative stronger correlations is H_2S and Fe^{2+} (rho = -0.85) and H_2S and SO_4^{2-} (rho = -0.54). From the resulting Spearman Rho correlations a PCA was evaluated. Results shown in Table 4.2 include eigenvalues (a measure of the variability of a factor), percent of total variance, and cumulative percent variance. Factors with an eigenvalue greater than 1 were considered significant in explaining the variability of the dataset according to the Kaiser (1960) criterion. The first five factors explaining 76% of the variability contain eigenvalues greater than one, thus the varimax factor rotation was performed on five factors (Table 4.2).

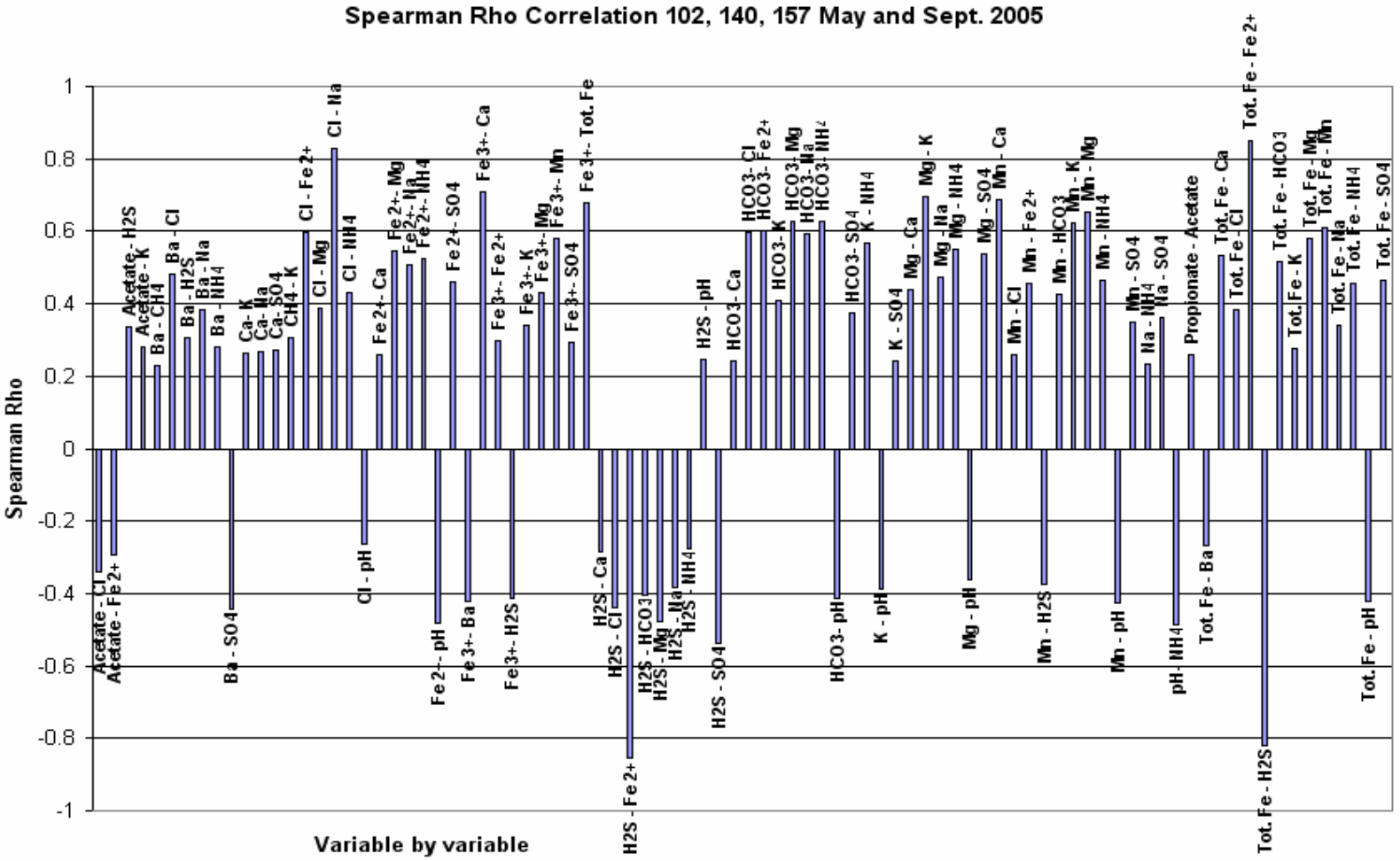

Figure 4.2. Spearman Rho correlation analysis with Rho probabilities <0.0001.

Table 4.2. Principal Component Analysis (PCA) on complete dataset from sites 102, 140, and 157 in May and September. Eigenvalues and percent variability accounted in each factor.

Factor	Eigenvalue	Percent	Cumulative Percent
1	4.745673	27.91572	27.91572
2	2.724971	16.02924	43.94496
3	2.362691	13.89818	57.84314
4	1.917538	11.27964	69.12278
5	1.136908	6.687694	75.81048
6	0.785584	4.621085	80.43156
7	0.675703	3.974726	84.40629
8	0.593126	3.488979	87.89526
9	0.463983	2.729313	90.62458
10	0.365181	2.148126	92.7727
11	0.333594	1.962316	94.73502
12	0.291701	1.71589	96.45091
13	0.230212	1.354187	97.8051
14	0.154139	0.906698	98.71179
15	0.137422	0.808364	99.52016
16	0.047799	0.281172	99.80133
17	0.033774	0.19867	100

Factor Interpretation

Factor loadings obtained from five factors are presented in Figure 4.3-4.7. Loadings approaching ±1 indicate a strong correlation of a variable with a factor, whereas loadings approaching 0 indicate weak correlations. Loadings higher than ±0.75 are considered strong correlations, while loadings between ±0.5 and ±0.74 are considered to be moderately correlated (McGuire et al., 2005; Wayland et al., 2003).

Based on the loadings, a factor can be interpreted as a process as indicated by the associations among parameters that load highly in each factor.

Factor 1 explains 28% of the variability and shows strong positive loadings by geochemical parameters SO_4^{2-}, Ca, Mg, Fe^{3+} and Mn (Figure 4.3). This factor was interpreted as *mineral dissolution* and *oxidation processes*. Other studies have interpreted factors containing Ca and Mg as dissolution processes by weathering (Puckett and Bricker, 1992; Schot and van der Waal, 1992; Wayland et al., 2003) from dissolution of calcite and dolomite. The grouping of SO_4^{2-} and Fe^{3+} in this factor is an indication of oxidation of iron sulfide minerals.

Factor 2 explains 16% of the variability in the dataset and is highly positively loaded with respect to Cl^-, Na, HCO_3^-, and Ba (Figure 4.4). These parameters are likely indicators of the presence of aquifer water. Cl, Na, and HCO_3^- have been found in elevated concentrations in the aquifer leachate plume and Cl^- is often used as an indicator of leachate transport (Grossman et al., 2002; Röling et al., 2001; van Breukelen and Griffioen, 2004). In this plume, elevated barium concentrations may also indicate the presence of landfill leachate. Previous studies have shown that the core of the leachate plume is depleted with respect to electron acceptors (Cozzarelli et al., 1999b). Under these conditions the mineral barite ($BaSO_4$) can be utilized as a source of sulfate by sulfate reducing bacteria. Barite utilization at this site has been previously suggested (Ulrich et al., 2003). This factor was interpreted as *plume advection*.

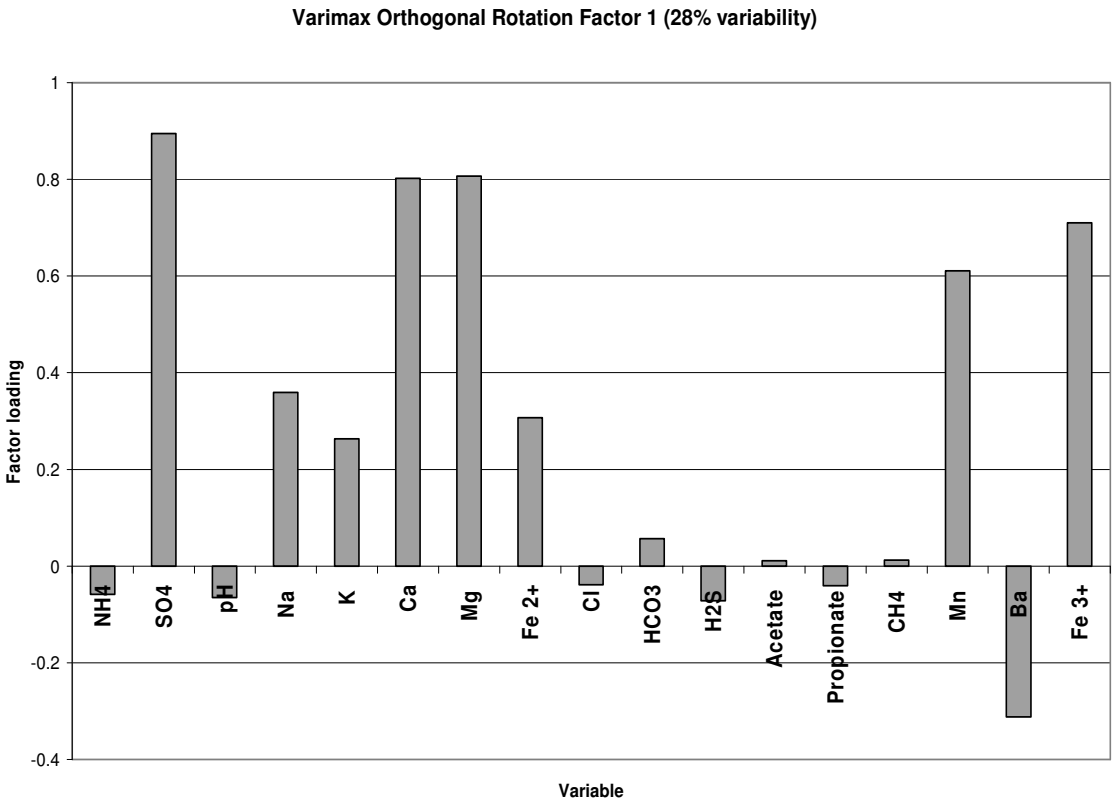

Figure 4.3. Factor loadings on rotated Factor 1. Loadings higher than 0.5 are considered to be significant in the factor. Factor processes were interpreted as *mineral dissolution* and *oxidation*.

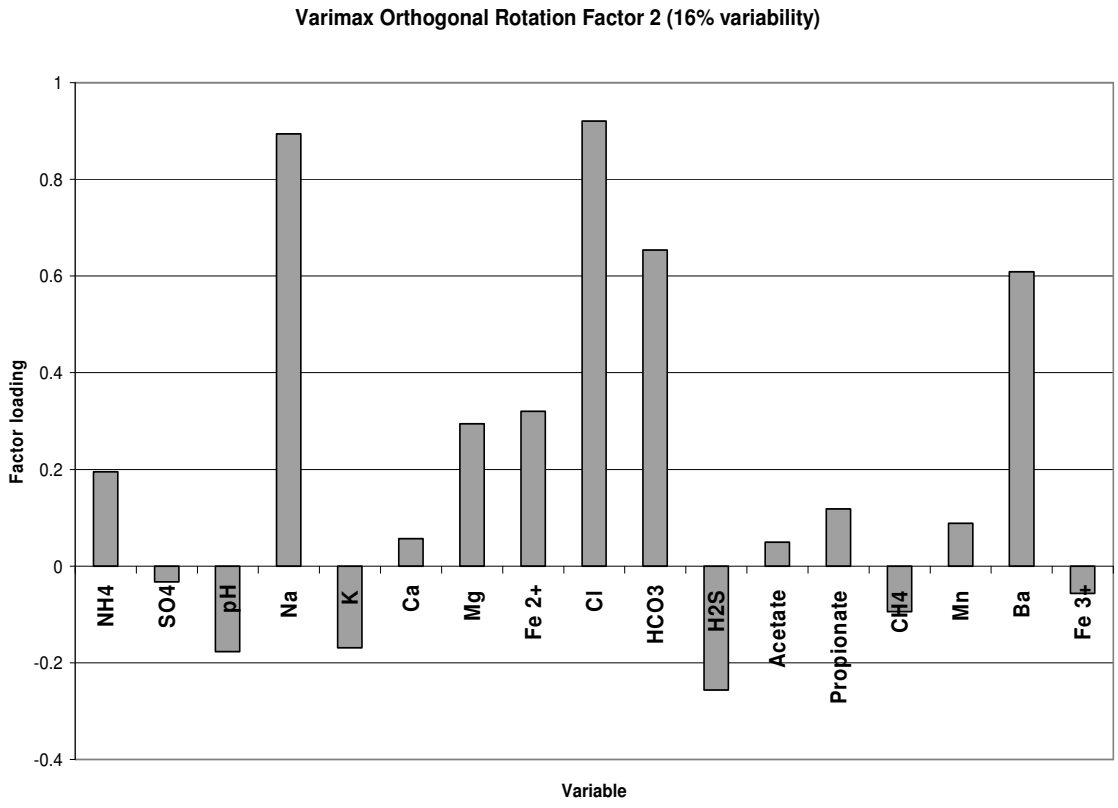

Figure 4.4. Factor loadings on rotated Factor 2. Loadings higher than 0.5 are considered to be significant in the factor. Factor process was interpreted as *plume advection*.

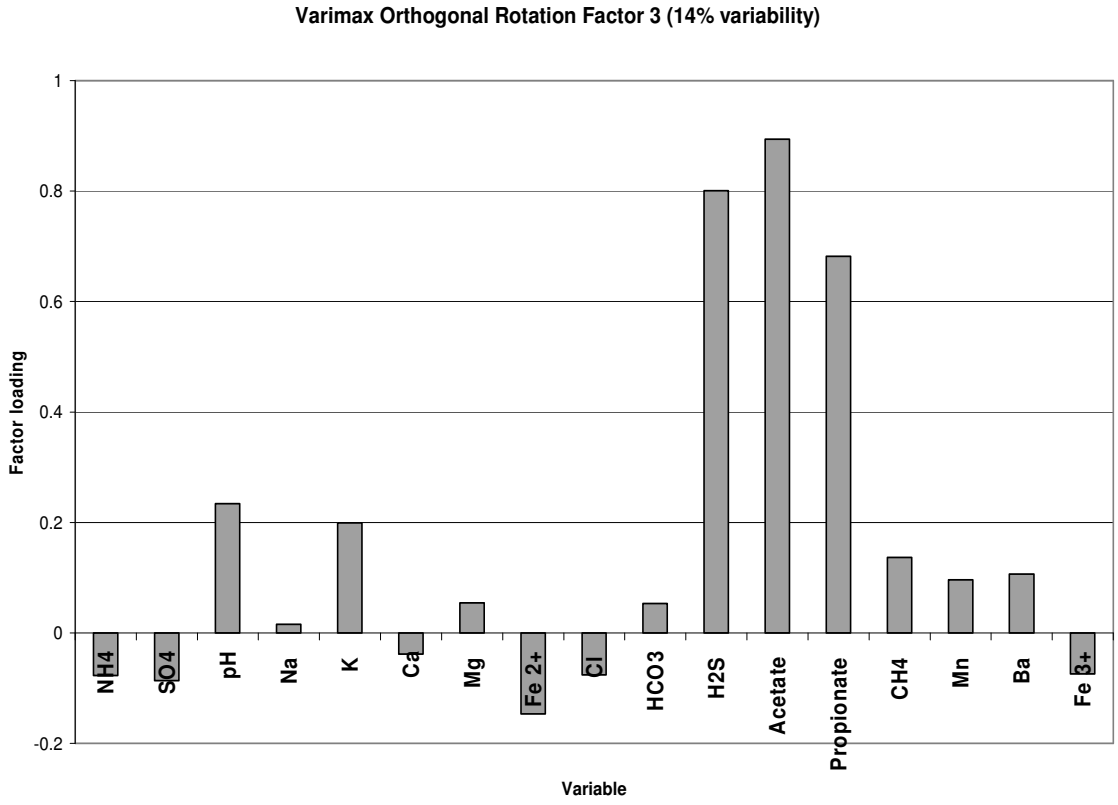

Figure 4.5. Factor loadings on rotated Factor 3. Loadings higher than 0.5 are considered to be significant in the factor. Factor processes were interpreted as *fermentation* and *sulfate reduction*.

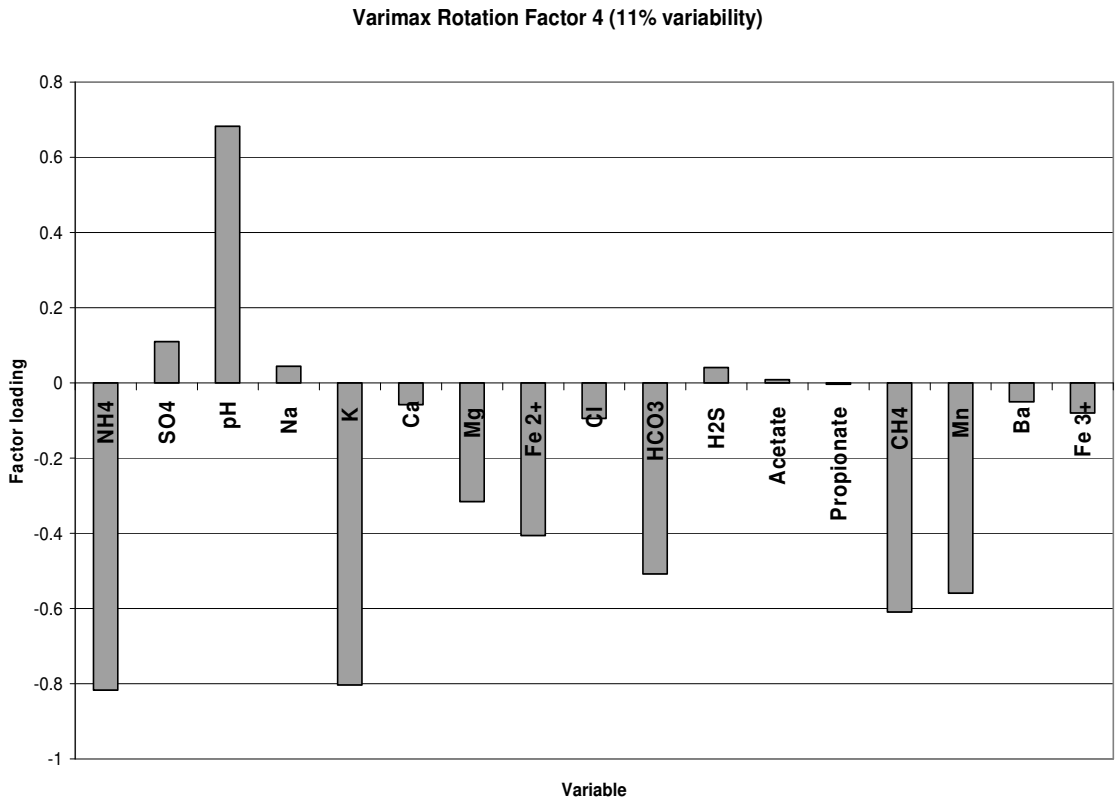

Figure 4.6. Factor loadings on rotated Factor 4. Loadings higher than 0.5 are considered to be significant in the factor. Factor processes were interpreted as *organic degradation* and *methanogenesis*.

Factor 3 explains 14% of the variability and contains high loadings by parameters acetate, propionate and sulfide (Figure 4.5). Acetate and propionate are byproducts of fermentation processes in wetland sediments (Duddleston et al., 2002; Hines et al., 1994; Kostka et al., 2002; Shannon and White, 1996; Wellsbury and Parkes, 1995), and can be quickly utilized as electron donors coupled to sulfate and iron reduction reactions. In this case, the high loading of sulfide in this factor suggests sulfate reduction correlates to the availability of organic acids. The processes assigned to this factor are *fermentation* and *sulfate reduction*.

Factor 4 explains 11% of the variability and is represented by strong negative correlations with NH_4^+, K, and CH_4, and a positive correlation in pH (Figure 4.6). High concentrations of NH_4^+ are indicators of organic matter degradation which have been observed in the wetland sediments (Baez-Cazull et al., 2007a) and in the aquifer leachate plume (Cozzarelli et al., 1999b). Methane is the result of organic matter degradation in highly reduced environments where methanogenesis becomes the favorable metabolic pathway. The high loading of K in this factor may indicate mineral dissolution of potassium-bearing minerals associated to the degradation of organic matter. In a previous study (Baez-Cazull et al., 2007b) K and CH_4 were found to be highly correlated and associated to the dissolution of Ba. It is hypothesized that the releases of K is a result of mineral dissolution reactions promoted by the use of electron acceptors from minerals in highly reduced environments. Thus this factor was interpreted as *organic matter degradation* via *methanogenesis* resulting in *K dissolution* (Baez-Cazull et al., 2007b).

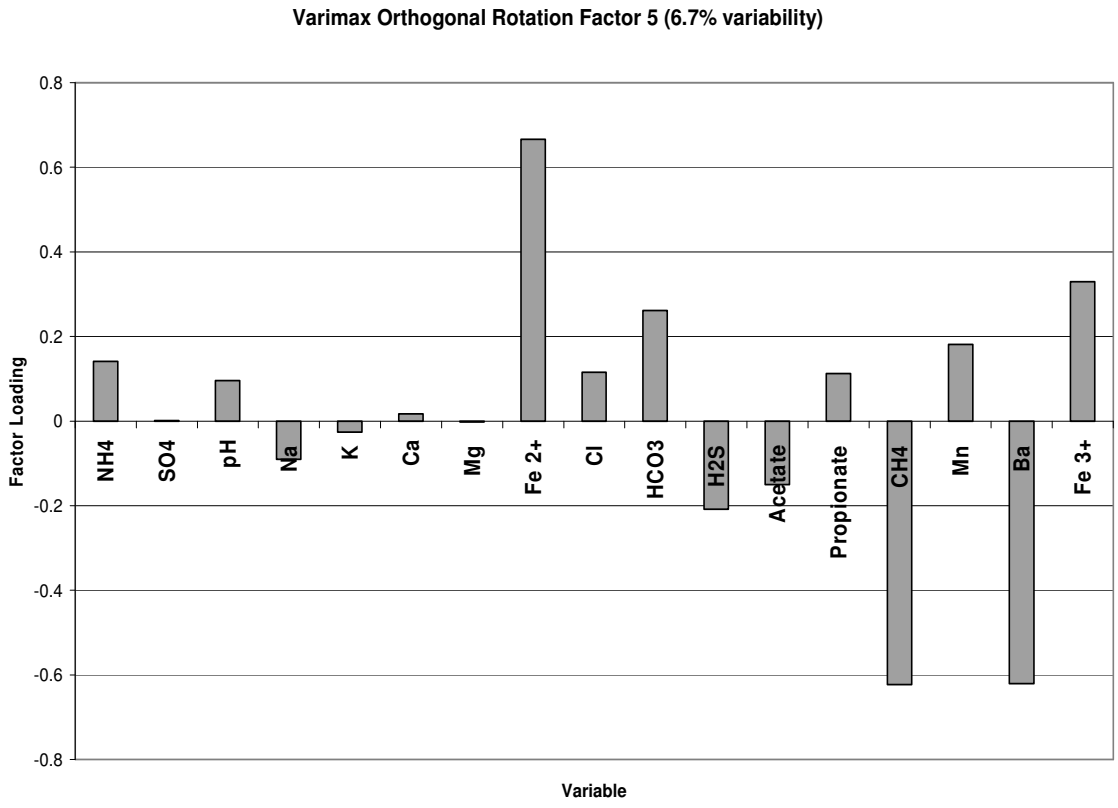

Figure 4.7. Factor loadings on rotated Factor 5. Loadings higher than 0.5 are considered to be significant in the factor. Factor processes were interpreted as *iron reduction*, *methanogenesis*, and *barite utilization* in sulfate reduction.

Factor 5 explains 6.7% of the variability and is represented with high positive factor loadings by Fe^{2+} and significant negative loadings by Ba and CH_4 (Figure 4.7). The high concentrations of Fe^{2+} in this environment are interpreted as a product of iron reduction reactions somewhere in the system. In the absence of sulfides, Fe^{2+} is subject to transport in anaerobic systems. The negative loadings of Ba and CH_4 are interpreted as methanogenesis and barite utilization for sulfate reduction in the absence of alternate electron acceptors. The opposite factor loadings (positive for Fe^{2+} and negative for CH_4 and Ba) is an indication that the processes are not occurring simultaneously. Thus this factor is expressed as *iron reduction* represented with positive scores and *methanogenesis/barite utilization* represented with negative scores.

One-Way ANOVA on Hydrologically Different Sites

To evaluate the effect of hydrological fluctuations for each factor (process), a one-way ANOVA (single factor) was performed using the nonparametric Wilcoxon/Kruskall-Wallis test. Results for each of the five tests are shown in Figures 4.8 through 4.12, which show diagrams comparing multiple groups. The factor scores' means are represented by diamond shapes. Diamonds that overlap in the y axis represent groups that have no difference in the means. An additional test for multiple comparisons, an all pairs Tukey Kramer, show which groups have similar means via overlapping circles. The table in the diagram marks the groups that have significant different means.

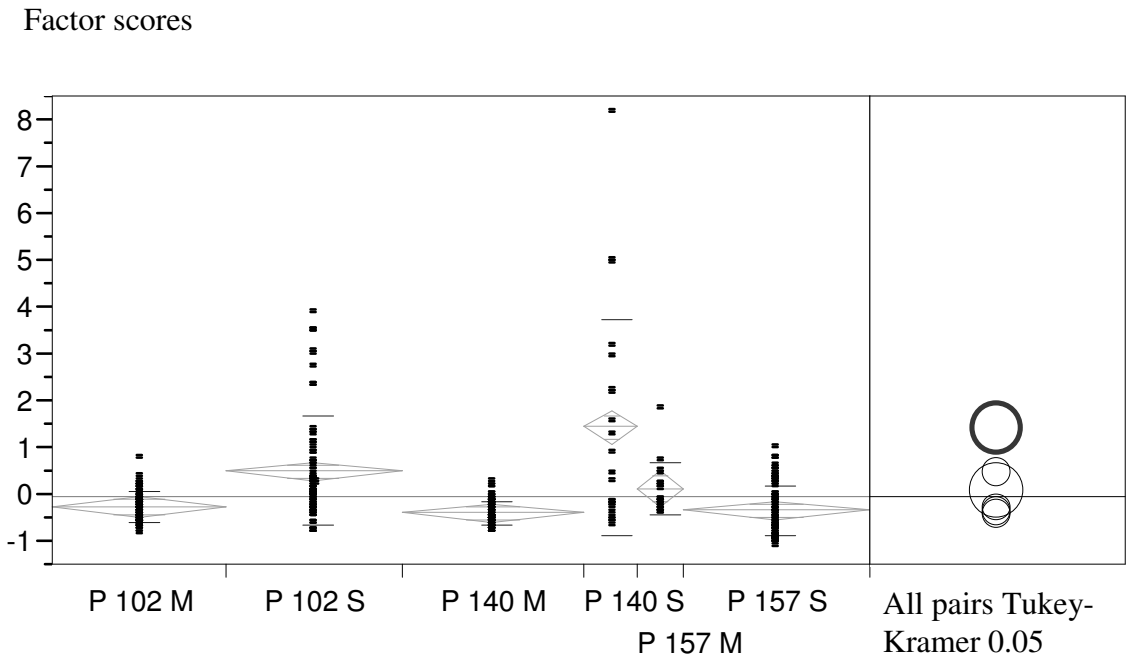

Factor 1	P140S	P102S	P157M	P102M	P157S	P140M
P140S		+	+	+	+	+
P102S	+			+	+	+
P157M	+					
P102M	+	+				
P157S	+	+				
P140M	+	+				

Figure 4.8. One-way ANOVA for Factor 1 (*mineral dissolution/oxidation*). Overlapping diamonds validate the null hypothesis which suggests there is no difference in means. Bars indicate range in homogeneity of variances using Levine's test. Multiple comparisons between groups were tested via Tukey-Kramer statistics and represented by circles in the diagram. Overlapping circles indicate no difference in means between pairs. Positive symbols in table show pairs of means that are significantly different.

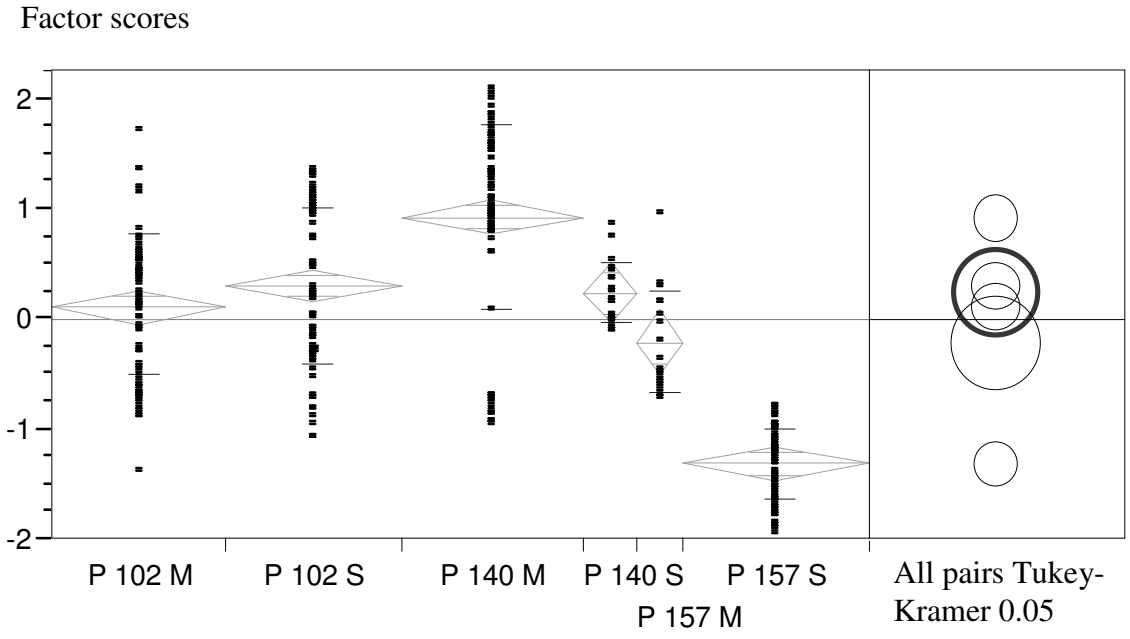

Factor 2	P140M	P102S	P140S	P102M	P157M	P157S
P140M		+	+	+	+	+
P102S	+				+	+
P140S	+					+
P102M	+					+
P157M	+	+				+
P157S	+	+	+	+	+	

Figure 4.9. One-way ANOVA for Factor 2 (*plume advection*). Overlapping diamonds validate the null hypothesis which suggests there is no difference in means. Bars indicate range in homogeneity of variances using Levine's test. Multiple comparisons between groups were tested via Tukey-Kramer statistics and represented by circles in the diagram. Overlapping circles indicate no difference in means between pairs. Positive symbols in table show pairs of means that are significantly different.

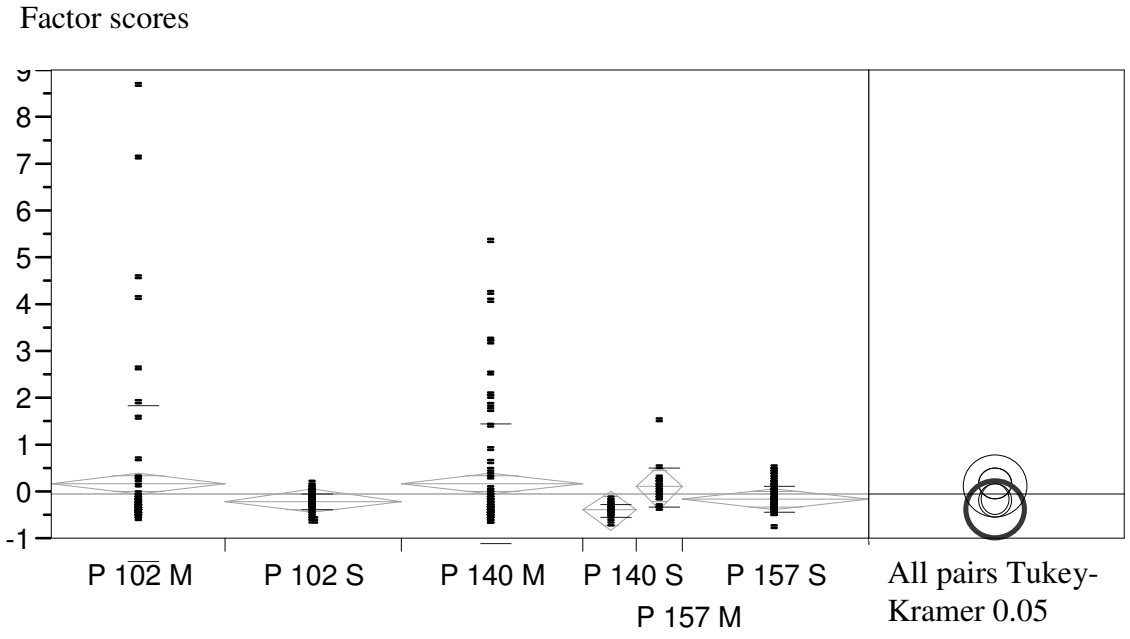

Factor 3	P140M	P102M	P157M	P157S	P102S	P140S
P140M						
P102M						
P157M						
P157S						
P102S						
P140S						

Figure 4.10. One-way ANOVA for Factor 3 (*fermentation/SO_4^{2-} reduction*). Overlapping diamonds validates the null hypothesis which suggests there is no difference in means. Bars indicate range in homogeneity of variances using Levine's test. Multiple comparisons between groups were tested via Tukey-Kramer statistics and represented by circles in the diagram. Overlapping circles indicate no difference in means between pairs. Positive symbols in table show pairs of means that are significantly different.

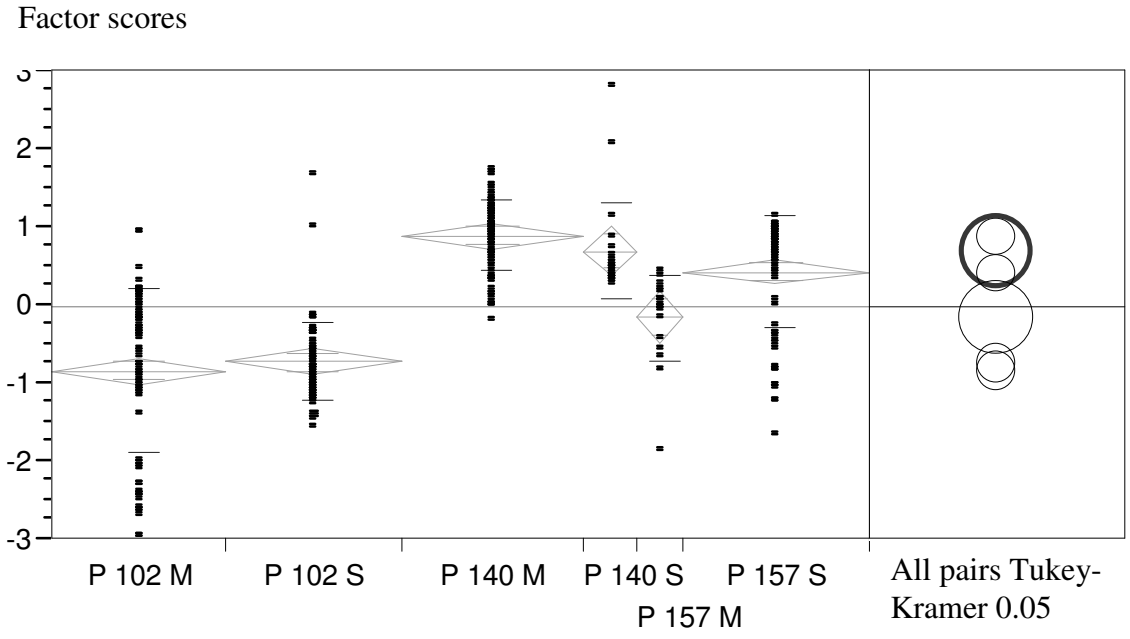

Factor 4	P140M	P140S	P157S	P157M	P102S	P102M
P140M			+	+	+	+
P140S				+	+	+
P157S	+			+	+	+
P157M	+	+	+		+	+
P102S	+	+	+	+		
P102M	+	+	+	+		

Figure 4.11. One-way ANOVA for Factor 4 (*organic degradation/methanogenesis*). Overlapping diamonds validates the null hypothesis which suggests there is no difference in means. Bars indicate range in homogeneity of variances using Levine's test. Multiple comparisons between groups were tested via Tukey-Kramer statistics and represented by circles in the diagram. Overlapping circles indicate no difference in means between pairs. Positive symbols in table show pairs of means that are significantly different.

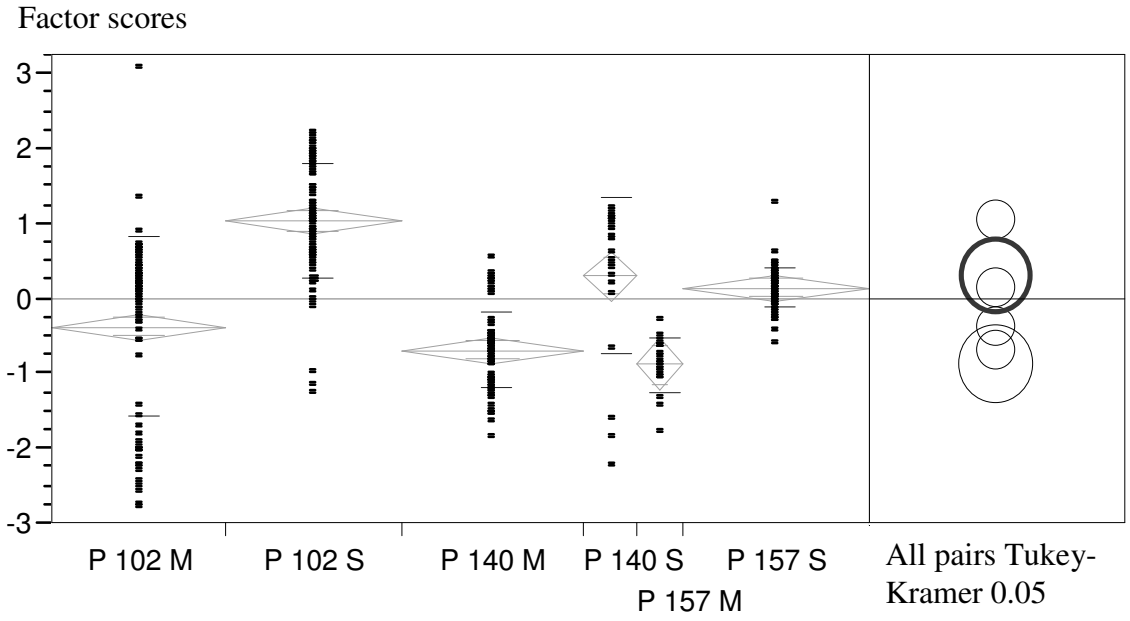

Factor 4	P102S	P140S	P157S	P102M	P140M	P157M
P102S		+	+	+	+	+
P140S	+			+	+	+
P157S	+			+	+	+
P102M	+	+	+			
P140M	+	+	+			
P157M	+	+	+			

Figure 4.12. One-way ANOVA for Factor 5 (*iron reduction/methanogenesis/barite utilization*). Overlapping diamonds validates the null hypothesis which suggests there is no difference in means. Bars indicate range in homogeneity of variances using Levine's test. Multiple comparisons between groups were tested via Tukey-Kramer statistics and represented by circles in the diagram. Overlapping circles indicate no difference in means between pairs. Positive symbols in table show pairs of means that are significantly different.

In Figure 4.8, the results for *Factor 1* are interpreted as *mineral dissolution* and *oxidation,* showing higher means overall in September than in May. In September the water table drops causing Fe-S and manganese-bearing minerals to oxidize in the upper 10 centimeters and become available at the water table interface. Sulfate concentrations above the water table interface are ~2350 ppm in September versus ~140 ppm in May. It has been demonstrated that increases in sulfate in oxic/anoxic zones stimulate dissimilatory sulfate reduction (Novák et al., 1994). The availability of Fe^{3+} also suggests that iron reduction may also be enhanced at the water table interface in September. The mineralization process of organic matter by the reduction of iron oxyhydroxides releases minerals and nutrients to the dissolved phase such as Fe^{2+} and Mn. The higher temperatures in September also increase mineralization of organic matter by enhancing microbial activity (Bally et al., 2004). Enhanced microbial activity and lower pH (data not shown) promote mineral dissolution and release of Ca and Mg.

Sites P102S and P140S were strongly associated with this factor because the lower water table conditions in September exposed previously reduced surface sediments to oxygen. Location 140 had no water ponded, and the water table was 10 cm below the surface. Thus, this factor was expressed more strongly here than at location 102 where a small stream of water was observed. According to the multiple comparisons test (Tukey-Kramer), location 140 in September showed a significantly different mean than all other sampling events and locations. Location 157 in September did not exhibit oxidation, as expected, because this location always has standing water due to a beaver dam.

Factor 2 representing *plume advection* best describes the hydrological regimes of the different locations. Generally, this indicates groundwater flow discharging into the wetland in May when recharge occurs and water table is high, and surface water flowing downward into the aquifer in September when the water table decreases. Site 140, which was the site with the most discharge from the contaminated aquifer into the wetland sediments (Table 4.1), exhibits high positive factor scores strongly indicating upward plume advection (Figure 4.9). Site 140 in May was significantly different than all other sites at either May or September as indicated by the Tukey-Kramer test. The factor mean for site 140 in May vs. September is different indicating a significant seasonal influence in the discharging fluxes when the aquifer is recharged in May with greater discharge into the wetland vs. when the aquifer is becoming depleted in September resulting in a lower mean in this factor. The positive factor scores for P140S indicate that the location is still discharging in September but not as much as it was for P140M. This is consistent with interpretations of geochemistry data from prior years (Lorah et al., 2007).

Location 157 was selected because water flows from the surface to the aquifer (Table 4.1). In the ANOVA results, the factor scores for this location and the means are represented with negative factor scores indicating that plume advection was not associated with this location. Na and Cl^- concentrations at site 157 are lower with a composition more like the surface water than the aquifer plume supporting this interpretation. There is also a seasonal difference in the means for location 157. In September, the mean is more negative and is interpreted as an increased flux of surface

water into the aquifer due to the lower water table in the aquifer during the dryer and warmer conditions.

Location 102 was selected because it shows neither recharge nor discharge. This is supported by the result that the means of the factor scores for locations P102M and P102S are not significantly different and the values fall closer to the 0 line indicating no effect from advection processes. However, their means are significantly different from the discharge fluxes in P140M and recharge in P157S.

One-way ANOVA comparing the different locations for *Factor 3*, *fermentation* and *sulfate reduction*, results in no significant differences in the means for all the locations and sampling events (Figure 4.10). This suggests that fermentation and sulfate reduction are not affected by changes in season or hydrological fluxes. Electron donors such as acetate and propionate are present in all sites and in both months indicating that electron donor availability is not limiting. Fermentation processes occur independent of hydrologic flows and seasonal changes. Sulfate reduction associated with the oxidation of acetate and propionate occurs at all sites and both months.

Factor 4 interpreted as an *organic degradation* and *methanogenesis* with negative factor scores show significant differences in means among locations 102 and 140, and 102 and 157 (Figure 4.11). Locations 140 and 157 did not show difference in their means. From this analysis the significant differences in the factors are attributed to hydrological fluxes specific to the sites and not to seasonal hydrological changes observed in May vs. September. Methanogenesis and organic degradation strongly associates with location 102 where no flow is detected. In the locations with discharge

or recharge fluxes as it is in site 140 and 157 methanogenesis and organic degradation were not observed. For a system to reach methanogenic conditions it should be limited in electron acceptors, and this often occurs in systems that are waterlogged and do not exhibit hydrological fluxes. In sites 140 and 157 electron donors can be supplied from water moving from oxygenated surface water or aquifer water. The constant flow in these two locations do not allow for methanogenic conditions to persist.

Results for the one-way ANOVA for *Factor 5*, *iron reduction*, *methanogenesis*, and *barite utilization* for sulfate reduction, are shown in Figure 4.12. For this factor, a hydrological, site specific component is not observed indicating that water flow is not a significant control for this factor. Rather this factor is controlled by seasonal hydrological changes such as the lowering of the water table as observed in the separation of means in May vs. September. Methanogenesis and barite utilization are significant in May as indicated by negative factor scores, whereas iron reduction is observed in September attributed to the availability of iron oxides when the water table drops exposing the first 10 cm of sediments to oxygen. The resulting increase in iron hydroxides stimulates microbial iron reduction at the oxic/anoxic interface and therefore we observed an increase in Fe^{2+} being produced in September. During the waterlogged conditions in May, electron acceptors such as SO_4^{-2} and Fe^{2+} become depleted resulting in alternate reaction pathways for the mineralization of organic matter such as methanogenesis and sulfate reduction utilizing barite minerals as a sulfate source (Baez-Cazull et al., 2007b). The only location with significantly different means was site 102

in September. This is an indication that iron reduction in this location was greater than in any of the other locations.

Description of Dominant Processes at Each Location in May and September

To identify the dominant biogeochemical processes at various hydrologic locations in May and September, an individual PCA was performed for each location at each month. In the first analysis, the entire dataset was used to obtain factors that were then analyzed via one-way ANOVAs for spatial and temporal comparisons. Here, the PCA was performed on the site specific datasets to identify the dominant processes at each location. The factor obtained from each PCA with the highest percentage in variability (i.e. factor 1) was considered to be the dominant process for that location.

In Table 4.3 significant factor loadings (greater than 0.5) for the first factor are displayed for each location and event. Due to the multiple parameters loading high in the first factor it is most likely that multiple processes describe each factor. These processes are loaded in the first factor because they are linked causing geochemical parameters to vary together. For example, Factor 1 for P102M, explaining 28% of the variability in the dataset, has high loadings in CH_4 and K which are interpreted as methanogenesis indicators. In addition, Ba, NH_4^+, and Mn are heavily loaded in this factor interpreted as mineral dissolution linked to mineralization of organic matter producing high concentrations of NH_4^+. Chloride and pH are loaded oppositely indicating that Cl^-, interpreted as plume advection, is not associated with methanogenic

Table 4.3. Factor loadings for the first factor explaining most of the variability in the dataset. Factors were rotated from a PCA on each sampling location by season. Shown are significant factor loadings greater than 0.5. Dashes were parameters that were not included in the analysis.

Variability Factor 1	**28%**	**32%**	**36%**	**47%**	**51%**	**36%**
Sample ID	**P102M**	**P102S**	**P140M**	**P140S**	**P157M**	**P157S**
NH4	0.731703	-0.70278	-0.64542		-0.71329	-0.89503
SO4		0.94525	0.805607	-0.84236	-	
pH	-0.63171		0.689515		0.781871	
Na			-0.90888	-0.91206	-0.78818	-0.69432
K	0.908455				-0.9425	-0.93435
Ca		0.521534		-0.8847		
Mg		0.828469		-0.8654	-0.97772	-0.92
Fe 2+				0.602329		
Cl	-0.56306	-0.61948	-0.84273	-0.82696	-0.89982	
HCO3		-0.80917	-0.78653		-0.97858	-0.83361
H2S						
Acetate					-0.84073	
Propionate		-		-	-	-
CH4	0.909026		-0.66022			
Mn	0.674339					
Ba	0.895575		-0.97399		-0.88071	-0.79955
Fe 3+				-0.90431		
Process	**(+)Methanogenesis / barium dissolution**	**(-) oxidation, mineral dissolution (-) organic degradation, evaporation**	**(-)Plume advection/ (-)barium dissolution (+)Oxidation**	**(-) Oxidation, Mineral dissolution, plume advection**	**(-) organic degradation, mineral dissolution, fermentation, plume advection**	**Organic degradation, mineral dissolution, barium**

conditions. These results suggest that in May, site 102 was highly reduced and mineralization of organic matter was mainly occurring by methanogenesis which caused mineral dissolution (Figure 4.13 a). In September, the dominant processes at site 102 differ from May, affected by the seasonal and hydrological conditions. Sulfate, magnesium, and calcium are positively loaded in this factor. Sulfate is an indicator of oxidation in the wetland. Sulfate is produced through oxidation of sulfide minerals when the lower water tables expose sediments to oxygen during this month. Sulfate concentrations are high in the upper 15 centimeters in the wetland sediments and decrease sharply below 20 cm at the water table interface (Figure 4.13 b). Higher sulfate stimulates sulfate reduction near the oxic/anoxic boundary and indirectly can cause mineral dissolution. Sulfate levels decrease at approximately 20 to 35 cm depth in the sediments; an increase of NH_4^+ and alkalinity is observed indicating organic mineralization (Figure 4.13 b). Unlike in May, sulfate concentrations increase at 35 to 45 cm depth, the location of a coarse sand layer. Elevated sulfate concentrations in conjunction with lower Cl^- concentrations at this location suggest that this zone is being recharged from the surface (Baez-Cazull et al., 2007b). The increased supply of sulfate into the sediments, both at the water table and sand-layer boundaries, cause sulfate reduction to be the dominant TEAP in September instead of methanogenesis as was observed in May. It is clear from this analysis that the dominant biogeochemical processes in location 102 in May and September have changed due to water table fluctuations.

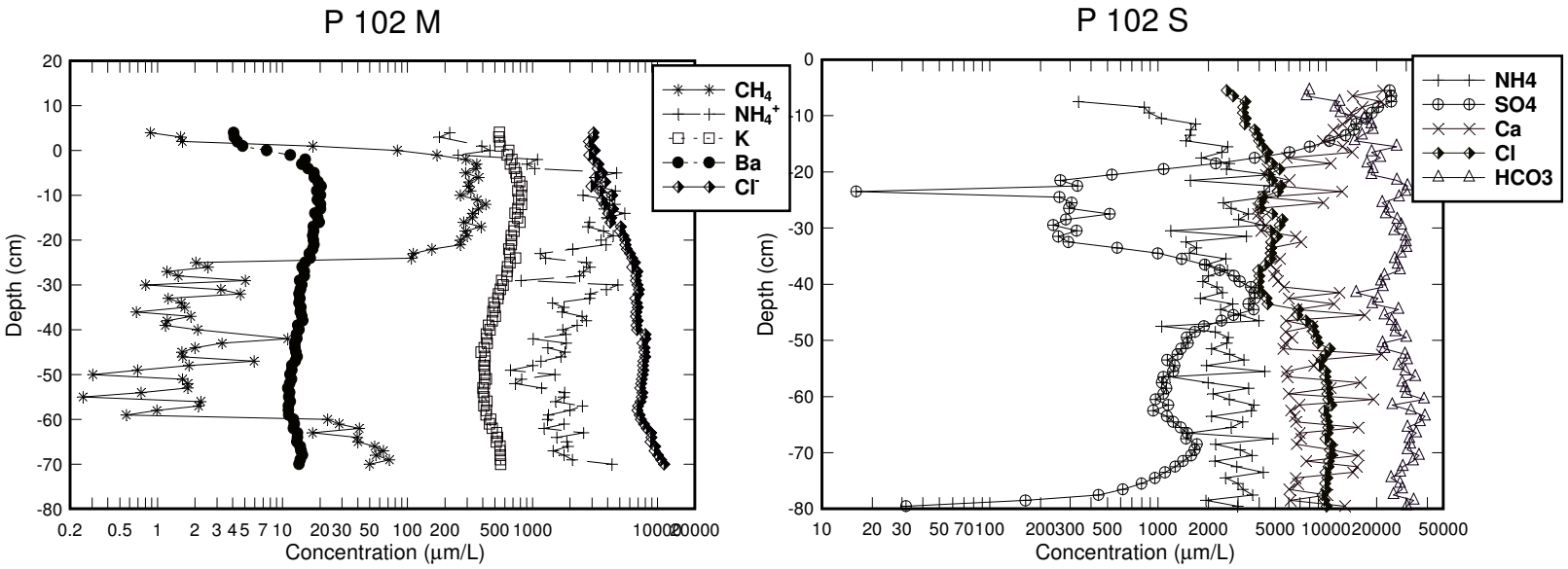

a) b)

Figure 4.13. Profiles of geochemical parameters in location 102 that yielded higher factor loadings for Factor 1 obtained from PCA. a) May and b) September.

Factor 1 for location 140 in May is positively loaded with sulfate and pH, and negatively loaded with Ba, Na, Cl^-, alkalinity, methane, and NH_4^+. Sulfate concentrations are high in the surface water of the wetland (Figure 4.14 a) and decrease at the sediment-water interface at 0 cm. CH_4 and NH_4^+ are loaded opposite to sulfate, indicating mineralization of organic matter in the absence of sulfate. Below the sediment-water interface, methane concentrations increase when sulfate concentrations decrease (Figure 4.14 a). Chloride concentrations are constant below the sediment-water interface, due to aquifer discharge since the composition of the sediments at this site are sandier than the other two sites which are mostly silt (data not shown). Alkalinity and ammonium, which are also found in elevated concentrations in the plume, are associated with Cl^- supporting upward plume advection. However, ammonium concentrations vary at the location where methanogenesis and sulfate reduction occur due to microbial activity (Figure 4.14 a).

Site 140 in September, exhibits positive high loadings for Fe^{2+} and negative high loadings for Fe^{3+}, sulfate, Cl^-, Mg and Ca. The processes inferred by these parameters include oxidation of iron minerals producing Fe^{3+} and sulfate due to the lower water table, evapotranspiration causing concentrated sodium chloride, and dissolution of minerals. Oxidizing conditions are found in the upper 10 cm of the sediments where Fe^{3+} and sulfate are high (Figure 4.14 b). Below this point iron reduction and sulfate reduction occur. Calcium concentrations correlate with sulfate concentrations in the upper 20 cm perhaps due to dissolution of gypsum minerals. Below this depth there is a decrease in iron reduction and an increase in sulfate reduction, causing the correlation of

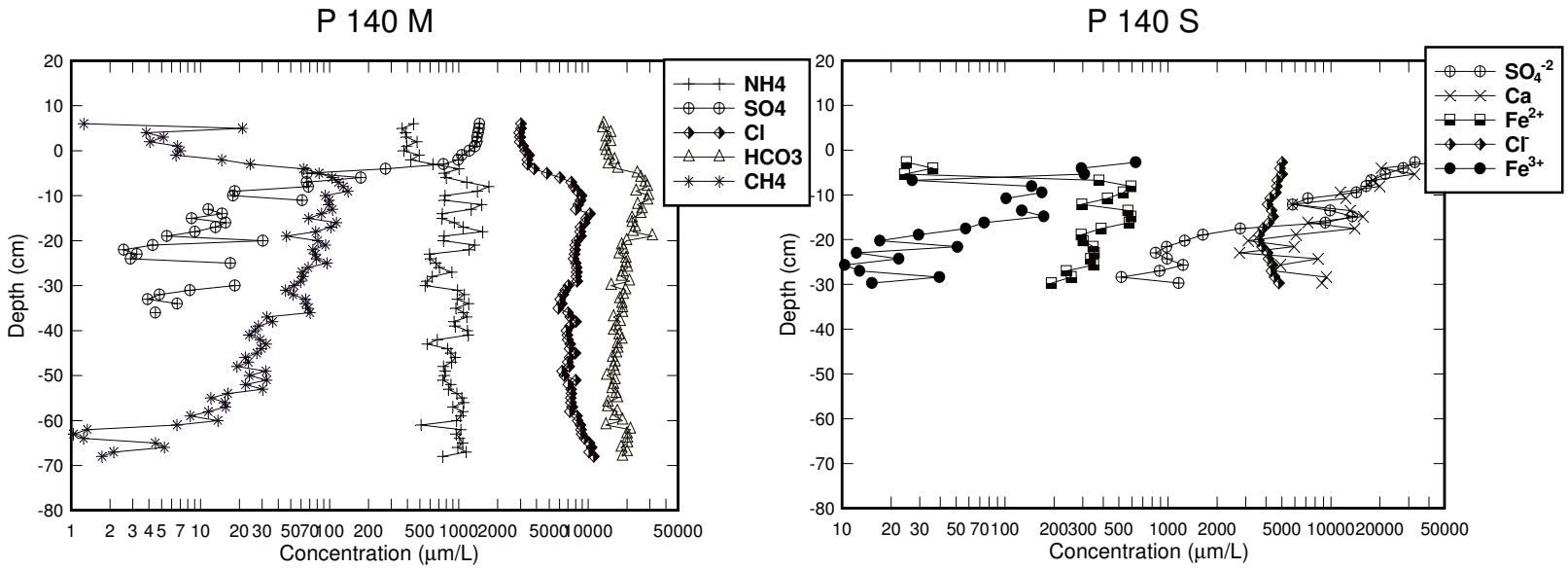

a) b)

Figure 4.14. Profiles of geochemical parameters in location 140 that yielded higher factor loadings for Factor 1 obtained from PCA. a) May and b) September.

Ca and SO_4^{-2} to decouple. Chloride concentrations are higher in the upper 20 cm attributed to evapotranspiration. From this analysis it can be concluded that location 140 is different in May and September due to seasonal changes such as temperature and plant growth causing evapotranspiration in September and hydrological fluctuations controlling the supply of electron acceptors. The dominant TEAPs are sulfate reduction and methanogenesis in May, and iron and sulfate reduction in September.

For May data from location 157, the principal factor was negatively loaded with parameters alkalinity, Mg, K, Cl^-, Ba, acetate, and ammonium and positively loaded with pH. From these geochemical indicators the processes interpreted are mineralization of organic matter producing ammonium and alkalinity, fermentation indicated by concentrations of acetate, and mineral dissolution (Figure 4.15 a). Note that Cl^- concentrations are constant throughout the profile including across the sediment-water interface. This supports the interpretation that water flow is from the surface water down into the aquifer due to the elevated water table caused by the beaver dam. This constant water flow is transporting biogeochemical products, therefore obscuring the chemical gradients observed at other locations (Figure 4.15 a). A specific terminal electron accepting process such as iron or sulfate reduction is not identified in this factor.

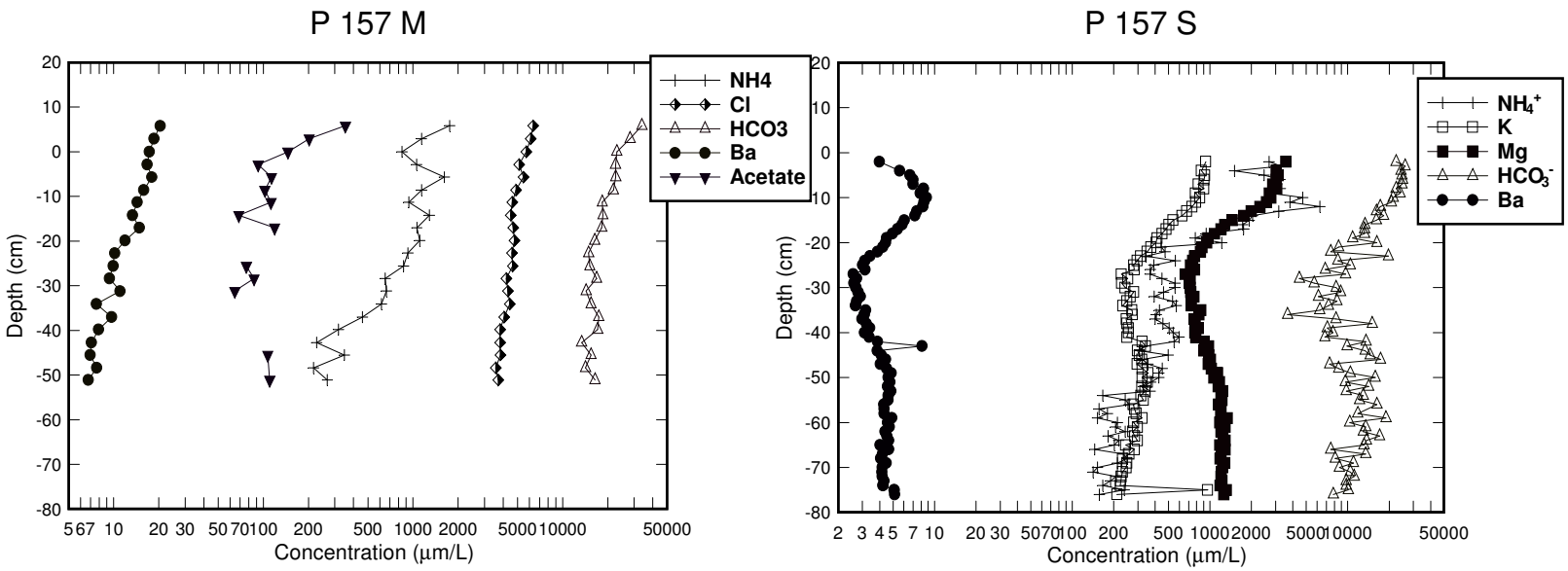

a) b)

Figure 4.15. Profiles of geochemical parameters in location 157 that yielded higher factor loadings for Factor 1 obtained from PCA. a) May and b) September.

In September, location 157 is dominated by parameters K, Mg, NH_4, HCO_3, Ba, and Na. This factor was identified as organic matter mineralization and mineral dissolution. The overall processes in September are no different than May for location 157, except that acetate and chloride are not important controls. There is a maximum gradient observed at approximately 10 cm deep where organic matter degradation is enhanced. An increase in Ba at this location might be an indication of sulfate reduction via dissolution of barium minerals. This location in September presents processes similar to those observed in May for other locations because the water recharge into the aquifer is decreased allowing for anaerobic respiration to occur in the upper sediments.

Performing a PCA on the data for each site allowed for the determination of dominant biogeochemical process interpreted from the first factor. These results, like the ANOVA comparison of the whole-dataset PCA, demonstrate that hydrologic fluctuations are a major control on biogeochemical variability. At sites 140 and 157, the direction of flow, upward and downward respectively, was the governing process determining the dominant biogeochemical process to the extent that the processes identified in the first factor of each PCA were similar in May and September. Site 140 was dominated by plume advection whereas site 157 exhibited organic degradation for both months. Site 102, where negligible flow was observed, was the only site where a seasonal difference in dominant biogeochemical process was indicated in May and September. In May, this site is mainly controlled by seasonal changes such as increasing temperature and increased inputs of organic matter from vegetation cycles, causing methanogenesis do be the dominant TEAP. In September, the mechanism controlling

the biogeochemistry in this location is the lowering of the water table, causing oxidation of iron sulfide minerals and an influx of electron acceptors Fe(III) and SO_4^{2-}.

SUMMARY

Hydrological fluctuations affecting a wetland-aquifer interface are an important control on biogeochemical processes in the system. The processes that exhibited significant differences among sites with different hydrologic regimes were plume advection into the wetland and methanogenesis. These processes were significantly different between sites that exhibited discharge, recharge, and no flow. Plume advection was strongly associated with 140, the site with upward flow. Methanogenesis was highly associated with the location lacking flow and was not dominant in locations with constant water flux.

Significant differences by season (May and September) were found for the processes oxidation, barite utilization, and iron reduction. The mechanism for oxidation is explained by changes in the water table elevation. In late summer, the water table elevation dropped below the surface exposing previously reduced sediments to oxygen and releasing electron acceptors, sulfate and Fe(III), to the system. Iron reduction is observed in September enhanced by the release of iron oxides. Barite utilization is strongly associated with the month of May showing significantly different means with respect to September. In waterlogged conditions, free sulfate is depleted and barite utilization by sulfate reducing bacteria becomes favorable.

The processes fermentation and sulfate reduction had equal factor score means by site and season, indicating that these processes were independent of hydrologic regime and seasonal differences. Analysis of dominant biogeochemical process by site revealed that seasonal differences in biogeochemical processes were only observed for the site with negligible flow.

The findings in this study demonstrate that the hydrologic linkage of a wetland and underlying aquifer controls the spatial and temporal changes in biogeochemistry. Seasonal changes in biogeochemical processes observed in the wetland and aquifer system are controlled by the direction of flow. Hydrologic fluctuations in other systems such as lakes, rivers, and wetlands may be the dominant control of the biogeochemistry in these systems. Therefore, spatial and temporal changes in biogeochemistry could then be predicted by knowledge of hydrological regimes. A better understanding of the physical, chemical and biological linkages among systems can be used for predicting biogeochemical cycling.

CHAPTER V

IN SITU EXPERIMENTS TO ASSESS MICROBIOLOGICAL RESPONSE TO INPUTS OF ELECTRON DONORS AND ELECTRON ACCEPTORS

SYNOPSIS

Biogeochemical dynamics in a wetland-aquifer system were studied by assessing microbiological response to changes in geochemistry. Native microorganisms were incubated in situ and isolated for geochemical experimentation. Recharge events were simulated by adding geochemical solutions containing electron acceptors and/or electron donors to a community of anaerobes contained in the microcosms with the purpose of quantifying metabolic rates and changes in community structure. Difficulties such as leakage in the experiments and reactions occurring in the test solutions compromised the analysis of the results. Although respiration rates could not be calculated, valuable information on microbial response to changes in geochemistry was obtained. Some of the results show sulfate and iron reduction occurring simultaneously in the presence of sulfate and ferrihydrite with the addition of electron donors (acetate and lactate). Sulfate reducers were dominant when sulfate concentrations exceeded iron oxide concentrations. Even though accurate respiration rates could not be calculated given the difficulties encountered, this chapter gives information that should be considered in the design and methodologies of future experiments.

INTRODUCTION

In an environment rich in electron donors, such a landfill plume or wetland sediment, electron acceptors are rapidly consumed making these systems highly anaerobic. In these systems, shifts in terminal electron accepting processes (TEAPs) have been observed resulting from the change in the distribution of electron acceptors. The observed changes in TEAPs are a result of the adaptation of microorganisms to the changing geochemical conditions utilizing the available electron acceptors that will yield the highest energy for their metabolic processes. However, microbial metabolic processes can also be limited by the availability of electron donors. In wetland and aquifer systems, organic matter is abundant but its quality (bioavailability) may be poor. An example is the recalcitrant fraction of dissolved organic matter in the landfill leachate plume (Cozzarelli et al., 2000). In dynamic systems such as wetland and aquifers, changes in electron acceptors and electron donors are driven by seasonal cycles and hydrological changes which result in adaptation and competition between microbial communities adjusting to the new environmental conditions.

Some electron acceptors such as oxygen, sulfate, and nitrate are naturally introduced in these systems by recharge events such as precipitation. The chemical composition of global atmospheric precipitation in the continents consists of electron acceptors such as NO_3^- and SO_4^{2-} in concentrations ranging from 6-21 and 10-30 µM respectively (Langmuir, 1997). In aquifers, recharge events contribute to the availability of electron acceptors, which stimulate microbial communities that thrive by utilizing nitrate and/or sulfate as an energy substrate. According to the redox zone theory

(Lensing et al., 1994; Lindberg and Runnells, 1984; Lyngkilde and Christensen, 1992b), sulfate reduction will occur sequentially after nitrate and iron (III) are depleted. But some studies suggest that these processes could occur simultaneously as long as there are sufficient electron donors for the organisms to compete (Chapelle and Bradley, 1998; McGuire et al., 2002; Motelica-Heino et al., 2003; Okabe et al., 2003). Fluctuating hydrological conditions, such as upward or downward flow, transport electron acceptors and/or electron donors to the aquifer and or wetland and therefore can control TEAPs (Baez-Cazull et al., 2007c). Water flowpaths become zones of increased microbial activity resulting from the transport of electron acceptors to zones limited in these nutrients. In systems with negligible flow, electron acceptors may be the limiting nutrient for respiration.

Previous studies have simulated a recharge event by introducing electron acceptors to an aquifer system in order to quantify respiration rates. McGuire et al. (2002) recreated an in situ recharge event in a reduced aquifer system using push-pull tests by introducing water rich in electron acceptors to measure microbial nitrate and sulfate reduction rates. Their results demonstrate stimulation of respiration activities but show a lag time before any change was observed which was attributed to the time necessary for organisms to adjust to the new conditions and/or the lack of electron donors in the solution. Another study by Kneeshaw et al. (2005) suggests that the lag time is attributed to incomplete mixing of the electron acceptor rich water with the reduced zone in direct contact with the microorganisms. These findings suggest that the addition of electron acceptors to a reduced redox environment stimulates anaerobic

respiration in the presence of electron donors at the zone where waters mix and are directly in contact with microorganisms.

Lower microbial respiration rates have been attributed to deficiencies in the availability of electron donors (e.g., Bakermans et al., 2002; Kostka et al., 2002; McGuire et al., 2002; Okabe et al., 2003). For example, nitrate reduction is strongly dependent on carbon availability. The supply of easily decomposable organic matter reduces oxygen levels, thus increasing the demand for nitrate as an electron acceptor (Paul and Clark, 1996). In the absence of nitrate, iron reducing bacteria and sulfate reducing bacteria compete for the carbon source. Therefore the availability of labile organic matter such as lactate and other organic acids produced in fermenting zones is greatly decreased when nitrate, iron and sulfate reducers compete for the same electron donor.

In the wetland, electron donors are supplied from vegetation cycles and aquatic biological activities. Vegetation cycles (Baez-Cazull et al., 2007a), peaking in the early spring and senescing in the late spring, are a main source of organic matter in the system. Fauna cycles in the wetland respond to seasonal and hydrological changes and can also be a source of organic matter to the wetland sediments. In addition, burrowing animals in the wetland can create paths for electron acceptors to reach deeper sediments (e.g., crawfish have been observed (Baez-Cazull et al., 2007a) and enhance microbial respiration.

To understand the effect of changing geochemical conditions on microbial activities in a linked wetland-aquifer system, a series of in situ experiments were

conducted at a region above the wetland-aquifer interface. This zone has been previously characterized with variable concentrations of organic acids suggesting that it is a zone of active microbial metabolism. The experiments were designed to quantify ideal iron and sulfate reduction rates from an in situ incubated bacterial community responding to a simulated recharge event by 1) addition of electron acceptors and 2) addition of electron acceptors and electron donors. This study uses small chambers that allow colonization of native microorganisms in situ and provide the loci for introducing the experimental solutions. It is hypothesized that the addition of electron acceptors will stimulate microbial activities and that the addition of electron acceptors and donors will result in higher and simultaneous iron and sulfate reduction rates. Another aspect of the experiment (not discussed here) will look at microbiological community changes during the exposure to the experimental geochemical solutions.

MATERIALS AND METHODS

Equipment

The experiment was designed as a microcosm study where microbial organisms colonized a sponge inside a chamber and were isolated for experimentation. The equipment used for incubating the organisms and supplying the test solutions was designed and constructed by Erik Smith in the Geology & Geophysics Department at TAMU. It consisted of six small tapered boxes (chambers) measuring 15 cm x 12.6 cm x 4.4 cm. Inside each chamber there were three perforated tubes that held three sets of

sponges (Figure 5.1). The sponges were made of polycarbonate material and had a surface area of 533 cm^2/cm^3 comparable to the surface area of ideal packed sand with a surface area of approximately 797 cm^2/cm^3. The sponges were selected because they could be sterilized, retrieved from the chamber and easily stored for microbiological analyses, thus eliminating cross contamination and impurities. One side of the chamber was open to allow microbial colonization in the sponges. This side was covered with a polycarbonate membrane, with track etched pores measuring 5 µm from Whatman Nuclepore® and secured to the chambers with a plastic screen to minimize sediments entering the chamber (Figure 5.2). The membrane material was chosen for its ability to resist mechanical stress and biodegradation (Jacobs, 2002).

PVC tubes were attached to the chambers to access each of the sponges from the surface and introduce the test solutions. To prevent bacterial contamination, the sponges were autoclaved and equipment was sterilized with bleach and rinsed with nanopure water. Six chambers were inserted in the sediments at a depth of 45 cm (previously characterized as a silty transitional zone, Figure 2.3) near the site of multilevel wells monitored by the USGS (Figure 5.3). Nanopure water was pumped in the chambers to equilibrate the hydraulic pressure and allow for passive diffusion through the membrane. The chambers were left for four weeks to allow colonization of bacteria.

After incubation, a second PVC tube inserted inside the PVC tube attached to the chambers was slid and sealed over the inner chamber tubes holding the sponges before introducing the test solutions (Figure 5.1). Argon gas was purged into the outer PVC tubes to prevent air from entering the chambers when placing the second PVC tube.

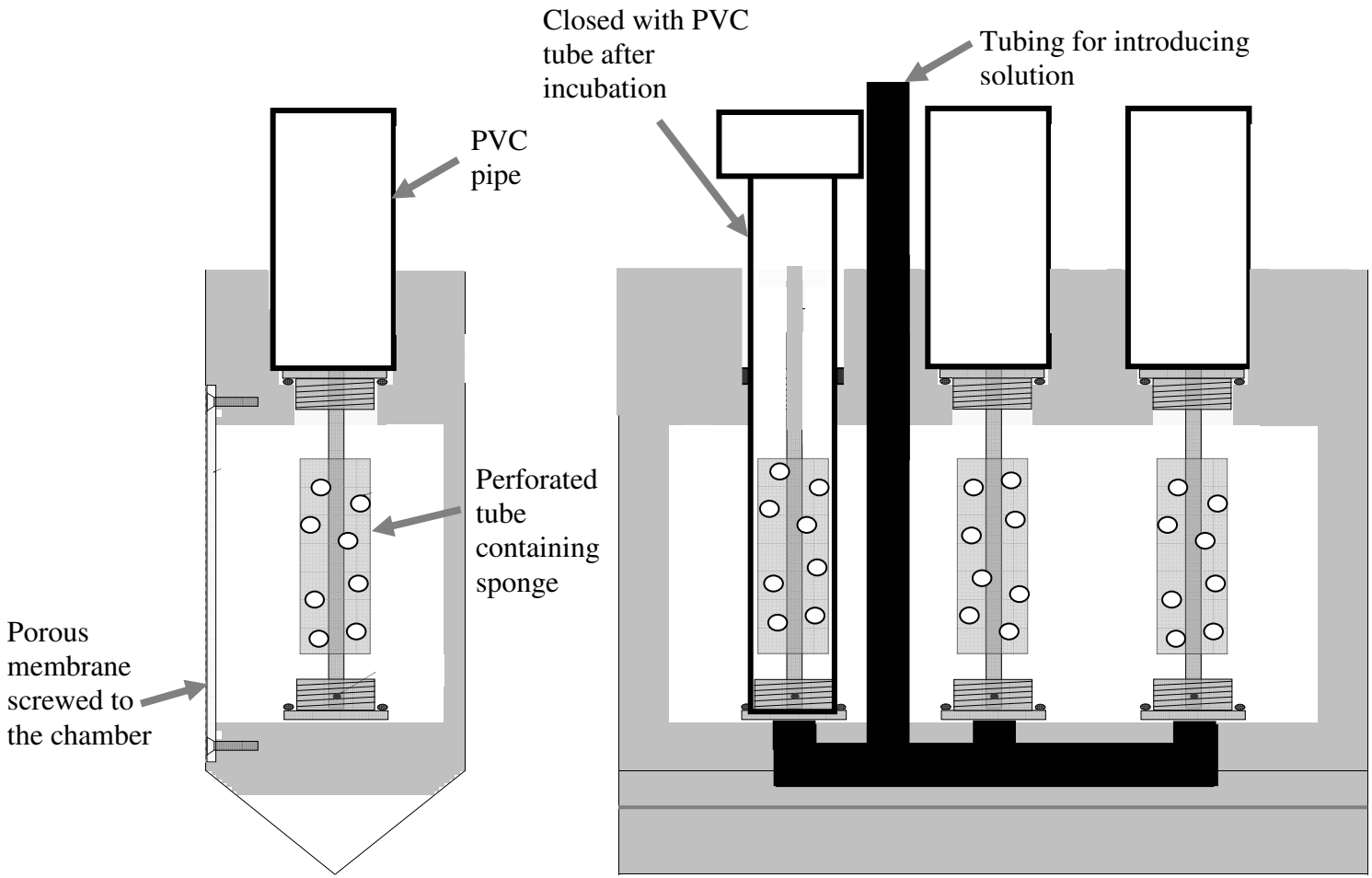

Figure 5.1. Side and front view sketch of a chamber utilized for microbial isolation and experimentation. Adapted from the design by Erik Smith (data not published).

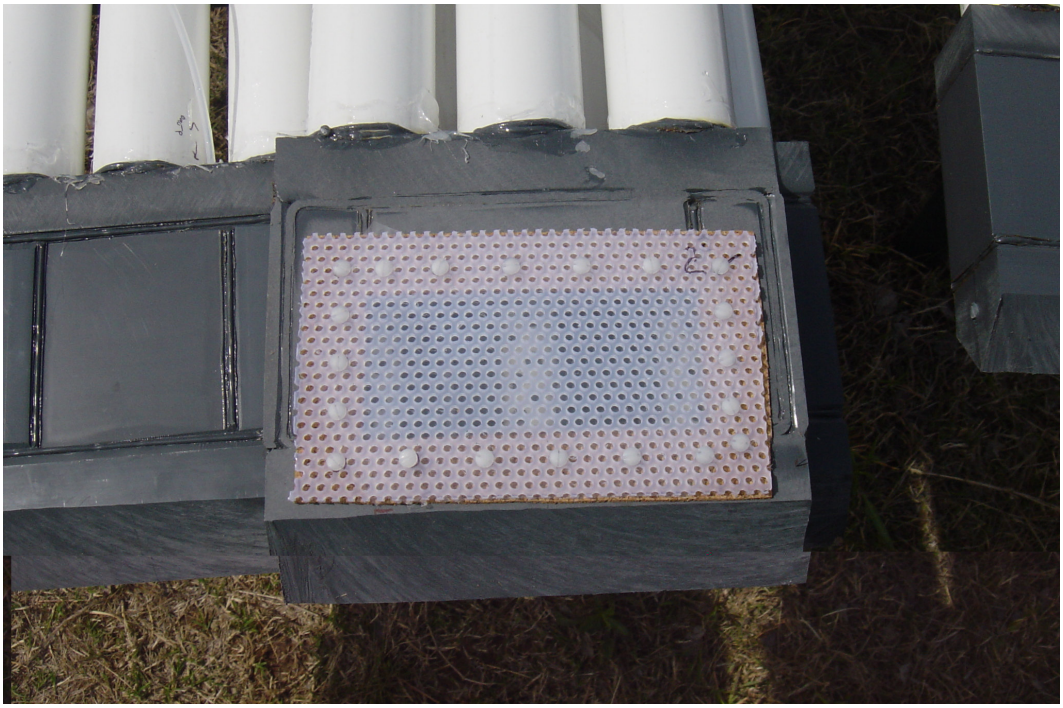

Figure 5.2. Photograph of front face of chamber showing the plastic screen holding the membrane.

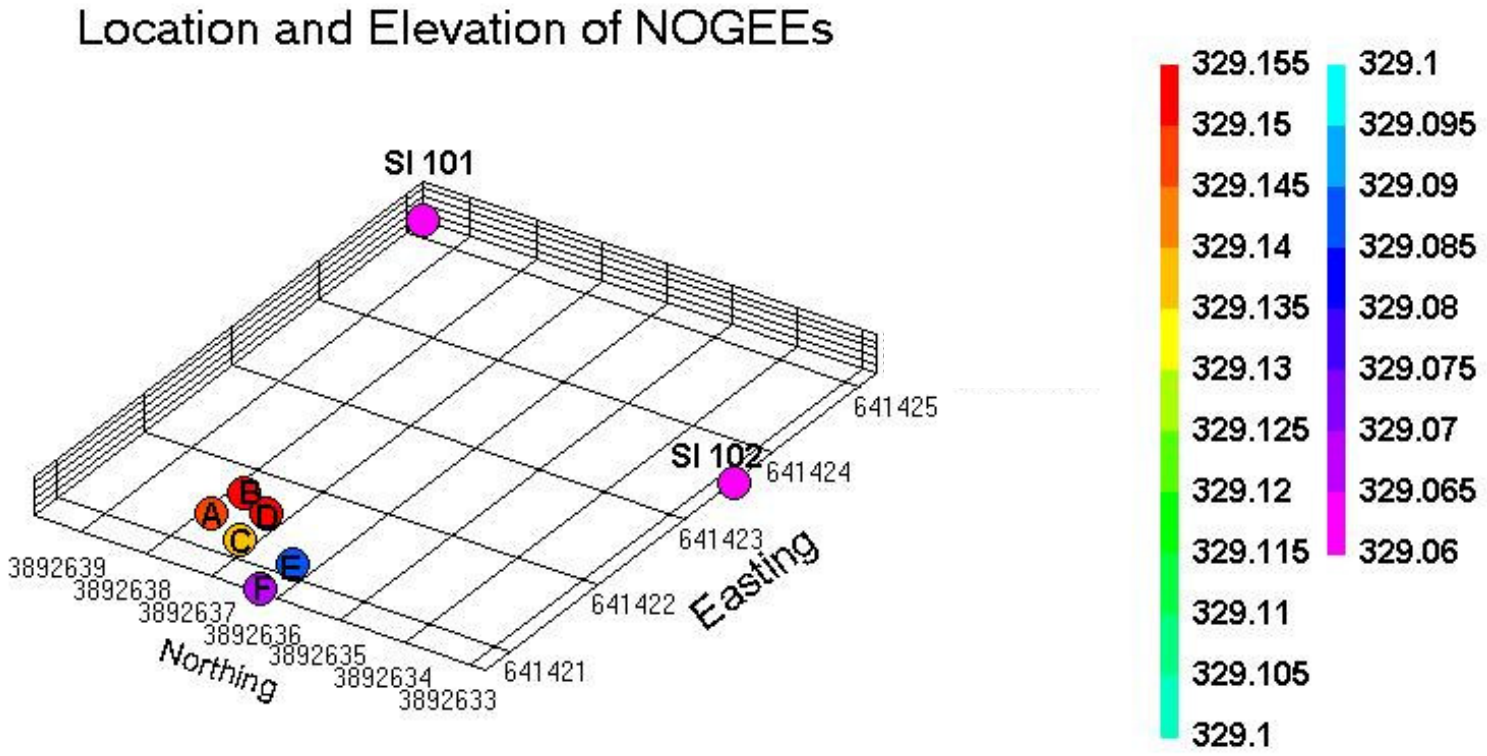

Figure 5.3. Location of experiments chambers A to F. Northings and eastings are in meters, while elevation is reported as meters above sea level. Purple circles SI 101 and SI 102 refer to the multilevel wells monitored by the USGS.

In Situ Measurements

The chambers named NOGEEs for Native Organism Geochemical Experimentation Enclosures, were labeled A through F. The experimental solutions consisted of native water collected from the aquifer, depleted in sulfate and assumed to be depleted in iron oxides, in which sulfate, ferrihydrite, lactate and acetate were added. Table 5.1 list the solutions injected to each NOGEE. The concentrations of sulfate and ferrihydrite in the solutions were 1mM each, and the concentrations for organic acids were calculated from the stoichiometry of sulfate and iron reduction reactions. Bromide was added to all the solutions to serve as a tracer.

Table 5.1. Solutions injected in each experimental chamber (NOGEE).

NOGEE Identification	Solutions (All prepared with aquifer water as a solvent and with Bromide added as tracer)
A	1mM Sulfate
B	1mM Sulfate + 1mM Acetate and 0.667 mM Lactate
C	1mM Ferrihydrite + 1mM Sulfate + 1mM Acetate and 1mM Lactate
D	Control (only native water and tracer)
E	1 mM Ferrihydrite
F	1 mM Ferrihydrite + 0.177 µM Acetate and 0.118 µM Lactate

The solutions were prepared the first day inside an anaerobic glovebag filled with N_2 gas and were used throughout the completion of the experiment. The solutions were kept in amber plastic jugs that were placed in a cooler to control the temperature and were continuously purged with N_2 gas and shaken before injection. Parts of these experimental solutions (~100 mL) were pumped each day simultaneously into each of the NOGEEs at a rate of 2 mL/min. The first day, an initial water sample from the water equilibrated in the NOGEE before experimentation was retrieved by pumping in the experimental solution. The time for sampling after each injection was decided on the time it took to obtain a measurable change, this time resulted in a 24 hour period. Each day the solutions in the jugs were sampled before injection (pumping) into the NOGEEs. Injecting new solution replaced the volume of water in contact with the sponges, this water was pumped from the NOGEE and sampled.

Geochemical Analyses

Samples obtained from each NOGEE consisted of a mix (an average) of the water contained in the three compartments containing the sponges. The geochemical parameters measured included sulfate, Fe^{2+}, and sulfide which are indicators of sulfate and iron reduction. Bromide was measured to trace the solution. Chloride found naturally in the system was also measured to serve as an additional tracer. Lactate and acetate as well as dissolved organic carbon DOC were measured to determine the consumption of electron donors.

Fe^{2+} and H_2S were measured immediately in the field using colorimetric spectroscopy adapted from standard methods (APHA et al., 2005) for Fe^{2+} and using a Thermo Orion Meter® combination electrode with silver sulfide for measuring H_2S. Anions (SO_4^{2-}, Cl^-, and Br^-) were preserved in 0.5% formaldehyde and analyzed by and Agilent Technologies, capillary electrophoresis (CE) (Baez-Cazull et al., 2007a). Samples collected for acetate and lactate measurements were flash-frozen with dry ice and analyzed in the laboratory by gas chromatography. Water samples for dissolved organic carbon (DOC) analyses were filtered in line through a 0.45 µm filter, collected in a baked glass bottle, and acidified with H_3PO_4 to a pH of 2. DOC was measured by high temperature combustion techniques following the method of Qian and Mopper (1996). DOC, lactate, and acetate samples were analyzed by Jeanne Jaeschke and Isabelle Cozzarelli at the U.S. Geological Survey Central Facility in Reston, VA.

Synthesis of Ferrihydrite

Two-line ferrihydrite ($Fe_{1.42}O_{1.26}(OH)_{1.74}$) was synthesized in the laboratory as described by Cornell and Schwertmann (2003), with slight modifications. To 500 mL of a 0.2 M $Fe(NO_3)_3 * 9H_2O$, 276 mL of 1M KOH was added at a fixed rate of addition of approximately 50 mL/min, during vigorous stirring with a magnetic stirrer. The pH of the suspension was then adjusted to 7.51 by the last 10 mL of KOH dropwise addition. Once the pH was stabilized for 30 minutes at the pH of 7.51 the suspension was washed 6 times with nanopure water by centrifugation to remove all the nitrate. Nitrate levels were below 0.06 ppm measured with CheMetrics VacuuVials®. The solution was

decanted and stored in the refrigerator at 2ºC as suggested by Raven et al. (1998). The identity of 2-line ferrihydrite (freeze dried) was confirmed by X-ray emission microscopy Electron Microscope Cameca SX50 performed under the direction or Dr. Ray Guillemette from Geology & Geophysics, TAMU. The analysis produced an Fe/O concentration ratio of 1:2 consistent with ferrihydrite. The particle size at a 20,000 magnification appears to be in the 1 µm range (Figure 5.4). The ferrihydrite used in the experiment was not freeze dried to preserve the small particle size.

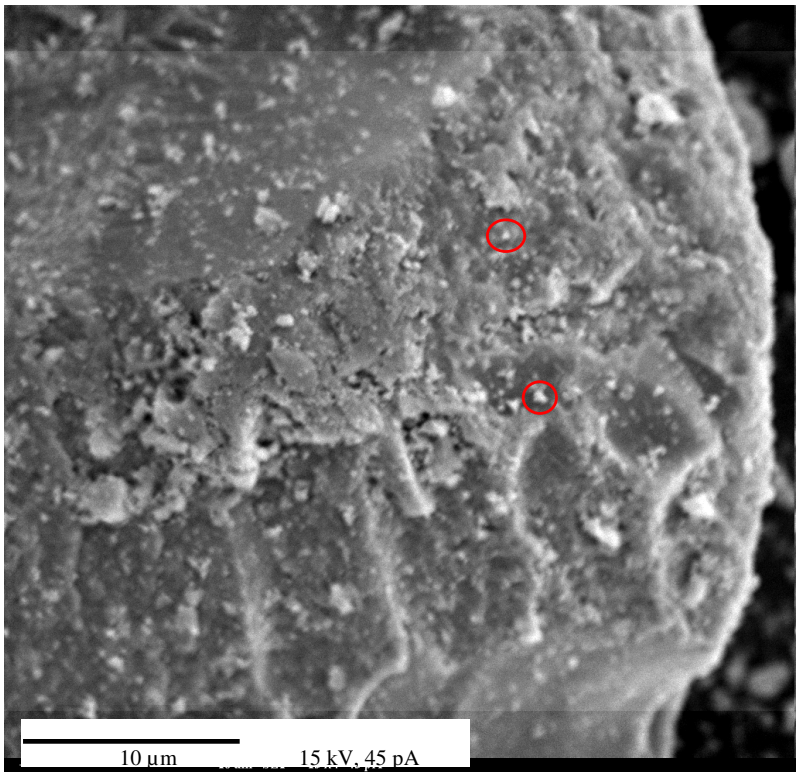

Figure 5.4. Electron microscope image of ferrihydrite. Particles are clumped together due to freeze drying however some individual particles are observed (circled in red).

RESULTS AND DISCUSSION

The data obtained for bromide concentrations indicate incomplete recovery of this tracer for all the experiments. There were some problems with administering the solutions to the chambers and leakage occurred in some of the chambers. Therefore rates of sulfate and iron reduction could not be calculated. The sections below discuss some of the data obtained for each NOGEE and explain some of the problems encountered. This chapter is intended to give information of problems in the methodology that could not be foreseen. For example, reactions ongoing in the solutions before injection into the chambers. Based on this first attempt, future experiments will be carried on after design improvements.

NOGEE A, Sulfate

Bromide was not recovered from the chamber, suggesting that the solution leaked (Figure 5.5). Chloride concentration recovered from the experimental chamber is half of the initial concentration sampled in the test solution before injected. The concentration of Cl^- is however similar to the initial concentration found in the chamber at a 45 cm depth. Sulfate concentrations are higher after incubation than in the initial solutions in the jug (Figure 5.6). These concentrations are similar to the sulfate concentrations found in the surface water and may indicate that surface water is entering the experimental chamber.

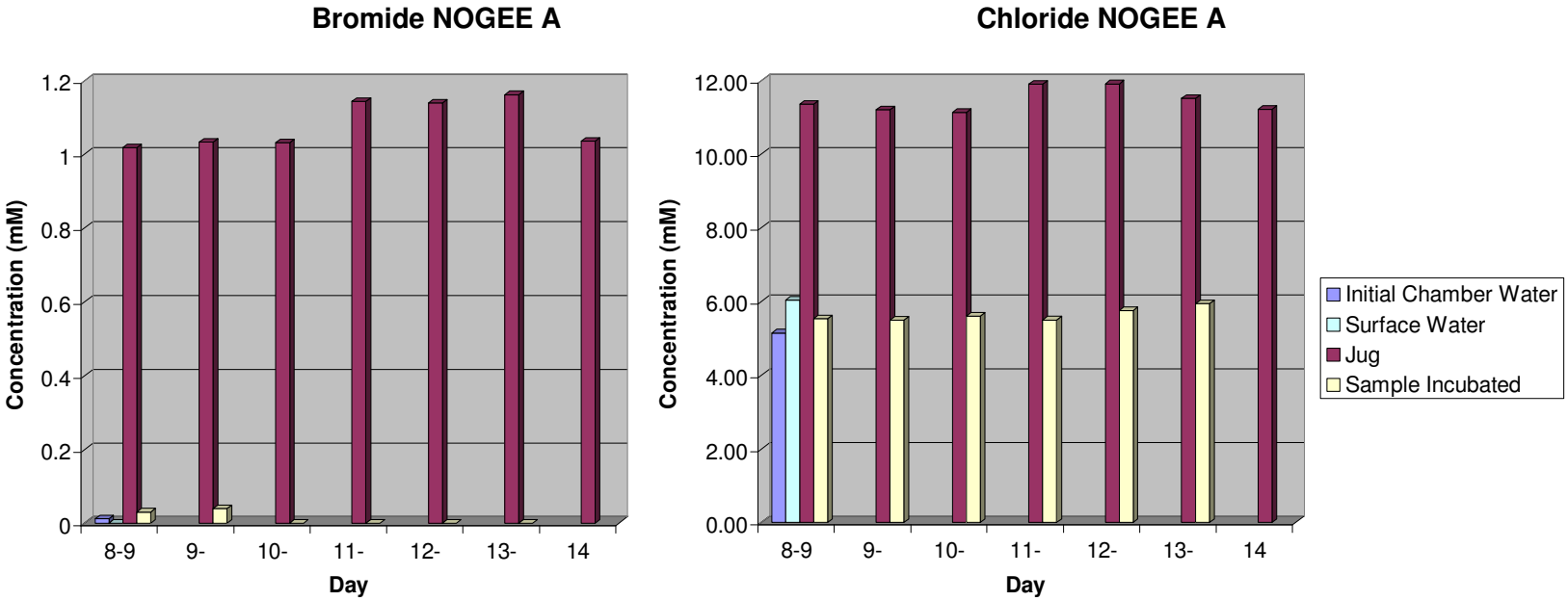

Figure 5.5. Bromide and chloride concentrations from NOGEE A obtained from the "initial chamber water" before experimentation, the wetland "surface water", the containers with the solutions ("jug") before adding to chamber, and the "sample incubated" which is the water recovered from the chamber after solution has been injected and incubated for a 24 hour period. Days represent the date in June 2006.

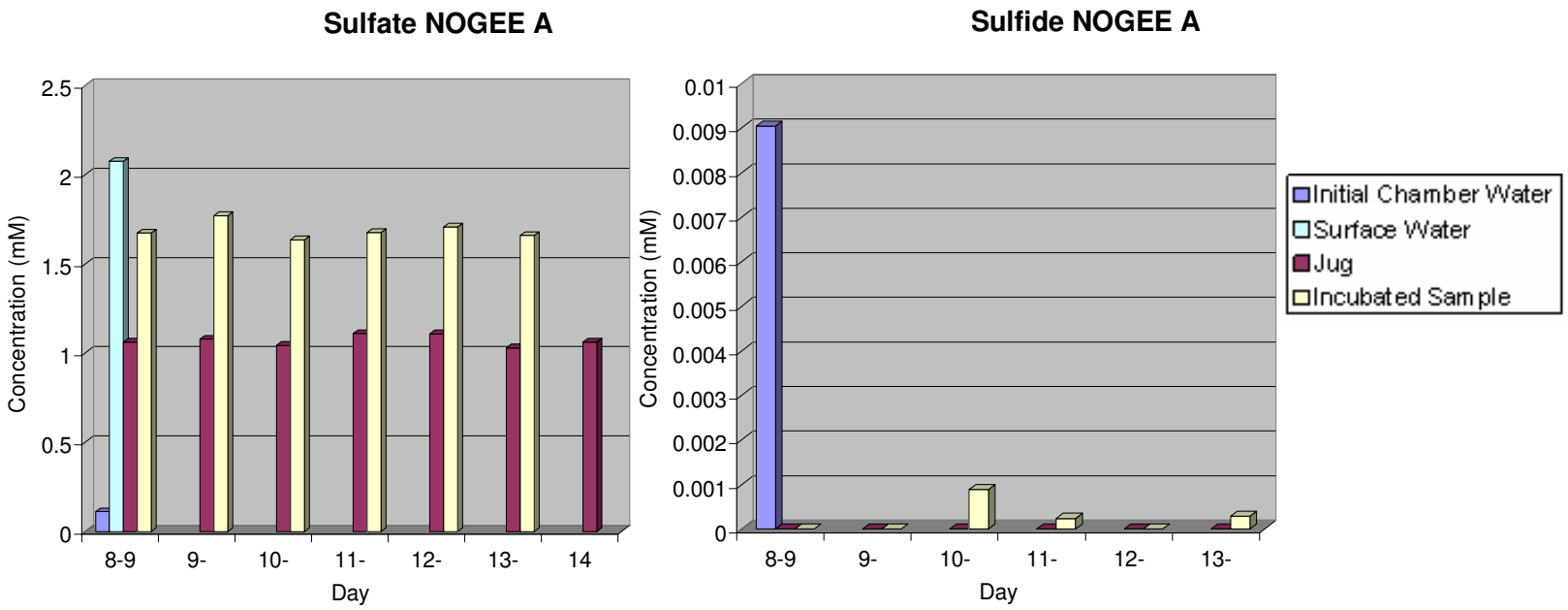

Figure 5.6. Sulfate and sulfide concentrations from NOGEE A obtained from the "initial chamber water" before experimentation, the wetland "surface water", the containers with the solutions ("jug") before adding to chamber, and the "sample incubated" which is the water recovered from the chamber after solution has been injected and incubated for a 24 hour period. Days represent the date in June 2006.

If this is the case, the solution injected is mixing with surface water consistent with the lower concentrations of chloride and bromide that could have been diffusing. Low sulfide and Fe^{2+} concentrations are consistent with surface water concentrations supporting the assumption of a surface water leak (Figure 5.6 and 5.7). Dissolved organic carbon concentration on the first day was found very high (~6.3 mM or 80 mg/L) but in the following days the concentrations are similar to the injected concentrations (~2.5 mM or ~30 mg/L) (Figure 5.7). The DOC concentration in the surface water was not collected therefore it cannot be determined if the increased concentrations in DOC recovered from the chambers are a contribution of surface water.

NOGEE B, Sulfate and Electron Donors

Bromide was not recovered suggesting a leak of the injected solution (Figure 5.8). Chloride concentration recovered from the chamber is lower than the Cl^- in the solution injected but higher than the Cl^- concentration initially in the chamber (Figure 5.8). This suggests that the leakage occurred in the chamber and that the sampled water may be mixed with pore water at a 45 cm depth. Sulfate concentrations recovered in the first two days are higher than the sulfate in the initial solution, the following days sulfate concentrations decrease slightly over time (Figure 5.9). Sulfide increases over time suggesting an increased activity in sulfate reduction (Figure 5.9). Since this water is mixed with pore water, it cannot be determined if the observed increase of sulfate reduction over time is produced by organisms in the sponge or organisms found in the pore water surrounding the chamber.

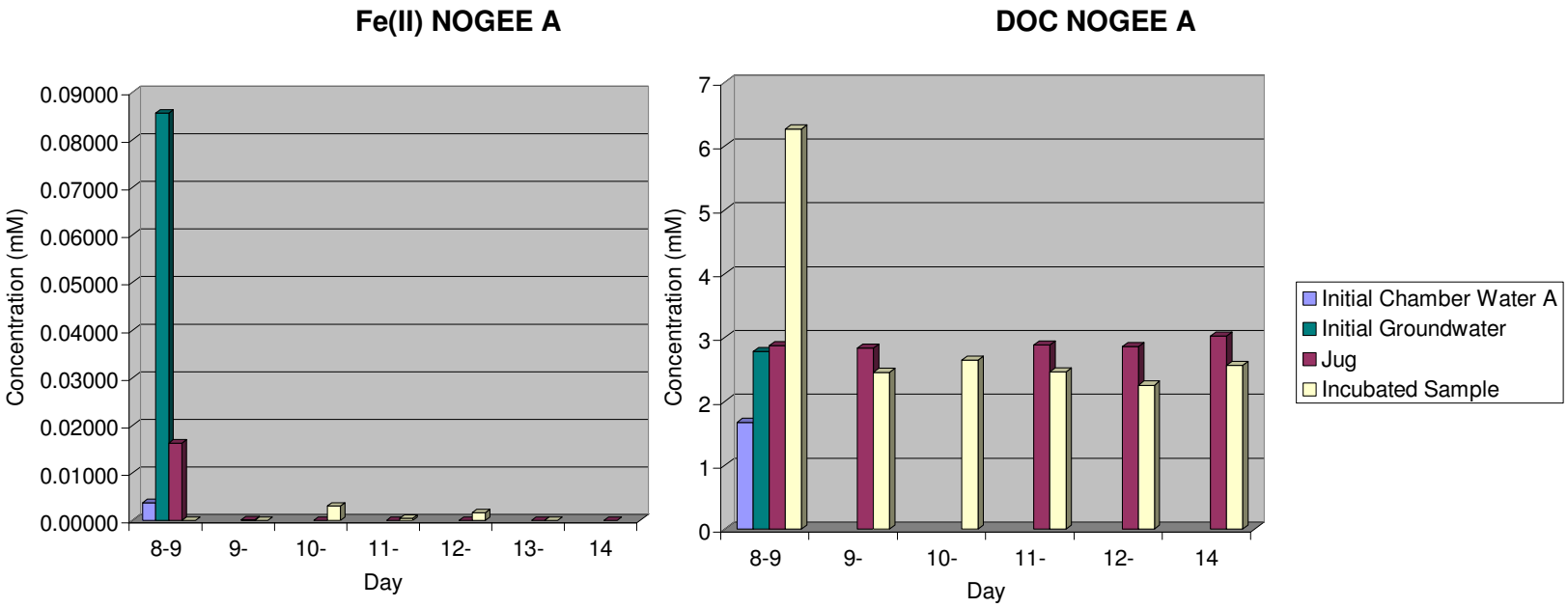

Figure 5.7. Fe^{2+} and dissolved organic carbon concentrations from NOGEE A obtained from the "initial chamber water" before experimentation, the wetland "surface water", the containers with the solutions ("jug") before adding to chamber, and the "sample incubated" which is the water recovered from the chamber after solution has been injected and incubated for a 24 hour period. Days represent the date in June 2006.

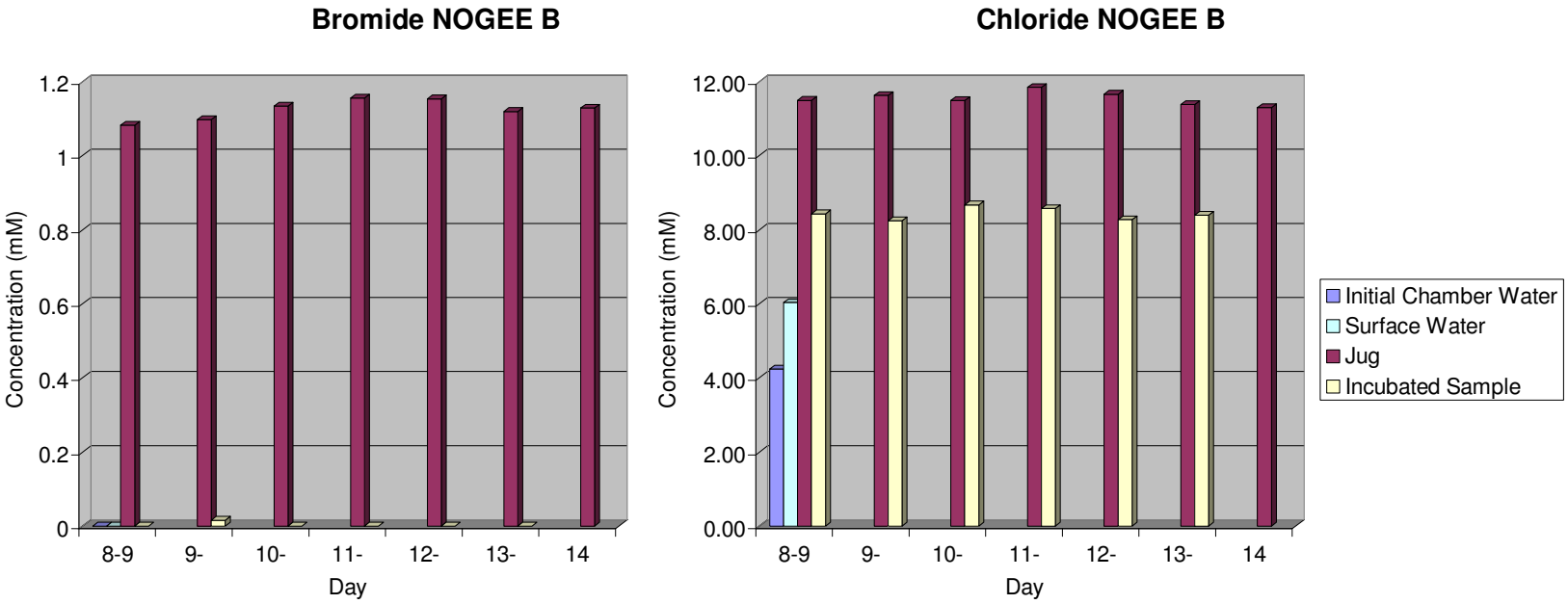

Figure 5.8. Bromide and chloride concentrations from NOGEE B obtained from the "initial chamber water" before experimentation, the wetland "surface water", the containers with the solutions ("jug") before adding to chamber, and the "sample incubated" which is the water recovered from the chamber after solution has been injected and incubated for a 24 hour period. Days represent the date in June 2006.

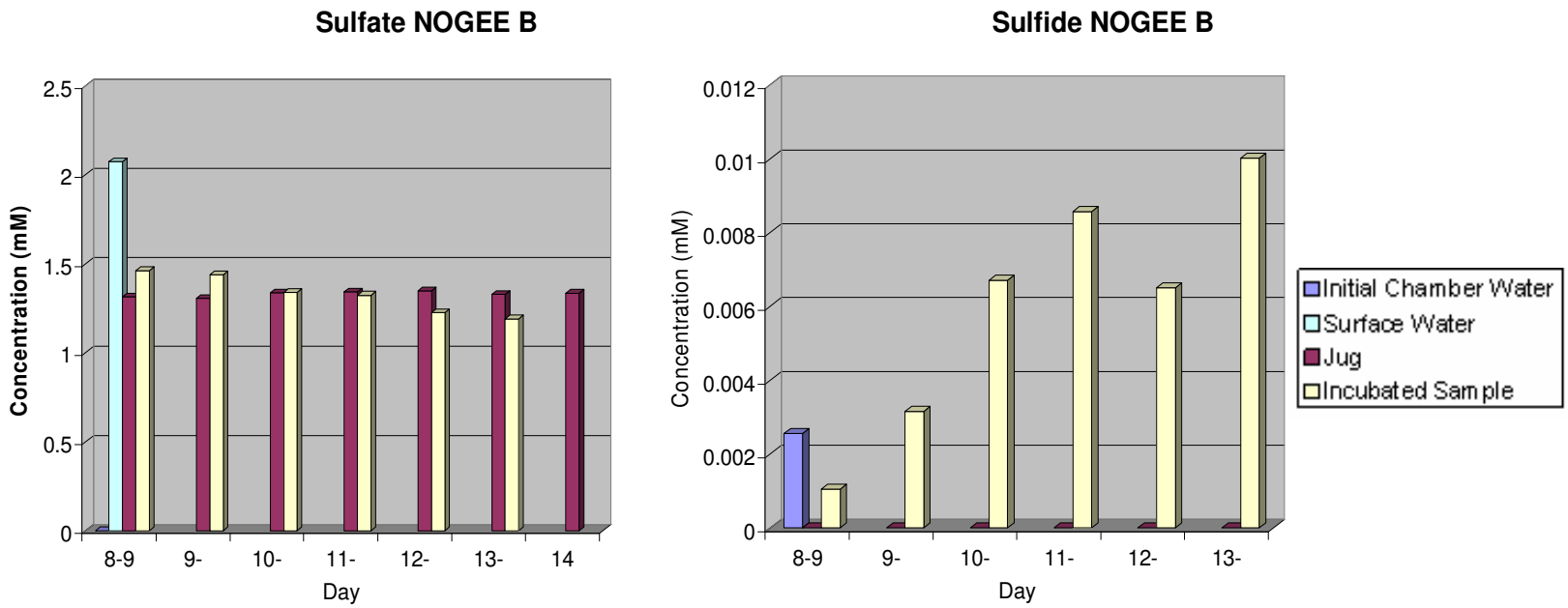

Figure 5.9. Sulfate and sulfide concentrations from NOGEE B obtained from the "initial chamber water" before experimentation, the wetland "surface water", the containers with the solutions ("jug") before adding to chamber, and the "sample incubated" which is the water recovered from the chamber after solution has been injected and incubated for a 24 hour period. Days represent the date in June 2006.

Concentration of Fe^{2+} in the groundwater used for the test solutions was 0.085 mM (4.7 mg/L) (Figure 5.10). As with NOGEE A (Figure 5.7) and also observed in the other NOGEES, Fe^{2+} concentrations in the jug were low compared to what was introduced from the groundwater. This indicates that Fe^{2+} was reacting in the jug possibly with oxygen. Concentrations of sulfate greater than 1 mM are also an indication of oxidation of sulfide in the groundwater transferred to the jugs. Oxygen in the test solution could introduce other electron acceptors that might be more favorable for microbial respiration and cause a lag time before sulfate could be used as electron acceptor. This can result in competition between organisms, in which organisms able to use higher energy yielding electron acceptors, such as iron oxides, would be favored. If oxygen was present it could have produced stress among the strictly anaerobe organisms found at depths in the sediments. However, all the oxygen could have been depleted by reacting with sulfide and Fe^{2+} producing high concentrations of sulfate and iron oxides. Having higher concentrations of sulfate can make the energy yields favorable for sulfate reduction even in the presence of other higher energy yielding electron acceptors found at lower concentrations (Blodau et al., 1998).

Over time, Fe^{2+} concentrations measured from the chambers after incubation varied (Figure 5.10). No Fe^{2+} was recovered on the first day even though there was Fe^{2+} present in the chamber before the experiment. This might be the result from oxidation. On the third, fourth and fifth day Fe^{2+} is produced but decreases over time. The production of Fe^{2+} indicates ongoing iron reduction but is not as dominant as sulfate reduction observed in Figure 5.9. The decrease in Fe^{2+} could be a result of ferrous iron

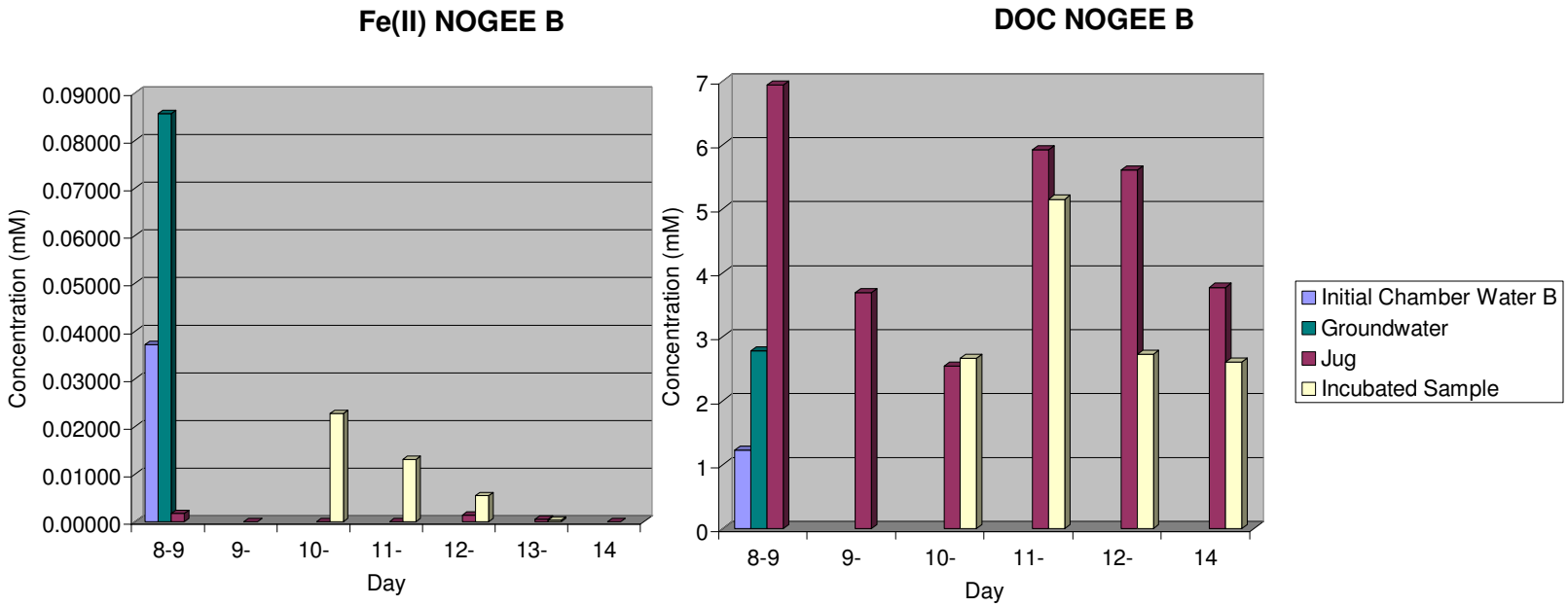

Figure 5.10. Ferrous iron and dissolved organic carbon concentrations from NOGEE B obtained from the "initial chamber water" before experimentation, the wetland "surface water", the containers with the solutions ("jug") before adding to chamber, and the "sample incubated" which is the water recovered from the chamber after solution has been injected and incubated for a 24 hour period. Days represent the date in June 2006.

reacting with sulfide or the result of a competition of iron and sulfate reducers for the electron donors, where sulfate reducers outcompeted the iron reducers given the increased productivity of sulfide over time and decreased productivity of Fe^{2+} (Koretsky et al., 2003). Transport of Fe^{2+} can also be occurring given the leak in the chamber. It seems that sulfate reducing bacteria were stimulated and sulfate reduction enhanced with the addition of sulfate and electron donors, even in the presence of iron oxides.

Concentrations of DOC varied over time in the jug containing solution for NOGGE B. The concentration in the jug should have been the same throughout time because each day part of the same solution was pumped into NOGEE B. An explanation for DOC variability is the potential for microbial activities occurring in the test solution. Since these solutions were prepared from groundwater filtered through 0.45 µm pores, microorganisms could have been introduced into the solution. Johanna Weiss at the USGS, Reston, VA has found significant microbial counts in the aqueous phase at this aquifer (data not published). DOC variability was not observed in the jug solution for NOGEE A, suggesting that the variability observed here, if attributed to microbial activities, may be a consequence of a) oxygen in the jug stimulating microbial respiration coupled to DOC, or b) cometabolism of DOC in conjunction with metabolism of acetate and lactate. Another explanation is organic matter complexing with iron resulting in adsorption and desorption processes (Blodau et al., 1998). In general DOC, recovered from the chamber, decreased to the original levels found in the NOGEE before the solution was added. The fourth day is an exception with higher DOC.

NOGEE C, Ferrihydrite, Sulfate, and Electron Donors

In this experiment bromide was recovered ~50% consistent throughout the seven days (Figure 5.11). Chloride was recovered about 90% (Figure 5.11) because it is mixing with pore water that already contains high levels of Cl^- differing from bromide which is low in the pore water. This indicates a leak of test solution mixing with pore water. The leak in this chamber was less than for any of the other chambers.

Sulfate concentrations higher than 1 mM in the jug containing the solution indicate oxidation in the containers (Figure 5.12). Sulfate concentrations recovered from the chamber after incubation were slightly variable and were about 60% the initial concentration (Figure 5.12). Like bromide, sulfate is found in lower concentrations in the pore water and 40% was diffused into the pore water given the leak in the equipment. Due to the loss of sulfate it cannot be determined if sulfate was reduced, although it seems to vary slightly over time. However, the increase in sulfide from the chamber-pore water mix indicates that sulfate reduction was enhanced (Figure 5.12). Sulfide was lower on the first day than the initial concentrations found in the chamber possibly due to oxidation and precipitation of iron sulfide minerals. During the second day through fourth day sulfide concentrations were maintained at concentrations of 0.0027 mM (0.9 mg/L). On the fifth day the concentration is decreased to 1/3 of the previous three days. The last day sulfide peaked to 0.0038 mM (0.13 mg/L) indicating higher activities of sulfate reduction after five days of exposure to the test solution. Sulfide produced in the jug on the second day may indicate sulfate reduction occurring in the jug supporting the idea of bacteria in the test solution.

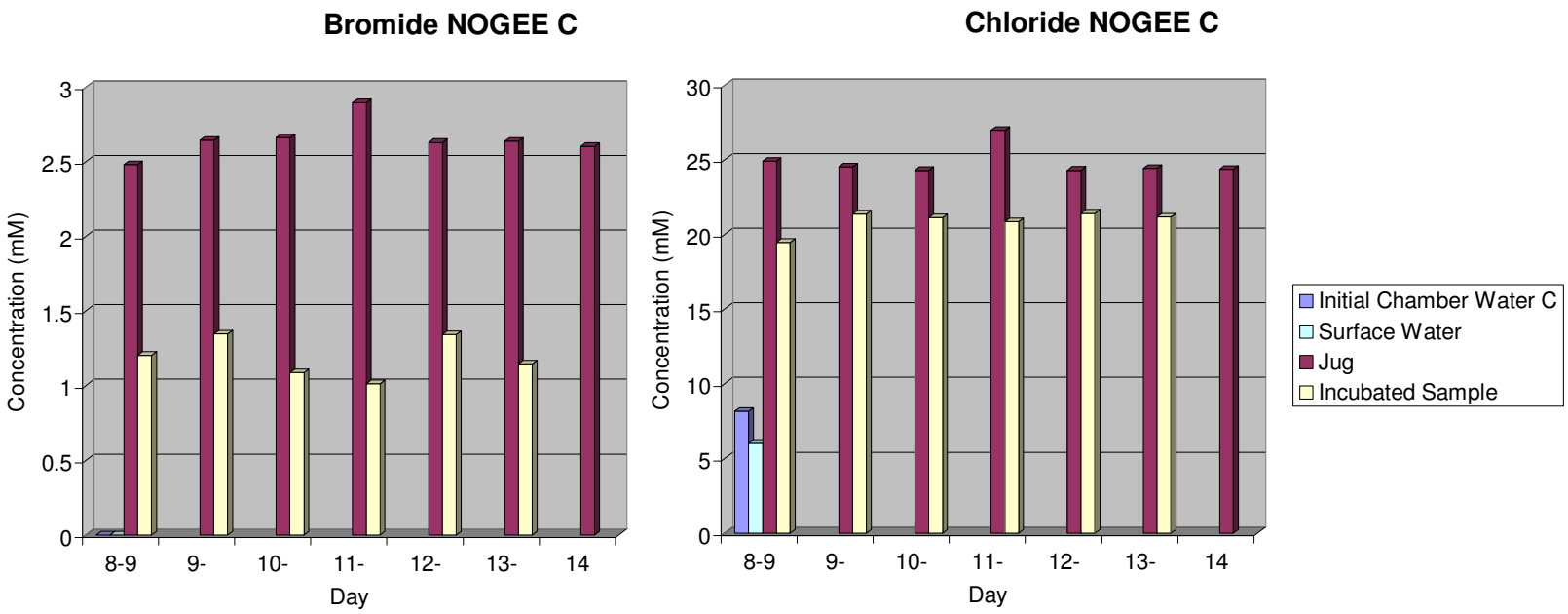

Figure 5.11. Bromide and chloride concentrations from NOGEE C obtained from the "initial chamber water" before experimentation, the wetland "surface water", the containers with the solutions ("jug") before adding to chamber, and the "sample incubated" which is the water recovered from the chamber after solution has been injected and incubated for a 24 hour period. Days represent the date in June 2006.

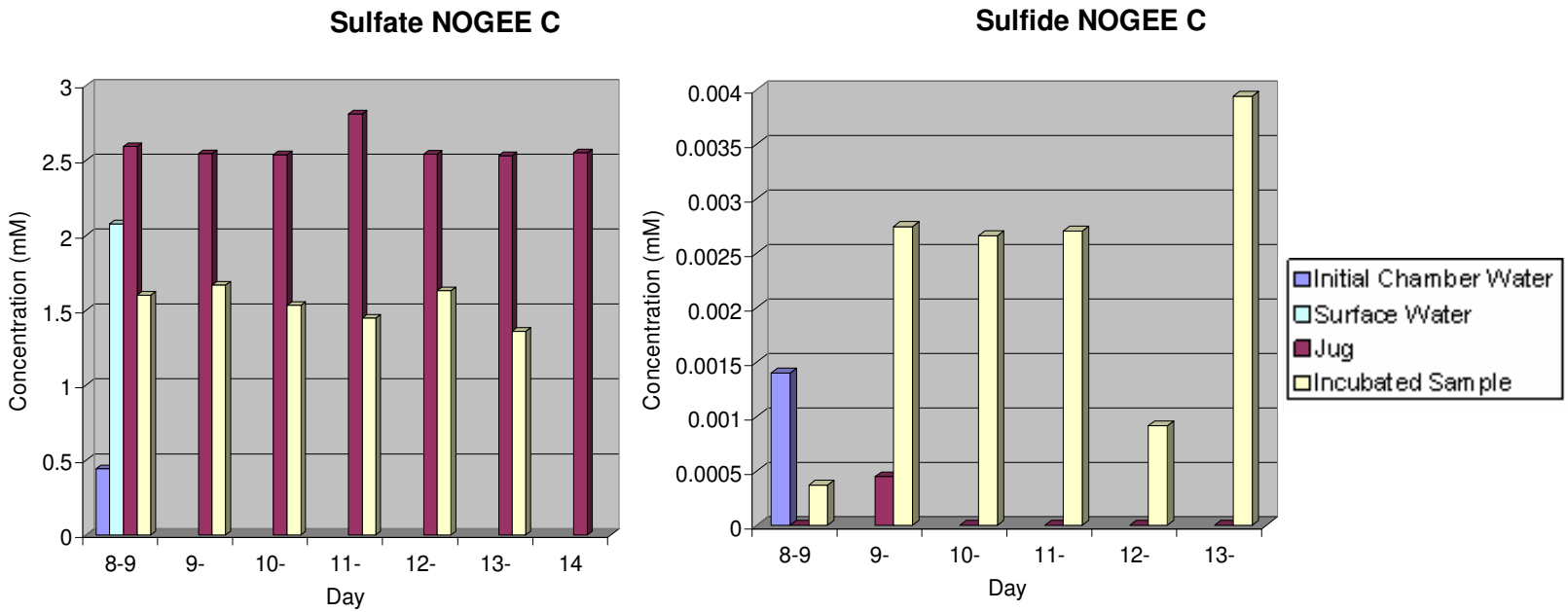

Figure 5.12. Sulfate and sulfide concentrations from NOGEE C obtained from the "initial chamber water" before experimentation, the wetland "surface water", the containers with the solutions ("jug") before adding to chamber, and the "sample incubated" which is the water recovered from the chamber after solution has been injected and incubated for a 24 hour period. Days represent the date in June 2006.

Fe^{2+} concentrations in the jugs are below detection limits (<0.1 mg/L) suggesting oxidation given that Fe^{2+} concentrations in the groundwater were 0.085 mM (Figure 5.13). Ferrous iron recovered from the chamber show a linear increase over time suggesting that iron reduction was stimulated in the chamber-pore water mix. The linear response may be a response to iron reducers' growth over time. The slight variability observed in recovered Fe^{2+} is attributed to the leak in the equipment since it correlates with tracer fluctuations.

Dissolved organic carbon is variable in the test solution and in the samples recovered from the chamber, making it very difficult to interpret (Figure 5.13). The first day DOC concentration in the sample was very high and it appears to be decreasing over time, suggesting utilization of DOC by bacteria over time. The fluctuations in DOC in the test solutions might be the result of cometabolism of DOC with metabolism of acetate and lactate by bacteria or adsorption and desorption dynamics by organic iron complexes as discussed in NOGEE B.

Although there is a leak in the experiment and the results cannot be attributed to the organisms in the sponge, this experiment demonstrates that iron and sulfate reducing bacteria were stimulated in the chamber-pore water mix. Iron and sulfate reducers competed for electron donors allowing the processes to occur simultaneously as found in other studies (Koretsky et al., 2003; Ludvigsen et al., 1998). The results show iron reduction favored over sulfate reduction interpreted from an increased linear production of Fe^{2+} vs. low and variable sulfide concentrations. This is expected given that iron reduction is the reaction that yields the highest Gibbs free energy.

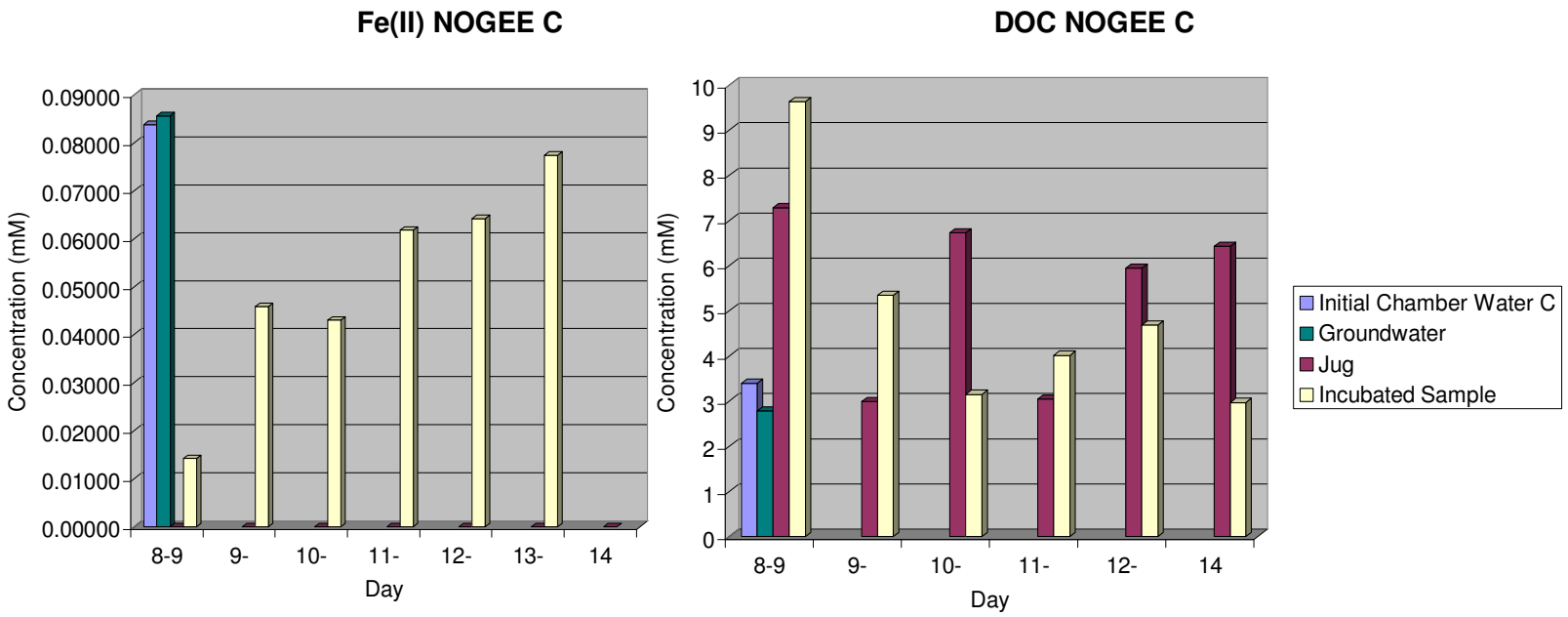

Figure 5.13. Ferrous iron and dissolved organic carbon concentrations from NOGEE C obtained from the "initial chamber water" before experimentation, the wetland "surface water", the containers with the solutions ("jug") before adding to chamber, and the "sample incubated" which is the water recovered from the chamber after solution has been injected and incubated for a 24 hour period. Days represent the date in June 2006.

NOGEE D, Control

Bromide and chloride on the first day of experimentation were recovered almost completely (Figure 5.14). Recoveries for the rest of the time period decreased with time indicating leakage after the second day.

Due to oxidation in the jug, where sulfate was found in the test solution at a concentration of 0.25 mM (18 mg/L) (Figure 5.15) and Fe^{2+} concentrations were below detection limits after the first day (Figure 5.16) indicating the presence of iron oxides, this NOGEE cannot be represented as a control. In the chambers, increased sulfide and ferrous iron concentrations were found over time indicating iron and sulfate reduction (Figure 5.15 and 5.16). The increase over time may be representing bacterial activities in the sponges or in the pore water enhanced by the introduction of sulfate and iron oxides from the control solution and by the leaks of test solutions from adjacent NOGEEs.

Dissolved organic carbon concentrations recovered from the chamber are higher than the concentrations in the test solution (Figure 5.16). This may result from higher DOC found in the pore water. In the test solutions DOC appear to hold constant concentrations, which may indicate that the variability observed in NOGEEs B and C might be attributed due to the presence of both electron acceptors and electron donors.

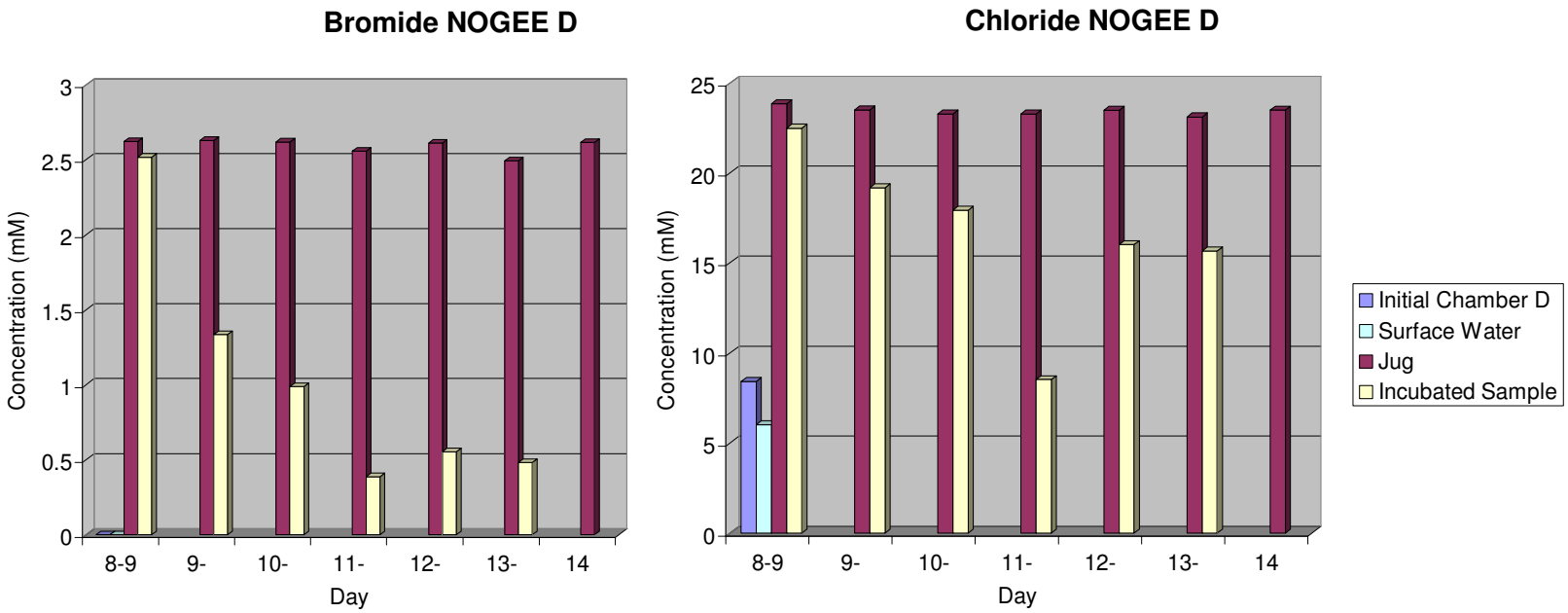

Figure 5.14. Bromide and chloride concentrations from NOGEE D obtained from the "initial chamber water" before experimentation, the wetland "surface water", the containers with the solutions ("jug") before adding to chamber, and the "sample incubated" which is the water recovered from the chamber after solution has been injected and incubated for a 24 hour period. Days represent the date in June 2006.

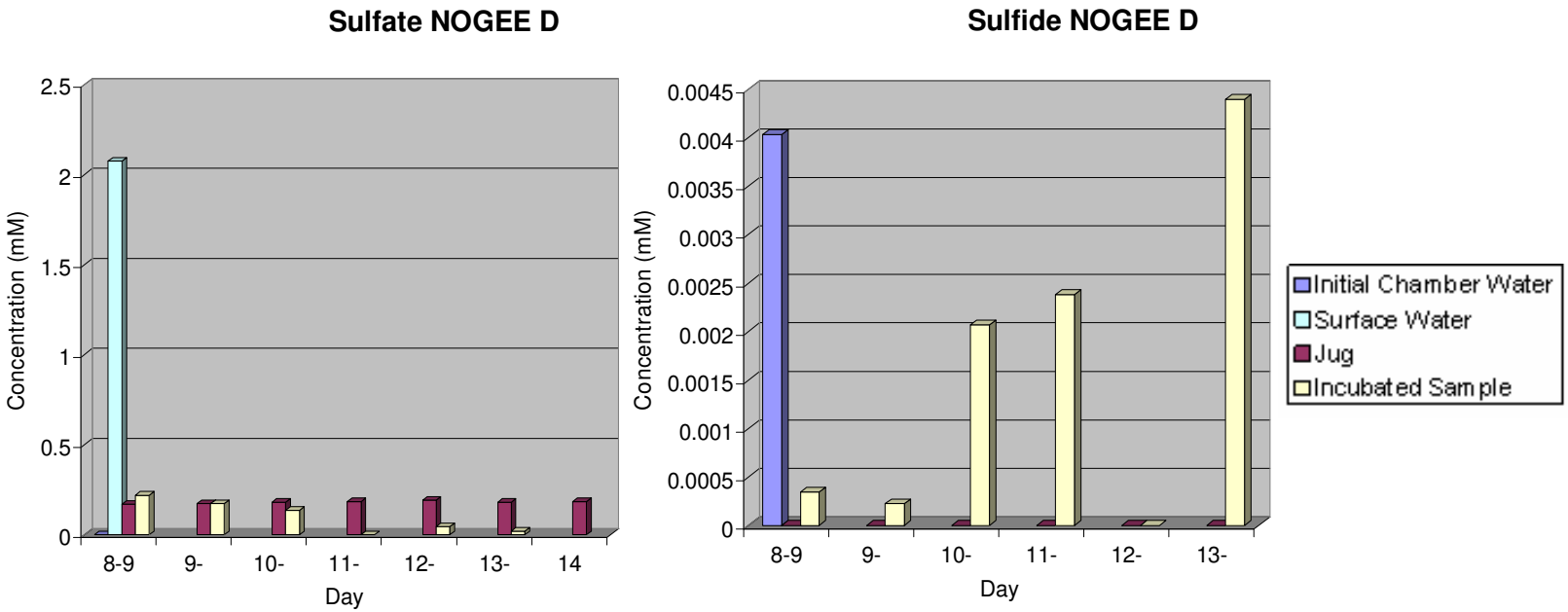

Figure 5.15. Sulfate and sulfide concentrations from NOGEE D obtained from the "initial chamber water" before experimentation, the wetland "surface water", the containers with the solutions ("jug") before adding to chamber, and the "sample incubated" which is the water recovered from the chamber after solution has been injected and incubated for a 24 hour period. Days represent the date in June 2006.

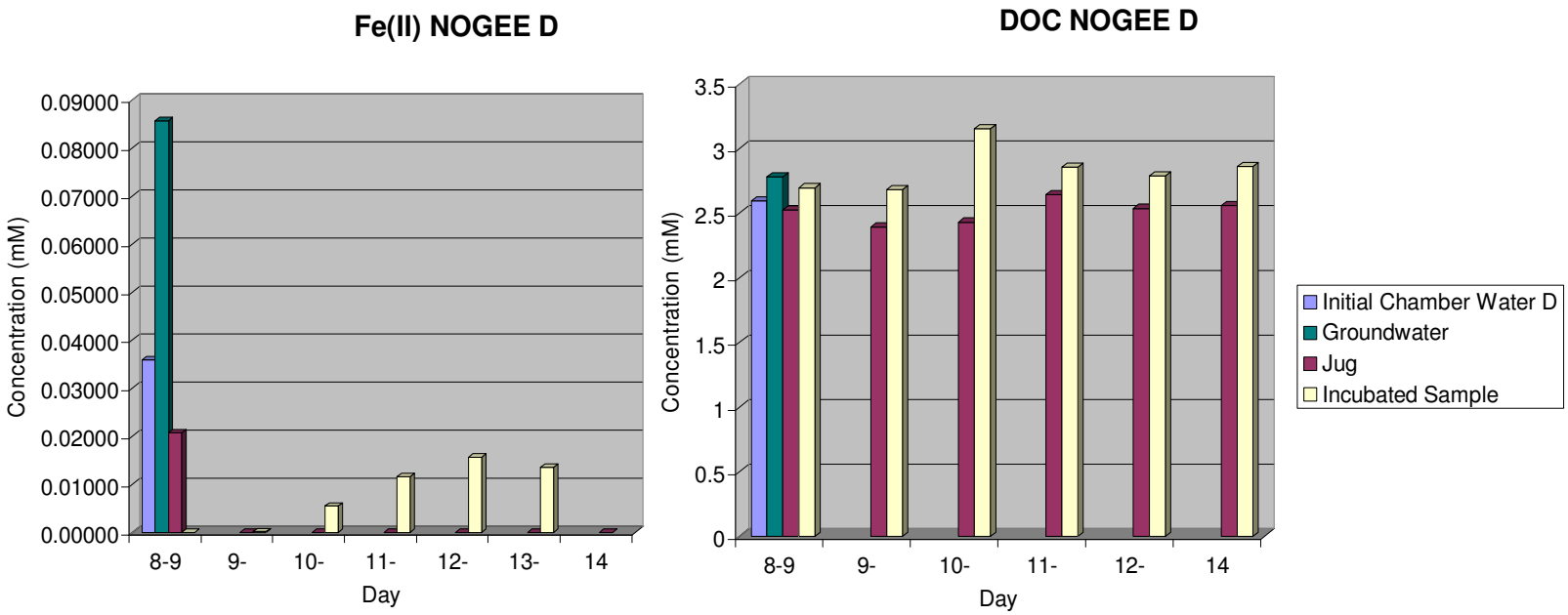

Figure 5.16. Ferrous iron and dissolved organic carbon concentrations from NOGEE D obtained from the "initial chamber water" before experimentation, the wetland "surface water", the containers with the solutions ("jug") before adding to chamber, and the "sample incubated" which is the water recovered from the chamber after solution has been injected and incubated for a 24 hour period. Days represent the date in June 2006.

NOGEE E, Ferrihydrite

This chamber had many problems including difficulty pumping, and when it was removed it was discovered that the chamber was cracked open. Therefore leakage occurred as shown in the bromide and chloride plots (Figure 5. 17).

High concentrations of sulfate recovered from the chamber (>3.5 mM) indicate that the source of sulfate is from the surface water (Figure 5.18). Sulfide concentrations were below detection limits except for the second and fifth day were sulfide is observed but the concentrations were very low (0.000013 mM) compared to sulfide produced in other NOGEEs. Ferrous iron concentrations were not detected, except in the test solution on the third day (Figure 5.19). The lack of Fe^{2+} is consistent with oxygenation in the test solution, and with surface water contamination.

In the test solution, dissolved organic carbon did not vary as much as in NOGEE B and C (Figure 5.19), suggesting that the variability observed in these other NOGEEs is dominated by the cometabolism of DOC with acetate and lactate. DOC concentrations of ~2.25 mM recovered from the chambers might be the DOC concentrations found in the surface water which are similar to the concentrations found in the initial chamber water.

Although experimentation with NOGEE E failed, the analysis of the solution in the jug provides more information on the reactions that are affecting the DOC in the test solutions.

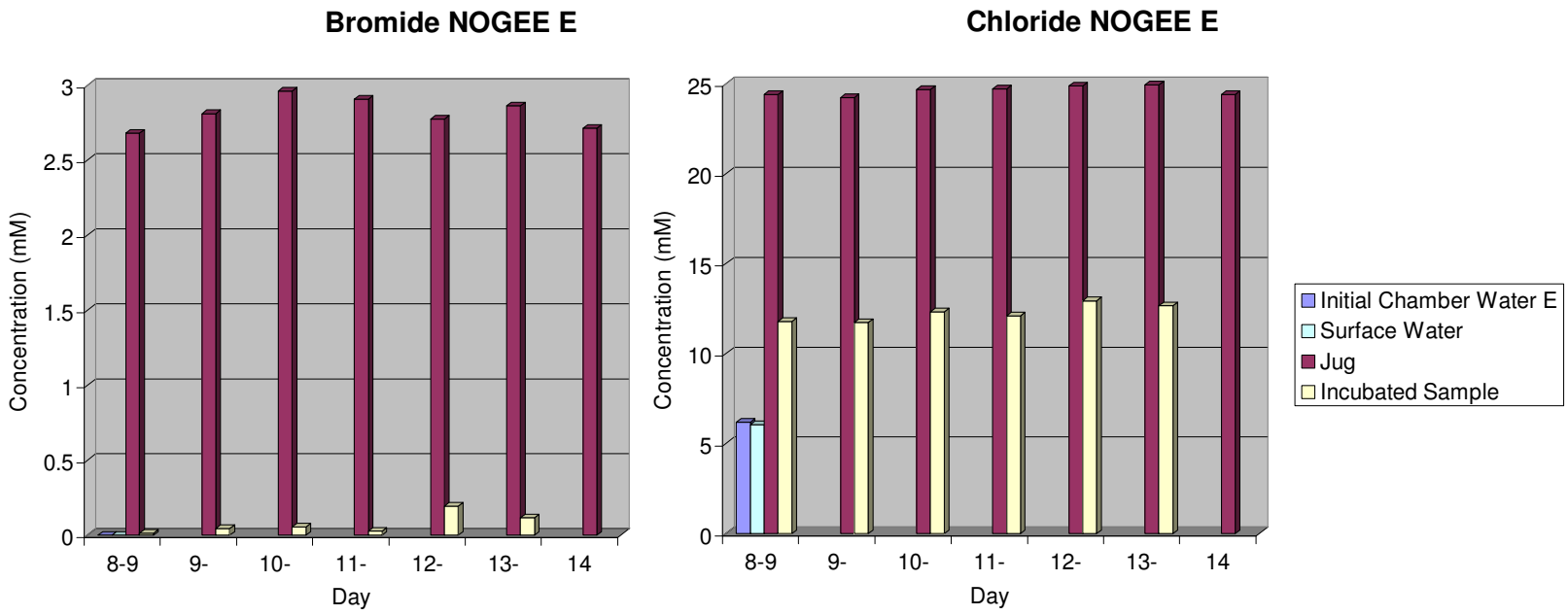

Figure 5.17. Bromide and chloride concentrations from NOGEE E obtained from the "initial chamber water" before experimentation, the wetland "surface water", the containers with the solutions ("jug") before adding to chamber, and the "sample incubated" which is the water recovered from the chamber after solution has been injected and incubated for a 24 hour period. Days represent the date in June 2006.

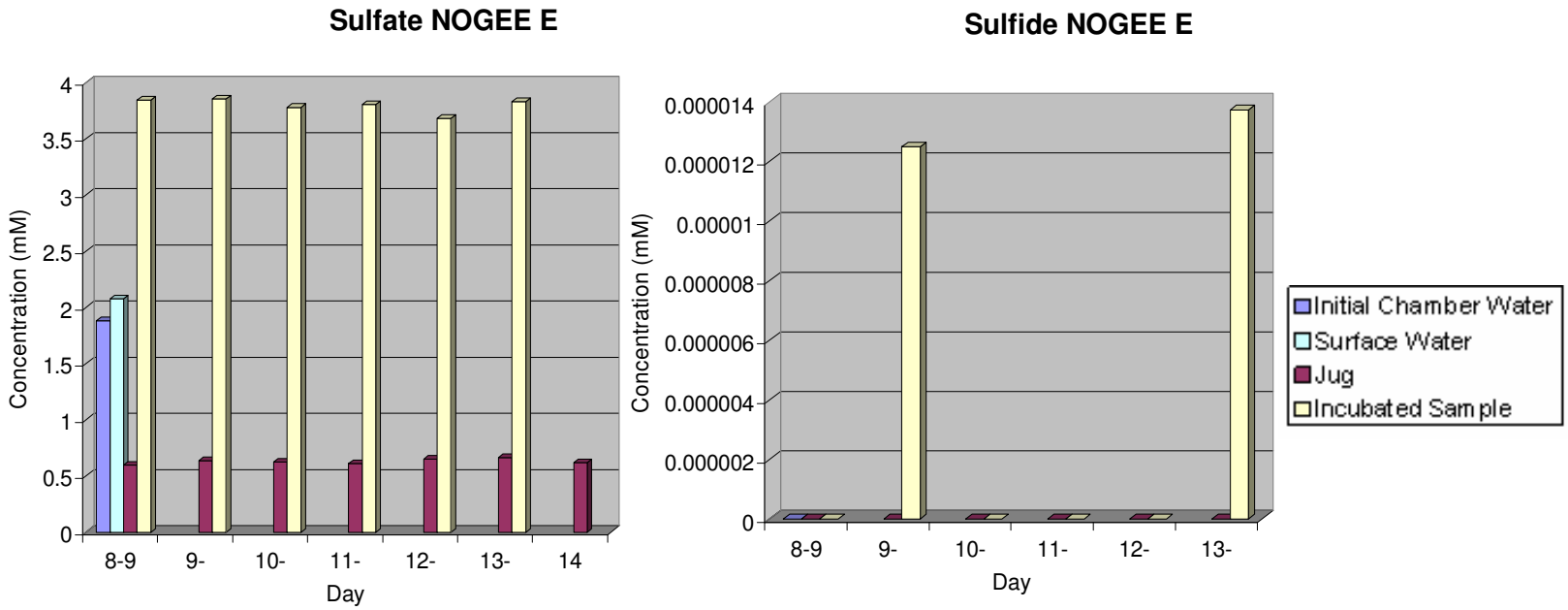

Figure 5.18. Sulfate and sulfide concentrations from NOGEE E obtained from the "initial chamber water" before experimentation, the wetland "surface water", the containers with the solutions ("jug") before adding to chamber, and the "sample incubated" which is the water recovered from the chamber after solution has been injected and incubated for a 24 hour period. Days represent the date in June 2006.

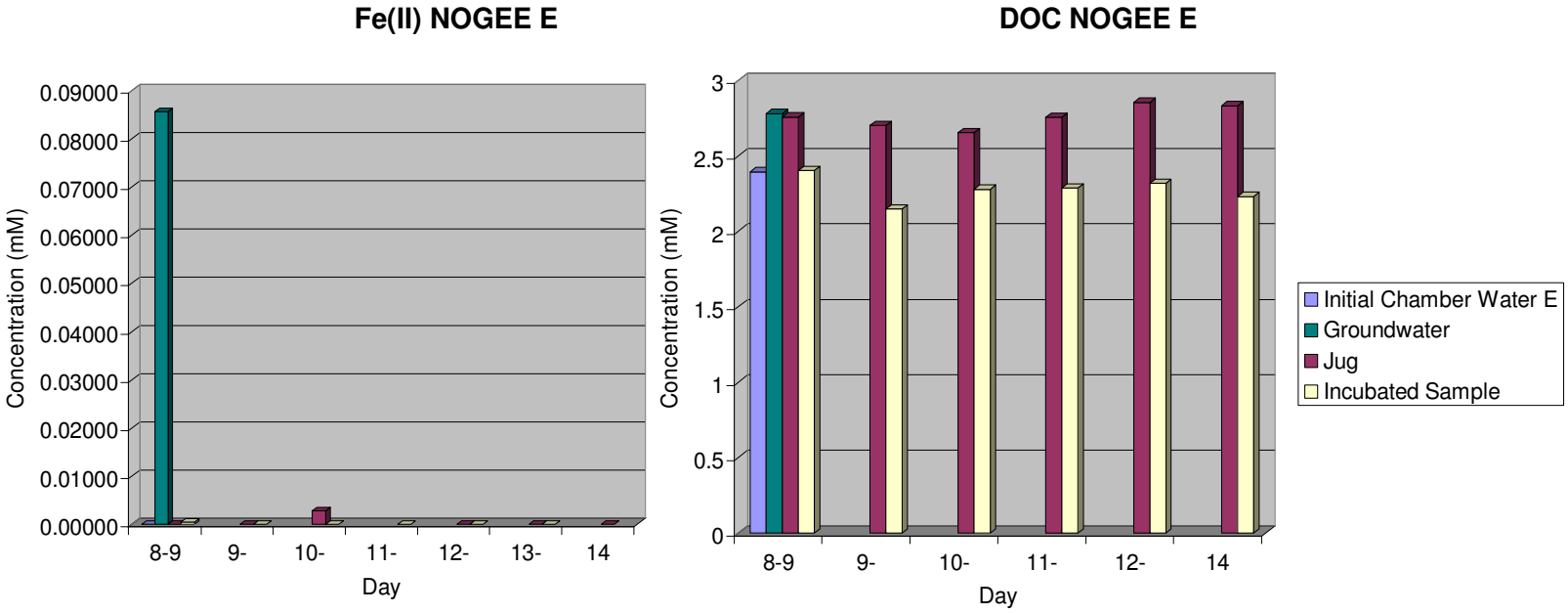

Figure 5.19. Ferrous iron and dissolved organic carbon concentrations from NOGEE E obtained from the "initial chamber water" before experimentation, the wetland "surface water", the containers with the solutions ("jug") before adding to chamber, and the "sample incubated" which is the water recovered from the chamber after solution has been injected and incubated for a 24 hour period. Days represent the date in June 2006.

NOGEE F, Ferrihydrite and Electron Donors

Total recovery of the tracer was achieved on the first day, however it was not the case for the following days as seen in the plots for bromide and chloride (Figure 5.20) and test solution was mixed with the pore water surrounding the chamber. Sulfate was found in the test solution (Figure 5.21) even though sulfate was not detected in the groundwater used to prepare the solution (data not shown). It appears that oxygen was not removed from the jug, oxidizing sulfide in the solution. During the first and second days some of this sulfate was recovered from the chamber, but afterward sulfate was not detected. Sulfide was produced during the period of experimentation (Figure 5.21). The sulfide produced on the first day is indicative of sulfate reduction by the organisms incubated in the sponge. The sulfide concentrations during the following days may represent sulfate reduction occurring in the sponge and in the surrounding pore water. These concentrations varied with time and the concentrations were not as high for NOGEE F as the concentrations found in NOGEE B (highest sulfide concentration 0.0016 vs. 0.01 mM respectively).

Fe^{2+} was not detected on the first day when total recovery of the solution was obtained (Figure 5.22). It cannot be determined if Fe^{2+} was produced because it might have been oxidized or precipitated as iron sulfides. However, the fact that a measurable amount of sulfide was detected on the first day when the solution was completely recovered may indicate that sulfate reduction was dominant over iron reduction even though iron oxides were introduced in this test. An interpretation is that the bacterial community in the sponge consisted mainly of sulfate reducers during the first day.

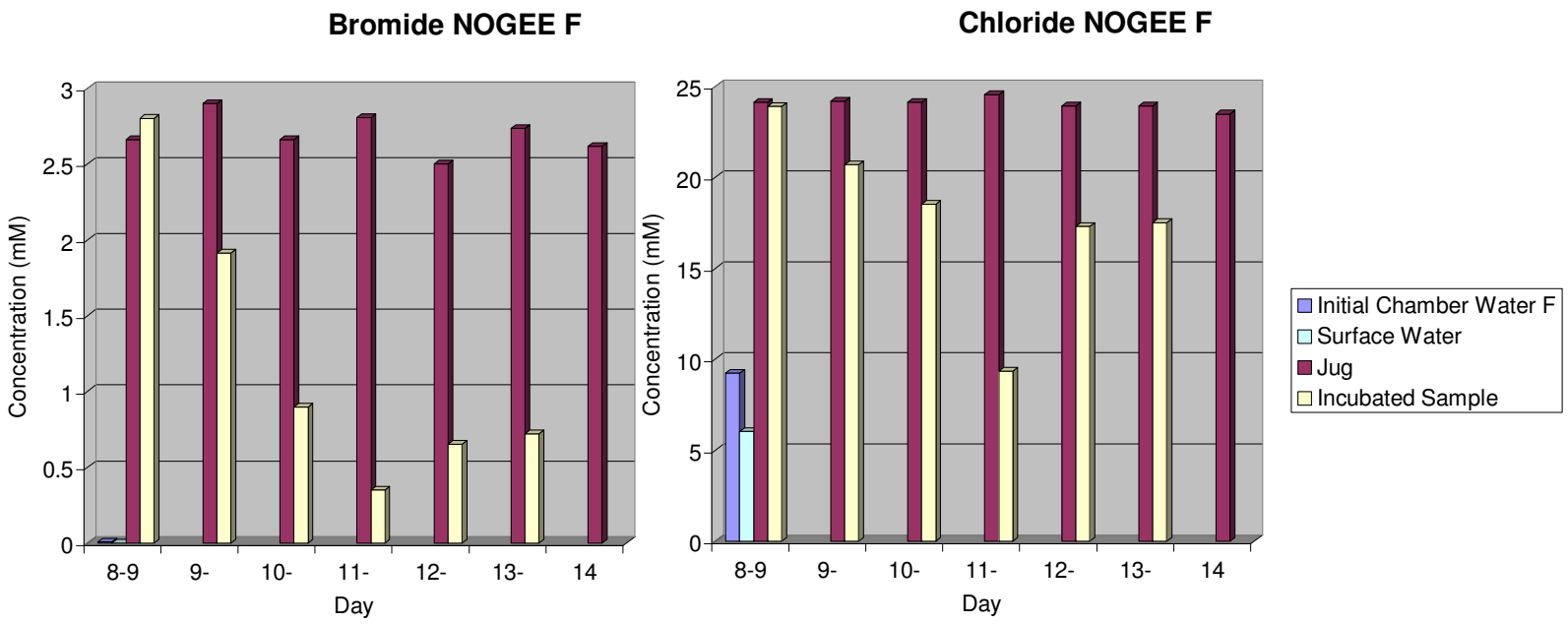

Figure 5.20. Bromide and chloride concentrations from NOGEE F obtained from the "initial chamber water" before experimentation, the wetland "surface water", the containers with the solutions ("jug") before adding to chamber, and the "sample incubated" which is the water recovered from the chamber after solution has been injected and incubated for a 24 hour period. Days represent the date in June 2006.

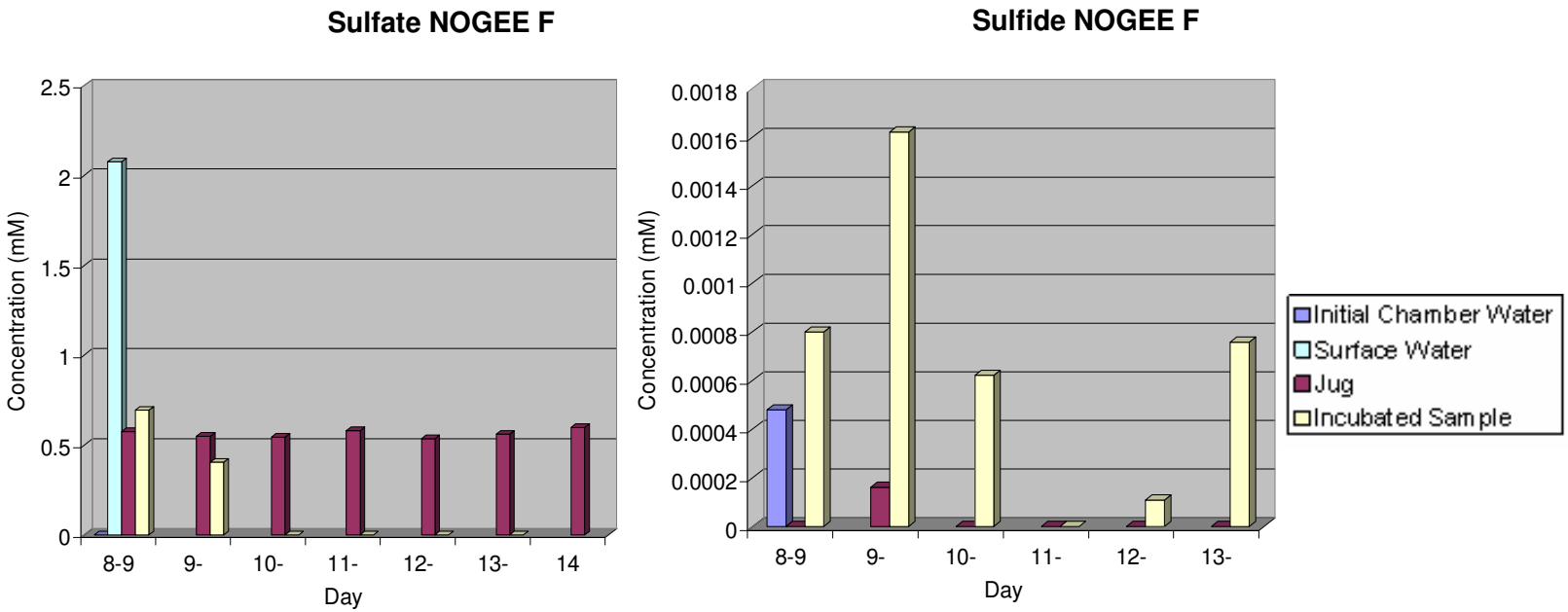

Figure 5.21. Sulfate and sulfide concentrations from NOGEE F obtained from the "initial chamber water" before experimentation, the wetland "surface water", the containers with the solutions ("jug") before adding to chamber, and the "sample incubated" which is the water recovered from the chamber after solution has been injected and incubated for a 24 hour period. Days represent the date in June 2006.

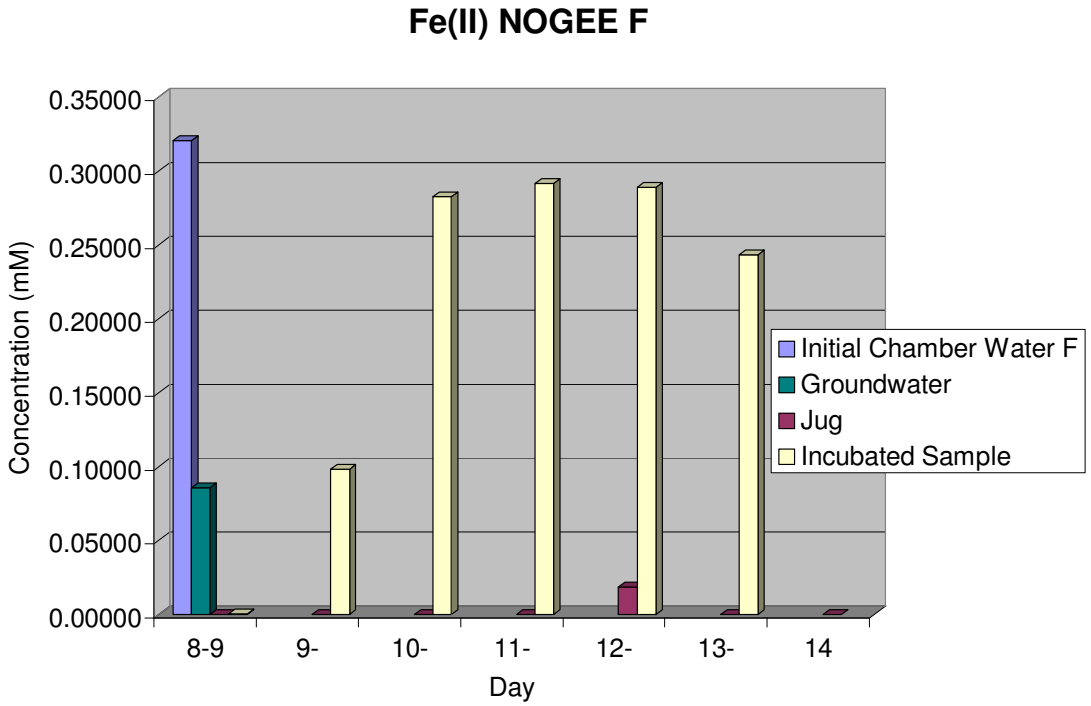

Figure 5.22. Ferrous iron concentrations from NOGEE F obtained from the "initial chamber water" before experimentation, the wetland "surface water", the containers with the solutions ("jug") before adding to chamber, and the "sample incubated" which is the water recovered from the chamber after solution has been injected and incubated for a 24 hour period. Days represent the date in June 2006.

During the second day, with 65% of the solution recovered, Fe^{2+} concentrations are 30% of the initial concentration found in the chamber before experimentation, meaning that the Fe^{2+} observed is from the mixing of the pore water which originally contained high concentrations of Fe^{2+} (Figure 5.22). The following days Fe^{2+} concentrations are high approximately 16 mg/L, but as in the case for the second day these concentrations may be contributed by ferrous iron previously found in the pore water and not necessary by stimulation of iron reduction given the addition of ferrihydrite. It is difficult to determine if there is iron reduction when sulfide is present because iron and sulfide react and precipitate as iron sulfide minerals. The decrease in sulfide during the fourth and fifth day suggests ongoing precipitation.

Samples for DOC are missing for this NOGEE. It is suspected that DOC concentrations in the jug would be variable given the addition of labile electron donors. Further studies to explore the factors affecting concentrations of DOC would be needed.

SUMMARY

The effect of changing geochemical conditions on microbial activities was explored using in situ microcosms at a wetland-aquifer interface characterized with changing geochemical gradients resulting from activities of anaerobic bacteria. Microorganisms were incubated in the microcosms and were isolated for experimentation with various test solutions. These consisted of natural groundwater with additions of electron donors and electron acceptors to stimulate microbial activities

and promote change in community structure enhanced by the growth of specific organisms adapted to the new geochemical conditions.

Rates of sulfate and iron reduction could not be determined due to difficulties encountered in the experiments such as leakage of the test solutions from the microcosm enclosures. Sulfate and iron reduction were observed but the activities could not be attributed solely to the microorganisms incubated in the microcosm. However, it was found that the addition of sulfate and electron donors in the presence of iron oxides (originated in the test solution by reoxidation of ferrous iron) promoted simultaneous iron and sulfate reduction. Sulfate reduction was dominant over iron reduction in the instances were sulfate concentrations were higher than concentrations of iron oxides.

In the tests where ferrihydrite was added, iron reduction was observed but the source of ferric iron utilized cannot be determined given that there was oxidation of ferrous iron in the test solution. The tests containing ferrihydrite, sulfate and electron donors proved that sulfate and iron reduction occur simultaneously competing for electron donors. With equal quantities of sulfate and iron oxides, iron reduction was dominant over sulfate reduction.

Another finding was that some reactions were taking place in the test solutions. Oxygen diffused into the test solutions causing sulfide and ferrous iron to oxidize. In addition, sulfide and ferrous iron were produced in the jugs in some instances suggesting microbial activity occurring in the test solution. Another indication for microbial activity in the test solution was given by the variability of dissolved organic carbon. This variability was only observed in the solutions that contained electron acceptors and

electron donors. It is suspected that microorganisms in the groundwater were stimulated by the presence of electron acceptors and electron donors metabolizing lactate and acetate and cometabolizing DOC.

Although the experiments leaked, there was information obtained from this first attempt that should be considered in the design of future experiments. Some of the problems encountered that should be avoided in future experiments include a better design to 1) seal the microcosms, 2) prevent diffusion of oxygen into the test solutions, and 3) filter bacteria from the groundwater to prevent contamination in the test solution. Based on this first trial, future experiments will be carried on after improvements in the design.

CHAPTER VI

CONCLUSIONS

This dissertation presented a high-resolution biogeochemical study targeting the mixing interface zones within a wetland-aquifer system near the Norman Landfill in Norman, Oklahoma. Temporal and spatial characterization of biogeochemical processes in the freshwater system was achieved in conjunction with determining the seasonal and hydrological controls on these processes.

In Chapter II, steep geochemical gradients indicating zones of significant biogeochemical cycling were observed at the sediment-water and silt-sand interfaces within a wetland-aquifer system which appear to be contact zones between waters of different redox potential. At the sediment-water interface the surface water is a source of electron acceptors whereas the wetland sediments supply organic acids to serve as electron donors. The dominant TEAPs are sulfate and iron reduction, which appear to be occurring at the same location or in reversed thermodynamic order. These trends can be explained by the abundant electron donors present at the sediment-water interface available from the contribution of senescing vegetation. The interface between the upper silt zone and coarse sand lens presents a contact between zones of differing redox potential indicated by a steep gradient of organic acids, which suggest a zone where microbial metabolism is enhanced by the mixing of electron donors and electron acceptors. In this zone sulfate is depleted allowing organic acids and ammonium to

accumulate to high levels. Below this point, these electron donors decrease coincident with the transition to the coarse sand unit where methanogenesis might be occurring. Centimeter-scale sampling allowed for resolution of steep geochemical gradients (sulfate, ferrous iron, sulfide, ammonium, acetate, propionate, and butyrate) supporting the idea that increased microbial activity occurs over small spatial scales at mixing interfaces. This resolution was made possible by the use of capillary electrophoresis (CE) to analyze the majority of geochemical parameters on the low sample volumes available in cm-scale pore waters.

In Chapter III, multivariate statistics were used to elucidate relationships between biogeochemical parameters to determine the dominant biogeochemical processes occurring in the system. Relationships between linked geochemical parameters could not be accomplished by graphical and numerical techniques alone. For example, processes affecting Fe^{2+} concentrations result from various processes including transport and solid phase precipitation/exchange reactions. By using Principal Component Analysis (PCA) the processes affecting Fe^{2+} cycling over time and space were revealed, such as transport from the aquifer, anaerobic respiration, and mineral precipitation/dissolution reactions. In addition, the greatest variability in the dataset was explained by fermentation and is thus considered to be the primary process governing biogeochemical cycling in the system. Sulfate and iron reduction were found to be the dominant TEAPs followed by methanogenesis and sulfate reduction via utilization of barite ($BaSO_4$). Seasonal hydrological patterns (wet and dry periods) were found to be an important control on the availability of electron acceptors through the reoxidation of

reduced iron-sulfur species enhancing iron and sulfate reduction. Variable patterns of geochemical associations as calculated using PCA (factor scores) provide a robust means of interpreting spatial and temporal variations on dominant biogeochemical processes in the wetland-aquifer system.

Chapter IV demonstrates that the spatial and temporal changes in biogeochemistry observed in the system are controlled by the hydrologic linkage of the wetland and underlying aquifer. Biogeochemical processes were determined by interpretation of factors using PCA and the effect of season and hydrologic fluctuations was evaluated by Analysis of Variance (ANOVA) which determined significant differences in the factor scores for each biogeochemical process. Significant differences among sites with different hydrologic regimes (sites with discharge, recharge, or negligent flow) were found for the processes plume advection into the wetland and methanogenesis, where plume advection was strongly associated with the site with upward flow and methanogenesis was highly associated with the location lacking flow. Significant differences by season (May and September) were found for the processes oxidation, barite utilization, and iron reduction. Oxidation varies with changes in the water table elevation, resulting in reoxidation of reduced minerals, making electron acceptors available and iron reduction feasible in September. Barite utilization is strongly associated with the month of May explained by the depletion of sulfate ions under waterlogged conditions. Fermentation and sulfate reduction were not affected by hydrologic fluctuations or seasonal differences. The site most affected by seasonal

conditions was the site that presented negligible water flow, for all the other sites the controlling factor on the biogeochemistry is the hydrological regime.

In Chapter V, rates of sulfate and iron reduction could not be determined due to leakage of the test solutions from the microcosm enclosures. Although indication of sulfate and iron reduction was observed, the activity could not be attributed solely to the microorganisms incubated in the microcosm, instead the reactions observed might have been produced by organisms in the sponges in conjunction with organisms in the pore water surrounding the microcosm enclosures. Indicators of simultaneous iron and sulfate reduction were observed in the instances were iron oxides, sulfate, and electron donors were added. It appears that sulfate reduction dominates over iron reduction when sulfate concentrations were higher than concentrations of iron oxides. With equal quantities of sulfate and iron oxides, iron reduction was dominant over sulfate reduction. Variability of DOC in the test solutions was observed only in the solutions that contained electron donors and electron acceptors, attributed to contamination of microorganisms in the test solution. Even though the experiments leaked, there was information obtained from this first attempt that should be considered in the design of future experiments. Some of the problems encountered that should be avoided in future experiments include a better design to 1) seal the microcosms, 2) prevent diffusion of oxygen into the test solutions, and 3) filter bacteria from the groundwater to prevent contamination in the test solution. Based on this first trial, future experiments will be carried on after improvements in the design.

These results suggest that quantifying the redox reactions occurring at small interface zones and understanding the hydrological and seasonal controls affecting the reactions may be critical to assessing overall biogeochemical cycling in aquifer systems. In addition, the use of multivariate statistics for data reduction of a large database containing geochemical parameters proved to be powerful in the interpretation of dominant biogeochemical processes. A better understanding of the physical, chemical and biological linkages among systems can be used for predicting biogeochemical cycling in other systems such as lakes and rivers and should be considered in conceptual and numerical models of anaerobic systems to improve understanding of the controls on chemical fate and transport, including the ability of systems to naturally attenuate pollutants.

REFERENCES

Achtnich, C., Bak, F., Conrad, R., 1995. Competition for electron donors among nitrate reducers, ferric iron reducers, sulfate reducers, and methanogens in anoxic paddy soil. Biology and Fertility of Soils 19, 65-72.

Adler, M., Hensen, C., Kasten, S., Schulz, H.D., 2000. Computer simulation of deep sulfate reduction in sediments of the Amazon Fan. International Journal of Earth Sciences 88, 641-654.

Albrechtsen, H.-J., Christensen, T.H., 1994. Evidence for microbial iron reduction in a landfill leachate-polluted aquifer (Vejen, Denmark). Applied and Environmental Microbiology 60, 3920-3925.

Aller, R.C., Hall, P.O.J., Rude, P.D., Aller, J.Y., 1998. Biogeochemical heterogeneity and suboxic diagenesis in hemipelagic sediments of the Panama Basin. Deep-Sea Research Part I-Oceanographic Research Papers 45, 133-165.

Amini, M., Abbaspour, K.C., Khademi, H., Fathianpour, N., Afyuni, M., Schulin, R., 2005. Neural network models to predict cation exchange capacity in arid regions of Iran. European Journal of Soil Science 56, 551-559.

APHA, AWWA, WEF. 2005. Standard methods for the examination of water & wastewater. In: Eaton, A. D., et al., (Eds.), 21 ed. American Public Health Association, American Water Works Association, Water Environment Federation, Washington, D.C., pp. 3-77, 4-174.

Aulenta, F., Gossett, J.M., Papini, M.P., Rossetti, S., Majone, M., 2005. Comparative study of methanol, butyrate, and hydrogen as electron donors for long-term dechlorination of tetrachloroethene in mixed anaerobic cultures. Biotechnology and Bioengineering 91, 743-753.

Azcue, J.M., Rosa, F., Lawson, G., 1996. An improved dialysis sampler for the in situ collection of larger volumes of sediment pore waters. Environmental Technology 17, 95-100.

Babu, Y.J., Nayak, D.R., Adhya, T.K., 2006. Potassium application reduces methane emission from a flooded field planted rice. Biology and Fertility of Soils 42, 532-541.

Baedecker, M.J., Cozzarelli, I.M. 1992. The determination and fate of unstable constituents in contaminated ground water. In: Lesage, S. and Jackson, R. (Eds.), Groundwater Auality and Analysis at Hazardous Waste Sites. Marcel Dekker, Inc., New York, pp. 425-461.

Baedecker, M.J., Cozzarelli, I.M., Eganhouse, R.P., Siegel, D.E., Bennett, P.C., 1993. Crude oil in a shallow sand and gravel aquifer: 3. Biogeochemical reactions and mass balance modeling in anoxic groundwater. Applied Geochemistry 8, 569-586.

Baez-Cazull, S.E., McGuire, J.T., Cozzarelli, I.M., Raymond, A., Welsh, L., 2007a. Centimeter-scale characterization of biogeochemical gradients at a wetland-aquifer interface using capillary electrophoresis. In press Applied Geochemistry DOI: 10.1016/j.apgeochem.2007.06.003.

Baez-Cazull, S.E., McGuire, J.T., Cozzarelli, I.M., Voytek, M.A., 2007b. Determination of dominant biogeochemical processes in a contaminated aquifer-wetland system using multivariate statistical analysis. In press Journal of Environmental Quality.

Baez-Cazull, S.E., McGuire, J.T., Cozzarelli, I.M., Voytek, M.A., 2007c. Seasonal hydrological controls on biogeochemical processes at a wetland-aquifer interface. In preparation.

Bakermans, C., Hohnstock-Ashe, A.M., Padmanabhan, S., Padmanabhan, P., Madsen, E.L., 2002. Geochemical and physiological evidence for mixed aerobic and anaerobic field biodegradation of coal tar waste by subsurface microbial communities. Microbial Ecology 44, 107-117.

Bally, G., Mesnage, V., Deloffre, J., Clarisse, O., Lafite, R., Dupont, J.P., 2004. Chemical characterization of porewaters in an intertidal mudflat of the Seine estuary: relationship to erosion-deposition cycles. Marine Pollution Bulletin 49, 163-173.

Baun, A., Reitzel, L.A., Ledin, A., Christensen, T.H., Bjerg, P.L., 2003. Natural attenuation of xenobiotic organic compounds in a landfill leachate plume (Vejen, Denmark). Journal of Contaminant Hydrology 65, 269-291.

Bekins, B.A., Cozzarelli, I.M., Godsy, E.M., Warren, E., Essaid, H.I., Tuccillo, M.E., 2001. Progression of natural attenuation processes at a crude oil spill site: II. Controls on spatial distribution of microbial populations. Journal of Contaminant Hydrology 53, 387-406.

Blodau, C., Hoffmann, S., Peine, A., Peiffer, S., 1998. Iron and sulfate reduction in the sediments of acidic mine lake 116 (Brandenburg, Germany). Water, Air, and Soil Pollution 108, 249-270.

Bolze, C.E., Malone, P.G., Smith, M.J., 1974. Microbial mobilization of barite. Chemical Geology 13, 141-143.

Boschker, H.T.S., Nold, S.C., Wellsbury, P., Bos, D., de Graaf, W., Pel, R., Parkes, R.J., Cappenberg, T.E., 1998. Direct linking of microbial populations to specific biogeochemical processes by C-13-labelling of biomarkers. Nature 392, 801-805.

Breit, G.N., Tuttle, M.L.W., Cozzarelli, I.M., Christenson, S.C., Jaeschke, J.B., Fey, D.L., Berry, C.J., 2005. Results of chemical and isotopic analyses of sediment and water from alluvium of the Canadian River near a closed municipal landfill, Norman, Oklahoma. U.S. Geological Survey, Open-File Report 2005-1091, 1-37.

Brune, A., Frenzel, P., Cypionka, H., 2000. Life at the oxic-anoxic interface: microbial activities and adaptations. FEMS Microbiology Reviews 24, 691-710.

Bruner, M.A., Rao, M., Dumont, J.N., Hull, M., Jones, T., Bantle, J.A., 1998. Ground and surface water developmental toxicity at a municipal landfill: description and weather-related variation. Ecotoxicity and Environmental Safety 39, 215-226.

Capone, D.G., Kiene, R.P., 1988. Comparison of microbial dynamics in marine and freshwater sediments: contrasts in anaerobic carbon catabolism. Limnology and Oceanography 33, 725-749.

Champ, D.R., Gulens, J., Jackson, R.E., 1979. Oxidation-reduction sequences in groundwater flow systems. Canadian Journal of Earth Sciences 127, 85-108.

Chapelle, F.H., McMahon, P.B., 1991. Geochemistry of dissolved inorganic carbon in a coastal-plain aquifer: 1. Sulfate from confining beds as an oxidant in microbial CO_2 production. Journal of Hydrology 127, 85-108.

Chapelle, F.H., McMahon, P.B., Dubrovsky, N.M., Fujii, R.F., Oaksford, E.T., Vroblesky, D.A., 1995. Deducing the distribution of terminal electron-accepting processes in hydrologically diverse groundwater systems. Water Resources Research 31, 359-371.

Chapelle, F.H., Haack, S.K., Adriaens, P., Henry, M., Bradley, P.M., 1996. Comparison of Eh and H_2 measurements for delineating redox processes in a contaminated aquifer. Environmental Science & Technology 30, 3565-3569.

Chapelle, F.H., Bradley, P.M., 1998. Selecting remediation goals by assessing the natural attenuation capacity of groundwater systems. Bioremediation Journal 227-238.

Chen, J., Xuan, J., Du, C., Xie, J., 1997. Effect of potassium nutrition of rice on rhizosphere redox status. Plant and Soil 188, 131-137.

Chen, Z.L., Naidu, R., 2003. Separation of sulfur species in water by co-electroosmotic capillary electrophoresis with direct and indirect UV detection. International Journal of Environmental Analytical Chemistry 83, 749-759.

Christensen, T.H., Bjerg, P.L., Banwart, S., Jakobsen, R., Heron, G., Albrechtsen, H.J., 2000. Characterization of redox conditions in groundwater contaminant plumes. Journal of Contaminant Hydrology 45, 165-241.

Christenson, S., Cozzarelli, I.M., 1999. Geochemical and microbiological processes in ground water and surface water affected by municipal landfill leachate. In: Morganwalp, D.W., and Buxton, H.T. (Eds.), U.S. Geological Survey Toxic Substances Hydrology Program, Proceedings of the technical meeting, Charleston, South Carolina, March 8-12, 1999: U.S. Geological Survey,

Subsurface Contamination from Point Sources: Water-Resources Investigations Report 99-4018, 3, 499-500.

Christenson, S., Scholl, M.A., Schlottmann, J.L., Becker, C.J., 1999. Ground-water and surface-water hydrology of the Norman Landfill Research Site. In: Morganwalp, D.W., and Buxton, H.T. (Eds.), U.S. Geological Survey Toxic Substances Hydrology Program, Proceedings of the technical meeting, Charleston, South Carolina, March 8-12, 1999: U.S. Geological Survey, Subsurface Contamination from Point Sources: Water-Resources Investigations Report 99-4018C, 3, 501-507.

Ciglenecki, I., Caric, M., Krsinic, F., Vilicic, D., Cosovic, B., 2005. The extinction by sulfide-turnover and recovery of a naturally eutrophic, meromictic seawater lake. Journal of Marine Systems 56, 29-44.

Clément, J.-C., Aquilina, L., Bour, O., Plaine, K., Burt, T.P., Pinay, G., 2003. Hydrological flowpaths and nitrate removal rates within a riparian floodplain along a fourth-order stream in Brittany (France). Hydrological Processes 17, 1177-1195.

Cornell, R.M., Schwertmann, U., 2003. The Iron Oxides: Structure, Properties, Reactions, Occurrences, and Uses. 2nd ed. Wiley-VCH, Weinheim.

Cozzarelli, I.M., Baedecker, M.J., Eganhouse, R.P., Goerlitz, D.F., 1994. The geochemical evolution of low-molecular-weight organic acids derived from the degradation of petroleum contaminants in groundwater. Geochimica et Cosmochimica Acta 58, 863-877.

Cozzarelli, I.M., Herman, J.S., Baedecker, M.J., Fischer, J.M., 1999a. Geochemical heterogeneity of a gasoline-contaminated aquifer. Journal of Contaminant Hydrology 40, 261-284.

Cozzarelli, I.M., Suflita, J.M., Ulrich, G.A., Harris, S.H., Scholl, M.A., Schlottmann, J.L., Jaeschke, J.B., 1999b. Biogeochemical processes in a contaminant plume downgradient from a landfill, Norman, Oklahoma. In: Morganwalp, D.W., and Buxton, H.T. (Eds.), U.S. Geological Survey Toxic Substances Hydrology Program, Proceedings of the technical meeting, Charleston, South Carolina,

March 8-12, 1999: U.S. Geological Survey, Subsurface Contamination from Point Sources: Water-Resources Investigations Report 99-4018C, 3, 521-530.

Cozzarelli, I.M., Suflita, J.M., Ulrich, G.A., Harris, S.H., Schroll, M.A., Schlottmann, J.L., Christenson, S., 2000. Geochemical and microbiological methods for evaluating anaerobic processes in an aquifer contaminated by landfill leachate. Environmental Science & Technology 34, 4025-4033.

Cozzarelli, I.M., Bekins, B.A., Baedecker, M.J., Aiken, G.M., Eganhouse, R.P., Tuccillo, M.E., 2001. Progression of natural attenuation processes at a crude-oil spill site: I. Geochemical evolution of the plume. Journal of Contaminant Hydrology 53, 369-385.

Crowe, A.S., Shikaze, S.G., Ptacek, C.J., 2004. Numerical modelling of groundwater flow and contaminant transport to Point Pelee marsh, Ontario, Canada. Hydrological Processes 18, 293-314.

Dabek-Zlotorzynska, E., Kelly, M., Chen, H., Chakrabarti, C.L., 2003. Evaluation of capillary electrophoresis combined with a BCR sequential extraction for determining distribution of Fe, Zn, Cu, Mn, and Cd in airborne particulate matter. Analytica Chimica Acta 498, 175-187.

Dabek-Zlotorzynska, E., Aranda-Rodriguez, R., Graham, L., 2005. Capillary electrophoresis determinative and GC-MS confirmatory method for water-soluble organic acids in airborne particulate matter and vehicle emission. Journal of Separation Science 28, 1520-1528.

Dahm, C.N., Grimm, N.B., Marmonier, P., Valett, H.M., Vervier, P., 1998. Nutrient dynamics at the interface between surface waters and groundwaters. Freshwater Biology 40, 427-451.

Dempster, A., Ellis, P., Wright, B., Stone, M., Price, J., 2006. Hydrogeological evaluation of a Southern Ontario kettle-hole peatland and its linkage to a regional aquifer. Wetlands 26, 49-56.

Devlin, J.F., 1991. Field evidence for the effect of acetate on leachate alkalinity. Ground Water 28, 863-867.

Donahoe, R.J., Liu, C., 1998. Pore water geochemistry near the sediment-water interface of a zoned, freshwater wetland in the southeastern United States. Environmental Geology 33, 143-153.

Drexler, J.Z., Bedford, B.L., Scognamiglio, R., Siegel, D.I., 1999. Fine-scale characteristics of groundwater flow in a peatland. Hydrological Processes 13, 1341-1359.

Duddleston, K.N., Kinney, M.A., Kiene, R.P., Hines, M.E., 2002. Anaerobic microbial biogeochemistry in a northern bog: acetate as a dominant metabolic end product. Global Biogeochemical Cycles 16, 11-1 - 11-9.

Eganhouse, R.P., Cozzarelli, I.M., Scholl, M.A., Matthews, L.L., 2001. Natural attenuation of volatile organic compounds (VOCs) in the leachate plume of a municipal landfill: using alkylbenzenes as process probes. Ground Water 39, 192-202.

Eser, P., Rosen, M.R., 1999. The influence of groundwater hydrology and stratigraphy on the hydrochemistry of Stump Bay, South Taupo Wetland, New Zealand. Journal of Hydrology 220, 27-47.

Farnham, I.M., Johannesson, K.H., Singh, A.K., Hodge, V.F., Stetzenbach, K.J., 2003. Factor analytical approaches for evaluating groundwater trace element chemistry data. Analytica Chimica Acta 490, 123-138.

Fenner, N., Dowrick, D.J., Lock, M.A., Rafarel, C.R., Freeman, C., 2006. A novel approach to studying the effects of temperature on soil biogeochemistry using a thermal gradient bar. Soil Use and Management 22, 267-273.

Frías, S., Sánchez, M.J., Rodríguez, M.A., 2004. Determination of triazine compounds in ground water samples by micellar electrokinetic capillary chromatography. Analytica Chimica Acta 503, 271-278.

Froelich, P.N., Klinkhammer, G.P., Bender, M.L., Luedtke, N.A., Heath, G.R., Cullen, D., Dauphin, P., Hammond, D., Hartman, B., Maynard, V., 1979. Early oxidation of organic matter in pelagic sediments of the eastern equatorial Atlantic: suboxic diagenesis. Geochimica et Cosmochimica Acta 43, 1075-1090.

Fung, Y.S., Lau, K.M., 2001a. Determination of oxoanions in river water by capillary electrophoresis. Electrophoresis 22, 2251-2259.

Fung, Y.F., Lau, K.M., 2001b. Determination of trace metals by capillary electrophoresis. Electrophoresis 22, 2192-2200.

Grossman, E.L., Cifuentes, L.A., Cozzarelli, I.M., 2002. Anaerobic methane oxidation in a landfill-leachate plume. Environmental Science & Technology 36, 2436-2442.

Güler, C., Thyne, G., McCray, J.E., Turner, A.K., 2002. Evaluation of graphical and multivariate statistical methods for classification of water chemistry data. Hydrogeology Journal 10, 455-474.

Hemond, H.F., 1990. Acid neutralizing capacity, alkalinity, and acid-base status of natural waters containing organic acids. Environmental Science & Technology 24, 1486-1489.

Hesslein, R.H., 1976. An in situ sampler for close interval pore water studies. Limnology and Oceanography 21, 912-914.

Hines, M.E., Knollmeyer, S.L., Tugel, J.B., 1989. Sulfate reduction and other sedimentary biogeochemistry in a northern New England salt marsh. Limnology and Oceanography 34, 578-590.

Hines, M.E., Banta, G.T., Giblin, A.E., Hobbie, J.E., Tugel, J.B., 1994. Acetate concentrations and oxidation in salt-marsh sediments. Limnology and Oceanography 39, 140-148.

Ho, T.Y., Scranton, M.I., Taylor, G.T., Varela, R., Thunell, R.C., Muller-Karger, F., 2002. Acetate cycling in the water column of the Cariaco Basin: seasonal and

vertical variability and implication for carbon cycling. Limnology and Oceanography 47, 1119-1128.

Hsieh, Y.Z., Huang, H.Y., 1996. Analysis of chlorophenoxy acid herbicides by cyclodextrin-modified capillary electrophoresis. Journal of Chromatography A 745, 217-223.

Huang, X.F., Hu, M., He, L.Y., Tang, X.Y., 2005. Chemical characterization of water-soluble organic acids in PM2.5 in Beijing, China. Atmospheric Environment 39, 2819-2827.

Hunt, R.J., Krabbenhoft, D.P., Anderson, M.P., 1997. Assessing hydrogeochemical heterogeneity in natural and constructed wetlands. Biogeochemistry 39, 271-293.

Jacobs, P.H., 2002. A new rechargeable dialysis pore water sampler for monitoring sub-aqueous in situ sediment caps. Water Research 36, 3121-3129.

Jones, E.J.P., Nadeau, T.-L., Voytek, M.A., Landa, E.R., 2006. Role of microbial iron reduction in the dissolution of iron hydroxysulfate minerals. Journal of Geophysical Research 111, G01012.

Jones, W.B., Cifuentes, L.A., Kaldy, J.E., 2003. Stable carbon isotope evidence for coupling between sedimentary bacteria and seagrasses in a sub-tropical lagoon. Marine Ecology Progress Series 255, 15-25.

Kaiser, H.F., 1960. The application of electronic computers to factor analysis. Educational and Psychological Measurement 20, 141-151.

Kantrud, H.A., 1990. Sago pondweed (*Potamogeton pectinatus* L.): A literature review. [Online http://www.npwrc.usgs.gov/resource/plants/pondweed/index.htm]. Available by U.S. Fish and Wildlife Service, Fish and Wildlife Resource Publication 176. Jamestown, North Dakota: Northern Prairie Wildlife Research Center (posted Version 16JUL97; verified April 29, 2006).

Kappler, A., Emerson, D., Edwards, K., Amend, J.P., Gralnick, J.A., Grathwohl, P., Hoehler, T., Straub, K.L., 2005. Microbial activity in biogeochemical gradients-new aspects of research. Geobiology 3, 229-233.

Kemp, W.M., Sampou, P.A., Garber, J., Tuttle, J., Boynton, W.R., 1992. Seasonal depletion of oxygen from bottom waters of Chesapeake Bay - Roles of benthic and planktonic respiration and physical exchange processes. Marine Ecology-Progress Series 85, 137-152.

Kharaka, Y.K., Ambats, G., Thordsen, J.J., 1993. Distribution and significance of dicarboxylic-acid anions in oil-field waters. Chemical Geology 107, 499-501.

Kleikemper, J., Schroth, M.H., Sigler, W.V., Schmucki, M., Bernasconi, S.M., Zeyer, J., 2002. Activity and diversity of sulfate-reducing bacteria in a petroleum hydrocarbon-contaminated aquifer. Applied and Environmental Microbiology 68, 1516-1523.

Kleinmeyer, J.A., Rose, P.E., Harris, J.M., 2001. Determination of ultratrace-level fluorescent tracer concentrations in environmental samples using a combination of HPLC separation and laser-excited fluorescence multiwavelength emission detection: Application to testing of geothermal well brines. Applied Spectroscopy 55, 690-700.

Kneeshaw, T.A., Mcguire, J.T., Smith, E.W., Cozzarelli, I.M., 2007. Evaluation of sulfate reduction at experimentally induced mixing interfaces using small-scale push-pull tests in an aquifer-wetland system. In press Applied Geochemistry DOI: 10.1016/j.apgeochem.2007.06.006

Koch, M.S., Mendelssohn, I.A., Mckee, K.L., 1990. Mechanism for the hydrogen sulfide-induced growth limitation in wetland macrophytes. Limnology and Oceanography 35, 399-408.

Koretsky, C.M., Moore, C.M., Lowe, K.L., Meile, C., DiChristina, T.J., Van Cappellen, P., 2003. Seasonal oscillation of microbial iron and sulfate reduction in saltmarsh sediments (Sapelo Island, GA, USA). Biogeochemistry 64, 179-203.

Koretsky, C.M., Van Cappellen, P., DiChristina, T.J., Kostka, J.E., Lowe, K.L., Moore, C.M., Roychoudhury, A.N., Viollier, E., 2005. Salt marsh pore water geochemistry does not correlate with microbial community structure. Estuarine, Coastal and Shelf Science 62, 233-251.

Kostka, J.E., Wu, J., Nealson, K.H., Stucki, J.W., 1999. The impact of structural Fe(III) reduction by bacteria on the surface chemistry of smectite clay minerals. Geochimica et Cosmochimica Acta 63, 3705-3713.

Kostka, J.E., Roychoudhury, A., Van Cappellen, P., 2002. Rates and controls of anaerobic microbial respiration across spatial and temporal gradients in saltmarsh sediments. Biogeochemistry 60, 49-76.

Kumar, M., Ramanathan, A., Rao, M.S., Kumar, B., 2006. Identification and evaluation of hydrogeochemical processes in the groundwater environment of Delhi, India. Environmental Geology 50, 1025-1039.

Langmuir, D., 1997. Aqueous and Environmental Geochemistry. Prentice-Hall, Inc., Upper Saddle River, New Jersey.

Lensing, H.J., Vogt, M., Herrling, B., 1994. Modeling of biologically mediated redox processes in the subsurface. Journal of Hydrology 159, 125-143.

Lindberg, R.D., Runnells, D.D., 1984. Ground water redox reactions: An analysis of equilibrium state applied to Eh measurements and geochemical modeling. Science 225, 925-927.

Linhardt, R.J., Toida, T., 2002. Ultra-high resolution separation comes of age (Capillary Electrophoresis). Science 298, 1441-1442.

Liu, C.-W., Lin, K.-H., Kuo, Y.-M., 2003. Application of factor analysis in the assessment of groundwater quality in a blackfoot disease area in Taiwan. The Science of the Total Environment 313, 77-89.

Llobet-Brossa, E., Rabus, R., Bottcher, M.E., Konneke, M., Finke, N., Schramm, A., Meyer, R.L., Grotzschel, S., Rossello-Mora, R., Amann, R., 2002. Community structure and activity of sulfate-reducing bacteria in an intertidal surface sediment: a multi-method approach. Aquatic Microbial Ecology 29, 211-226.

Lorah, M.M., Cozzarelli, I.M., Böhlke, J.K., 2007. Biogeochemical effect of interaction of a landfill leachate plume with a seasonally ponded wetland (slough). In review Journal of Contaminant Hydrology.

Lovley, D.R., Phillips, E.J.P., 1987. Competitive mechanisms for the inhibition of sulfate reduction and methane production in the zone of ferric iron reduction in sediments. Applied and Environmental Microbiology 53, 2636-2641.

Lovley, D.R., Phillips, E.J.P., Lonergan, D.J., 1991. Enzymatic versus nonenzymatic mechanisms for Fe(III) reduction in aquatic sediments. Environmental Science & Technology 25, 1062-1067.

Ludvigsen, L., Albrechtsen, H.-J., Heron, G., Bjerg, P.L., Christensen, T.H., 1998. Anaerobic microbial processes in a landfill leachate contaminated aquifer (Grindsted, Denmark). Journal of Contaminant Hydrology 33, 273-291.

Lyngkilde, J., Christensen, T.H., 1992a. Fate of organic contaminants in the redox zones of a landfill leachate pollution plume (Vejen, Denmark). Journal of Contaminant Hydrology 10, 291-307.

Lyngkilde, J., Christensen, T.H., 1992b. Redox zones of a landfill leachate pollution plume (Vejen, Denmark). Journal of Contaminant Hydrology 10, 273-289.

Malard, F., Tockner, K., Dole-Olivier, M.J., Ward, J.V., 2002. A landscape perspective of surface-subsurface hydrological exchanges in river corridors. Freshwater Biology 47, 621-640.

Mathes, S.E., Rasmussen, T.C., 2006. Combining multivariate statistical analysis with geographic information systems mapping: a tool for delineating groundwater contamination. Hydrogeology Journal 14, 1493-1507.

Mayer, K.U., Benner, S.G., Frind, E.O., Thornton, S.F., Lerner, D.N., 2001. Reactive transport modeling of processes controlling the distribution and natural attenuation of phenolic compounds in a deep sandstone aquifer. Journal of Contaminant Hydrology 53, 341-368.

McGuire, J.T., Smith, E.W., Long, D.T., Hyndman, D.W., Haack, S.K., Kolak, J.J., Klug, M.J., Velbel, M.A., Forney, L.J., 1999. Temporal variations in biogeochemical processes that influence ground water redox zonation. In: Morganwalp, D.W., and Buxton, H.T. (Eds.), U.S. Geological Survey Toxic Substances Hydrology Program, Proceedings of the technical meeting, Charleston, South Carolina, March 8-12, 1999: U.S. Geological Survey, Subsurface Contamination from Point Sources: Water-Resources Investigations Report 99-4018C, 3, 641-652.

McGuire, J.T., Smith, E.W., Long, D.T., Hyndman, D.W., Haack, S.K., Klug, M.J., Velbel, M.A., 2000. Temporal variations in parameters reflecting terminal-electron-accepting processes in an aquifer contaminated with waste fuel and chlorinated solvents. Chemical Geology 169, 471-485.

McGuire, J.T., Long, D.T., Klug, M.J., Haack, S.K., Hyndman, D.W., 2002. Evaluating behavior of oxygen, nitrate, and sulfate during recharge and quantifying reduction rates in a contaminated aquifer. Environmental Science & Technology 36, 2693-2700.

McGuire, J.T., Long, D.T., Hyndman, D.W., 2005. Analysis of recharge-induced geochemical change in a contaminated aquifer. Ground Water 43, 518-530.

McMahon, P.B., Chapelle, F.H., 1991. Microbial-production of organic-acids in aquitard sediments and its role in aquifer geochemistry. Nature 349, 233-235.

McMahon, P.B., 2001. Aquifer/aquitard interfaces: mixing zones that enhance biogeochemical reactions. Hydrogeology Journal 9, 34-43.

Megonigal, J.P., Hines, M.E., Visscher, P.T., 2004. Anaerobic Metabolism: Linkages to Trace Gases and Aerobic Processes. Elsevier-Pergamon, Oxford, United Kingdom.

Molina, M., Perez-Bendito, D., Silva, M., 1999. Multi-residue analysis of N-methylcarbamate pesticides and their hydrolytic metabolites in environmental waters by use of solid-phase extraction and micellar electrokinetic chromatography. Electrophoresis 20, 3439-3449.

Mori, M., Hu, W., Haddad, P.R., Fritz, J.S., Tanaka, K., Tsue, H., Tanaka, S., 2002. Capillary electrophoresis using high ionic strength background electrolytes containing zwitterionic and non-ionic surfactants and its application to direct determination of bromide and nitrate in seawater. Analytical and Bioanalytical Chemistry 372, 181-186.

Motelica-Heino, M., Naylor, C., Zhang, H., Davison, W., 2003. Simultaneous release of metals and sulfide in lacustrine sediment. Environmental Science & Technology 37, 4374-4381.

Nealson, K.H., 1997. Sediment bacteria: Who's there, what are they doing, and what's new? Annual Review of Earth and Planetary Sciences 25, 403-434.

Neubauer, S.C., Givler, K., Valentine, S., Megonigal, J.P., 2005. Seasonal patterns and plant-mediated controls of subsurface wetland biogeochemistry. Ecology 86, 3334-3344.

Nicholson, R.V., Cherry, J.A., Reardon, E.J., 1983. Migration of contaminants in groundwater at a landfill: A case study. Journal of Hydrology 63, 131-176.

Novák, M., Wieder, R.K., Schell, W.R., 1994. Sulfur during early diagenesis in *Sphagnum* peat: Insights from $\delta^{34}S$ ratio profiles in ^{210}Pb-dated peat cores. Limnology and Oceanography 39, 1172-1185.

Okabe, S., Santegoeds, C.M., De Beer, D., 2003. Effect of nitrite and nitrate on in situ sulfide production in an activated sludge immobilized agar gel film as determined by use of microelectrodes. Biotechnology and Bioengineering 81, 570-577.

Parkhurst, D.L., 1995. PHREEQC: User's guide to PHREEQC: a computer program for speciation, reaction-path, advective-transport, and inverse geochemical

calculations. U.S. Geological Survey Water Resource, Investigations Report 95-4227, 1-143.

Paul, E.A., Clark, F.E., 1996. Soil Microbiology and Biochemistry. Second ed. Academic Press, San Diego, California.

Peterson, J.N., Sun, Y., 2000. An analytical solution evaluating steady-state plumes of sequentially reactive contaminants. Transport in Porous Media 41, 287-303.

Postma, D., Jakobsen, R., 1996. Redox zonation: Equilibrium constraints on the Fe(III)/SO_4^- reduction interface. Geochimica et Cosmochimica Acta 60, 3169-3175.

Puckett, L.J., Bricker, O.P., 1992. Factors controlling the major ion chemistry of streams in the Blue Ridge and Valley and Ridge physiographic provinces of Virginia and Maryland. Hydrological Processes 6, 79-98.

Qian, J., Mopper, K., 1996. Automated high performance, high temperature combustion total organic carbon analyzer. Analytical Chemistry 68, 3090-3097.

Raven, K.P., Jain, A., Loeppert, R.H., 1998. Arsenite and arsenate adsorption on ferrihydrite: kinetics, equilibrium, and adsorption envelopes. Environmental Science & Technology 32, 344-349.

Rennert, T., Mansfeldt, T., 2005. Iron-cyanide complexes in soil under varying redox conditions: speciation, solubility and modelling. European Journal of Soil Science 56, 527-536.

Reynolds, R.C., Jr., 1978. Polyphenol inhibition of calcite precipitation in Lake Powell. Limnology and Oceanography 23, 585-597.

Röling, W.F.M., van Breukelen, B.M., Braster, M., Lin, B., van Verseveld, H.W., 2001. Relationships between microbial community structure and hydrochemistry in a landfill leachate-polluted aquifer. Applied and Environmental Microbiology 67, 4619-4629.

Safarpour, H., Asiaie, R., Katz, S., 2004. Quantitative analysis of imazamox herbicide in environmental water samples by capillary electrophoresis electrospray ionization mass spectrometry. Journal of Chromatography A 1036, 217-222.

Sanchez, M.E., Rabanal, B., Otero, M., Martin-Villacorta, J., 2003. Solid-phase extraction for the determination of dimethoate in environmental water and soil samples by Micellar Electrokinetic Capillary Chromatography (MEKC). Journal of Liquid Chromatography & Related Technologies 26, 545-557.

SAS Institute, 1999. JMP Version 4. SAS Inst., Cary, North Carolina.

Sass, A.M., Eschemann, A., Kuhl, M., Thar, R., Sass, H., Cypionka, H., 2002. Growth and chemosensory behavior of sulfate-reducing bacteria in oxygen-sulfide gradients. FEMS Microbiology Ecology 40, 47-54.

Schlesinger, W.H., 1997. Biogeochemistry: An Analysis of Global Change. 2nd ed. Academic Press, San Diego, California.

Schlottmann, J.L. 2001. Water chemistry near the closed Norman Landfill, Cleveland County, Oklahoma, 1995. U.S. Geological Survey Water-Resources Investigations Report 00-4238 1-41.

Scholl, M.A., Christenson, S., 1998. Spatial variation in hydraulic conductivity determined by slug tests in the Canadian River alluvium near the Norman Landfill, Norman, Oklahoma. U.S. Geological Survey Water-Resources, Investigations Report 97-4292 1-28.

Scholl, M.A., Christenson, S.C., Cozzarelli, I.M., Ferree, D., Jaeschke, J., 2005. Recharge processes in an alluvial aquifer riparian zone, Norman Landfill, Norman, Oklahoma, 1998-2000. U.S. Geological Survey Scientific Investigations, Report 2004-5238 1-53.

Schot, P.P., van der Waal, J., 1992. Human impact on regional groundwater composition through intervention in natural flow patterns and changes in land use. Journal of Hydrology (Amsterdam) 134, 297-313.

Seidel, B.S., Faubel, W., 1998. Determination of iron in real samples by high performance capillary electrophoresis in combination with thermal lensing. Fresenius' Journal of Analytical Chemistry 360, 795-797.

Sène, M., Doré, T., Pellissier, F., 2000. Effect of phenolic acids in soil under and between rows of a prior sorghum (*Sorghum bicolor*) crop on germination, emergence, and seedling growth of peanut (*Arachis hypogea*). Journal of chemical Ecology 26, 625-637.

Seybold, C.A., Mersie, W., Huang, J.Y., McNamee, C., 2002. Soil redox, pH, temperature, and water-table patterns of a freshwater tidal wetland. Wetlands 22, 149-158.

Shakulashvili, N., Faller, T., Engelhardt, H., 2000. Simultaneous determination of alkali, alkaline earth and transition metal ions by capillary electrophoresis with indirect UV detection. Journal of Chromatography A 895, 205-212.

Shannon, R.D., White, J.R., 1996. The effects of spatial and temporal variations in acetate and sulfate on methane cycling in two Michigan peatlands. Limnology and Oceanography 41, 435-443.

Stacy, B.L., 1961. Ground water resources of the alluvial deposits of the Canadian River valley near Norman, Oklahoma. U.S. Geological Survey, Open-File Report 61-177 1-61.

Stucki, J.W., Shen, S. 1993. Effects of Iron Oxidation State on Potassium Fixation. University of Illinois, Urbana, Illinois.

Stucki, J.W., Kostka, J.E., 2006. Microbial reduction of iron in smectite. C.R. Geoscience 338, 468-475.

Suk, H., Lee, K.-K., 1999. Characterization of a ground water hydrochemical system through multivariate analysis: clustering into ground water zones. Ground Water 37, 358-366.

Thyne, G., Güler, C., Poeter, E., 2004. Sequential analysis of hydrochemical data for watershed characterization. Ground Water 42, 711-723.

Tuxen, N., Albrechtsen, H.-J., Bjerg, P.L., 2006. Identification of a reactive degradation zone at a landfill leachate plume fringe using high resolution sampling and incubation techniques. Journal of Contaminant Hydrology 85, 179-194.

Ulrich, G.A., Martino, D., Burger, K., Routh, J., Grossman, E.L., Ammerman, J.W., Suflita, J.M., 1998. Sulfur cycling in the terrestrial subsurface: Commensal interactions, spatial scales, and microbial heterogeneity. Microbial Ecology 36, 141-151.

Ulrich, G.A., Breit, G., Cozzarelli, I.M., 2003. Sources of sulfate supporting anaerobic metabolism in a contaminated aquifer. Environmental Science & Technology 37, 1093-1099.

USGS Water Resources of Oklahoma, 2007. Daily data of the Canadian River tributary at Norman, OK. [Online http://waterdata.usgs.gov/ok/nwis/inventory/?site_no=07229053&]. Available by U.S. Geological Survey, National Water Information System. (verified January 15, 2007).

van Breukelen, B.M., Röling, W.F.M., Groen, J., Griffioen, J., van Verseveld, H.W., 2003. Biogeochemistry and isotope geochemistry of a landfill leachate plume. Journal of Contaminant Hydrology 65, 245-268.

van Breukelen, B.M., Griffioen, J., 2004. Biogeochemical processes at the fringe of a landfill leachate plume: potential for dissolved organic carbon, Fe(II), Mn(II), NH_4, and CH_4 oxidation. Journal of Contaminant Hydrology 73, 181-205.

van Breukelen, B.M., Griffioen, J., Röling, W.F.M., van Verseveld, H.W., 2004. Reactive transport modelling of biogeochemical processes and carbon isotope geochemistry inside a landfill leachate plume. Journal of Contaminant Hydrology 70, 249-269.

van Griethuysen, C., Luitwieler, M., Joziasse, J., Koelmans, A.A., 2005. Temporal variation of trace metal geochemistry in floodplain lake sediment subject to dynamic hydrological conditions. Environmental Pollution 137, 281-294.

van Helvoort, P.-J., Filzmoser, P., van Gaans, P.F.M., 2005. Sequential Factor Analysis as a new approach to multivariate analysis of heterogeneous geochemical datasets: an application to a bulk chemical characterization of fluvial deposits (Rhine-Meuse delta, The Netherlands). Applied Geochemistry 20, 2233-2251.

Voicu, G., Hallbauer, D.K., 2005. Determination of the physico-chemical characteristics of hydrothermal fluids from the post-metamorphic Omai gold deposit, Guiana Shield, using analysis of ionic species by crush-leach technique and capillary electrophoresis. Mineralogy and Petrology 83, 243-270.

Wayland, K.G., Long, D.T., Hyndman, D.W., Pijanowski, B.C., Woodhams, S.M., Haack, S.K., Haack, S.K., 2003. Identifying relationships between baseflow geochemistry and land use with synoptic sampling and r-mode factor analysis. Journal of Environmental Quality 32, 180-190.

Webster, I.T., Teasdale, P.R., Grigg, N.J., 1998. Theoretical and experimental analysis of peeper equilibration dynamics. Environmental Science & Technology 32, 1727-1733.

Weiss, J.V., Emerson, D., Megonigal, J.P., 2004. Geochemical control of microbial Fe(III) reduction potential in wetlands: comparison of the rhizosphere to non-rhizosphere soil. FEMS Microbiology Ecology 48, 89-100.

Wellsbury, P., Parkes, R.J., 1995. Acetate bioavailability and turnover in an estuarine sediment. FEMS Microbiology Ecology 17, 85-94.

Welsh, L.W., Raymond, A., McGuire, J.T., Baez-Cazull, S., Smith, E., 2007. Burial and decomposition of particulate organic matter in a temperate, siliciclastic, freshwater wetland. In review Wetlands.

Wu, C.H., Lo, Y.S., Nian, H.C., Lin, Y.Y., 2003. Capillary electrophoretic analysis of the derivatives and isomers of benzoate and phthalate. Journal of Chromatography A 1003, 179-187.

Xie, Z., Sun, L., Zhang, P., Zhao, S., Yin, X., Liu, X., Cheng, B., 2005. Preliminary geochemical evidence of groundwater contamination in coral islands of Xi-Sha, South China Sea. Applied Geochemistry 20, 1848-1856.

Yang, W.P., Zhang, Z.J., Deng, W., 2003. Simultaneous, sensitive and selective on-line chemiluminescence determination of Cr(III) and Cr(VI) by capillary electrophoresis. Analytica Chimica Acta 485, 169-177.

Yao, W., Xu, S.K., 2002. Determination of nitrate and nitrite in environmental water samples with direct ultraviolet detection by flow injection-capillary electrophoresis. Chinese Journal of Analytical Chemistry 30, 836-838.

APPENDIX A

SULFIDE COLORIMETRIC METHOD

Sulfide Test

Reagents

1. Ferric Chloride Solution 250g/100mL Cat#NC 9404941
2. Sulfide Standard Solution 1000 ppm Cat#NC9652106
3. Amine-Sulfuric Acid Cat #610-32
4. 2N Zinc Acetate Solution Cat # 9450-4

Preparation of Amine-Sulfuric/Ferric Chloride Reagent

Combine 5 parts of amine-sulfuric acid with 1 part of ferric chloride reagent, shake and store in refrigerator. Shelf life 1 to 2 weeks. Shake before use.

Spectrophotometric Reading

Filter Position: 600-950 nm
Wavelength: 670 nm

Sample Preparation

0.5 mL Zinc Acetate
3 mL sample
0.5 mL Amine-Sulfuric/Ferric Chloride Reagent
1 mL deoxygenated nanopure water
wait time 20 minutes

Blank Preparation

0.5 mL Zinc Acetate
3 mL nanopure water
0.5 mL Amine-Sulfuric/Ferric Chloride Reagent
1 mL nanopure water
wait time 20 minutes

Note: The reaction in the sample will degrade over time making the readings unstable. Wait exactly 20 minutes before reading each sample. When placing sample in cuvette, invert cuvette three times to allow mixing, tap the cuvette to eliminate bubbles, and wipe the outside of the cuvette with lens paper.

APPENDIX B

FERROUS IRON COLORIMETRIC METHOD

Iron Test

Reagents

1. Certified Fe Standard Solution 1000 ppm Cat#A466-250
2. Hydroxylamine hydrochloride Cat#LC15530-1
3. HCl Optima® (Metal Grade) Cat#A466-500
4. 0.1% (w/v) 1,10-phenanthroline solution Cat#5520-16
5. 40% (w/w)Ammonium acetate solution Cat#620-1

Blank and Standard Solutions (1, 5, 10, 15, and 30 ppm)

1. In a 100 mL flask add 50 mL nanopure water
2. Add 2 mL HCL trace metal
3. Add 2 mL hydroxylamine hydrochloride
4. Add aliquot of Fe necessary for standard solutions (100, 500, 1000, 1500, and 3000 µL) (This step does not apply for the blank)
5. Add nanopure water to 100 mL mark
6. Wait at least 3 minutes before spectrophotometric readings

Spectrophotometric reading

Filter Position: 340-599 nm
Wavelength: 510 nm

Sample or standard Preparation

Add to cuvette:

100 µL of HCl Optima®
2 mL sample or standard
1 mL phenanthroline
0.5 mL acetate buffer
4 mL nanopure water
Wait time 3 minutes

Blank Preparation

Add to cuvette:

1. 100 µL of HCl Optima®
2. 2 mL nanopure water
3. 1 mL phenanthroline
4. 0.5 mL acetate buffer
5. 4 mL nanopure water
6. Wait time 3 minutes

Note: Reaction in sample is very stable, once the samples are fixed with reactants they can be measured at any time, minimum wait time for reading should be 3 minutes. When placing sample in cuvette, invert cuvette three times to allow mixing, tap the cuvette to eliminate bubbles, and wipe the outside of the cuvette with lens paper.

APPENDIX C

ALKALINITY METHOD

Alkalinity

Reagents:

1. **Sodium Carbonate 0.995-1.005 N (Na_2CO_3) #SS148-1**
2. **Concentrated H_2SO_4 (Sp. Gr. 1.84)**

Preparation of H_2SO_4 Solution

2 mL of concentrated sulfuric acid in 1 L H_2O.
If alkalinity in sample is suspected to be low then dilute solution to 1 mL sulfuric acid in 1 L H_2O.

Determination of normality of titrant (H_2SO_4)

Titration

Set up pH meter and calibrate with pH 4 and 7 buffers. If possible do a three point calibration using pH buffer 10.

Rinse and fill burette with H_2SO_4 for the titration.

Pipette 2 mL of the standard sodium carbonate solution to a 50 mL beaker.

Rinse pH electrode well with distilled water and dry with Kim wipe, then place it in the solution.

Measure and record initial pH, leave electrode in solution during the entire titration.

Titrate the sample by adding small amounts of titrant (0.2 or 0.4 mL) each time. After each addition stir solution until pH is stable. Record the volume of titrant added and the pH reading after every addition.

Continue doing this, until a pH of around 4.5 is reached, after this point keep adding the acid at increments of 0.1 mL until five additions. Record the volume of titrant added and the pH as in step 6.

Determining end point using the Gran Titration method

1. Plot Gran Function vs. Volume of Acid added.
2. Extrapolate back from the linear part of the curve to intersect with the x-axis. This intersection is the equivalence point.

Gran Function = $(V_0 + V) \times 10^{-pH}$)
Where V_0 is the starting volume of the sample or sodium carbonate solution and V is the volume of acid added.

Table C.1. Titration of sample with standardized sulfuric acid. Starting volume of sample was 1 mL.

pH	Vol. H2SO4 (µL)	GF H_2SO_4
8.35	0	4.5E-09
8.32	10	5.3E-08
6.95	110	1.2E-05
6.52	210	6.4E-05
5.98	310	3.3E-04
5.51	360	1.1E-03
3.56	410	1.1E-01
3.34	420	1.9E-01
3.2	430	2.7E-01
3.12	440	3.3E-01
3.04	450	4.1E-01

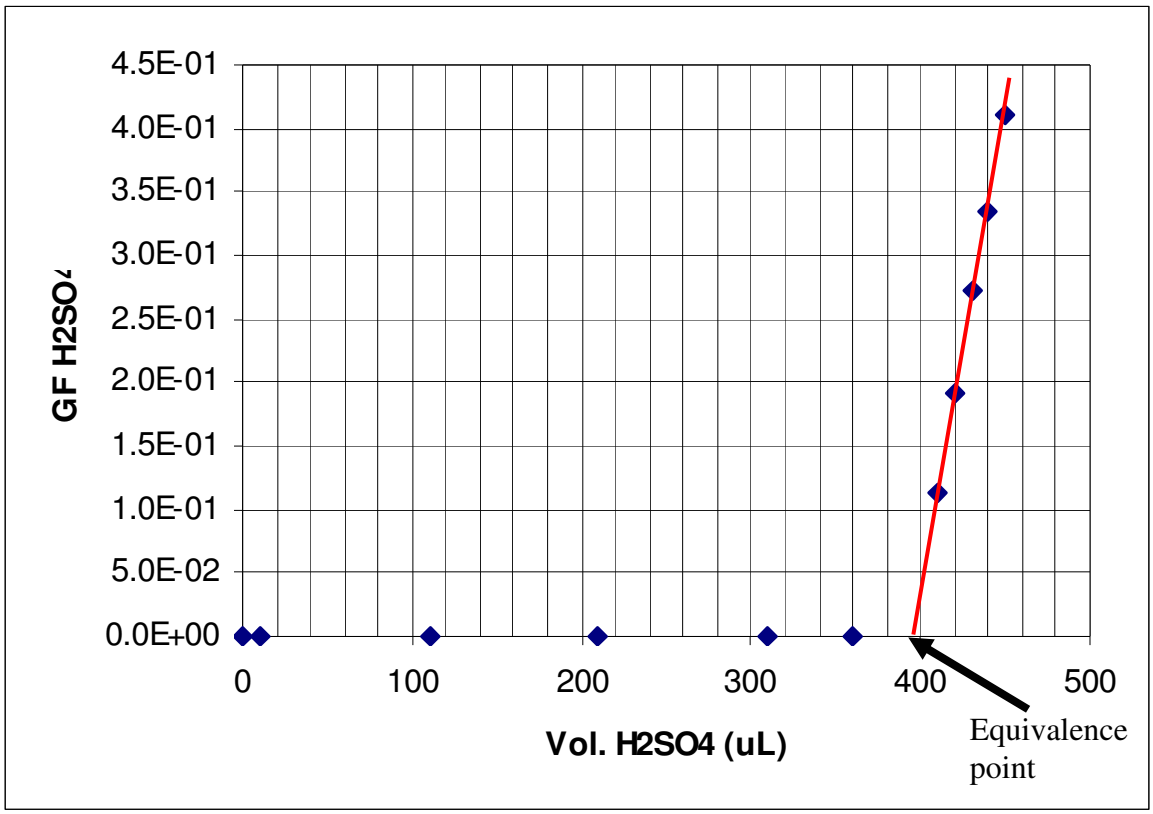

Figure C.1. Gran Function vs. volume of standardized sulfuric acid added during titration of sample or sodium carbonate solution showing equivalence or end point at pH of 4.5 (volume of H_2SO_4 added to reach equivalence point at pH 4.5 = 394 mL).

Equation to determine the Normality of H_2SO_4 after standardizing with standard solution of sodium carbonate.

Normality titrant= (V_0 x (Normality$_{Na2CO3}$ / $V_{eq.pt}$))

Where V_0 is the starting volume of Na_2CO3, Normality$_{Na2CO3}$ is the normality of sodium carbonate solution, and $V_{eq.pt}$ is the volume of H_2SO_4 added at equivalence point.

Calculating Alkalinity

Titrate sample using standardized H_2SO_4.

a. Set up pH meter and calibrate with pH 4 and 7 buffers. If possible do a three point calibration using pH buffer 10.
b. Pipette 2 mL of the sample into a 8 mL Nalgene vial.
c. Rinse pH electrode well with distilled water and dry with Kim wipe, then place it in the solution.
d. Measure and record initial pH, leave electrode in solution during the entire titration.
e. Titrate the sample by adding small amounts of titrant (0.2 or 0.4 mL) each time. After each addition stir solution until pH is stable. Record the volume of titrant added and the pH reading after every addition.
f. Continue doing this, until a pH of around 4.5 is reached, after this point keep adding the acid at increments of 0.1 mL until five additions. Record the volume of titrant added and the pH as in step 6.

Determine volume of titrant added using Gran Function method as explained above.

Determine the normality of H_2SO_4 using the equation explained above for Normality of Titrant

Determine the alkalinity with the following equation:

Alkalinity (mg/L HCO3-) = (N titrant * mL titrantpH4.5 * (1000mL/1L) * (61 mg HCO3/meq)/mL sample

APPENDIX D

PASSIVE DIFFUSION EQUILIBRATION TIME

Peeper was let to equilibrate in a tub containing a chloride solution.

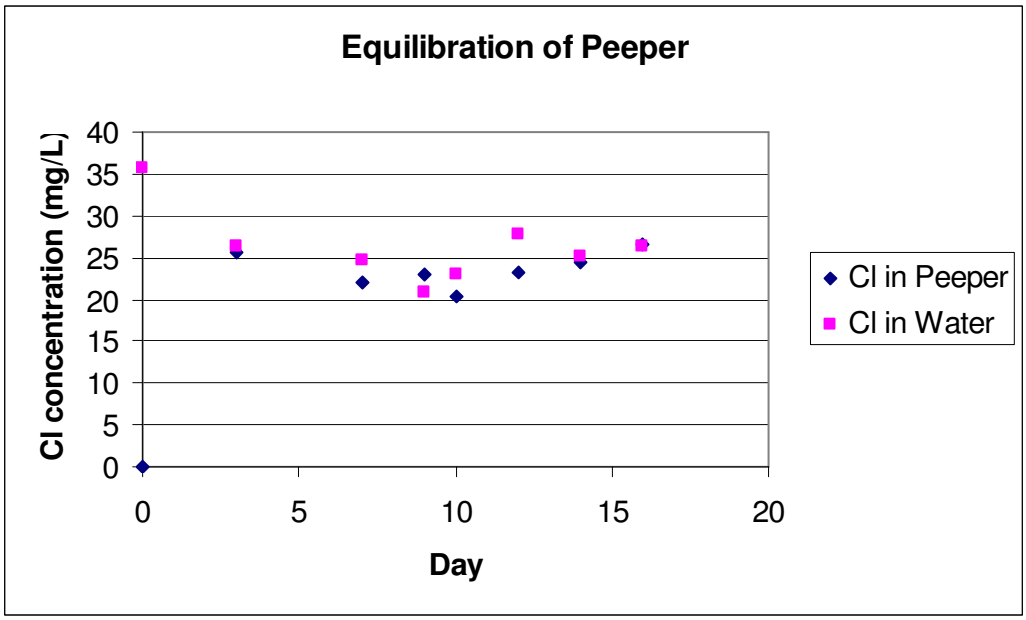

Figure D.1. Test to determine the time it takes the peeper to equilibrate with Cl^- in the surrounding solution. Membrane used is Inmobilion® Nylon Membrane 0.45 µm.

VITA

Susan Enid Baez-Cazull
Calle Lirio 3B4 Lomas Verdes
Bayamón, P.R. 00956
cazull@hotmail.com

EDUCATION

2000 B.S. in Chemistry, University of Puerto Rico, Río Piedras

2007 Ph.D. in Geology, Texas A&M University, College Station

PUBLICATIONS

Baez-Cazull, S., McGuire, J.T., Cozzarelli, I.M., Raymond, A., and Welsh, L. (2007) "Centimeter-Scale Characterization of Biogeochemical Gradients at a Wetland-Aquifer Interface Using Capillary Electrophoresis". Special Issue Applied Geochemistry. In press.

Baez-Cazull, S., McGuire, J.T., Cozzarelli, and Voytek, M.A. (2007) "Determination of Dominant Biogeochemical Processes in a Contaminated Aquifer-Wetland System Using Multivariate Statistical Analyses". Journal of Environmental Quality. In press.

Welsh, L.W., Raymond, A., McGuire, J.T., Baez-Cazull, S., and Smith, E. (2007) "Burial and decomposition of particulate organic matter in a temperate, siliciclastic, freshwater wetland". Wetlands. Submitted

Baez-Cazull, S., McGuire, J.T., Cozzarelli, and Voytek, M.A. (2007) "Biogeochemical processes at a wetland-aquifer interface: seasonal and hydrological linkages". In review by USGS. To be submitted to Applied Geochemistry.